

Semiconductor TCAD Fabrication Development for BCD Technology

A Major Qualifying Project Report:
submitted to the Faculty
of the

WORCESTER POLYTECHNIC INSTITUTE

in partial fulfillment of the requirements for the
Degree of Bachelor of Science

by

Matthew Hazel

Marc Cyr

Date: March 13, 2006

Submitted to:

Professor John McNeill, Co-Advisor

Abstract

As semiconductor devices evolve, it is important to understand the fabrication processes and issues that arise with each new generation of transistor technology. Through research, and the use of the SILVACO simulation tools, we successfully simulated and tested a series of Bipolar, CMOS, and DMOS devices, and optimized them in order to minimize issues such as leakage current and punch through. Additionally, comparisons between actual, and theoretical device characteristics were made.

Acknowledgements

We take this opportunity to thank the people that have supported us over the course of our project. Without their help and guidance, we would not have been able to complete this effort in a timely manner.

Professor Shela Aboud (Project Advisor): Whose knowledge of BCD technologies as well as the Silvaco simulation tools was a significant help during the completion of our project.

Professor John McNeill (Project Advisor): For graciously taking on the role of our project advisor for the third term, and completion of our MQP.

Jim McClay: Whose research paper on device fabrication proved to be the foundation of this project.

Table of Contents

Abstract.....	ii
Acknowledgements	iii
Table of Contents	iv
List of Figures	viii
List of Tables	x
Executive Summary	xi
1. Introduction.....	1
2. Background.....	3
2.1. Evolution of the Transistor in BCD Technology	3
2.2. The Fabrication Process.....	4
2.2.1. Lithography	5
2.2.2. Oxidation of Silicon.....	5
2.2.3. Diffusion and Ion Implantation	6
2.2.4. Ion Implantation.....	6
2.2.5. Film Deposition	7
2.3. BCD Masking Process	7
2.3.1. Locos Isolation	8
3. Silvaco Software Suite.....	10
3.1. How to Code with Athena.....	10
3.1.1. Overview	10
3.1.2. Research	12
3.1.3. Line-By-Line Analysis.....	13
3.2 How to Code with Atlas.....	13
3.2.1. Overview	13
3.2.2. Research	15
3.3. Deviance from Ideal Simulation Examples.....	16
3.3.1. Mesh Lines	16
3.3.2. Oxidation.....	16
3.3.3. Masking.....	18

3.3.4.	LOCOS Isolation process.....	20
3.3.5.	Contacts.....	27
3.4.	Conclusion.....	29
4.	CMOS Transistor	30
4.1.	Problem Statement.....	30
4.2.	Theoretical Device Characteristics	31
4.2.1.	Oxide Thickness	31
4.2.2.	Threshold Voltage.....	32
4.2.3.	I-V Characteristics	33
4.3.	Walkthrough of CMOS Fabrication	34
4.3.1.	PMOS Fabrication Summary	36
4.3.2.	NMOS Device Process.....	37
4.4.	Final Device Characteristics and Comparison	43
4.4.1.	Gate Oxide.....	43
4.4.2.	Threshold Voltage.....	44
4.4.3.	I-V Relationship.....	45
4.5.	Conclusion.....	46
5.	Bipolar Junction Transistor.....	48
5.1.	Problem Statement.....	48
5.2.	Theoretical Device Characteristics	49
5.2.1.	Gummel Plot.....	49
5.2.2.	I-V Characteristics	50
5.3.	Walkthrough of BJT Fabrication.....	51
5.3.1.	BJT Device Process	53
5.4.	Final Device Characteristics and Comparison	58
5.4.1.	Gummel Plot.....	59
5.4.2.	I-V Characteristics	61
5.5.	Conclusion.....	62
6.	LDMOS Transistor.....	62
6.1.	Problem Statement.....	62
6.2.	Theoretical Device Characteristics	63

6.2.1. Threshold Voltage.....	64
6.2.2. Leakage Current.....	64
6.2.3. Off-State Leakage Current	65
6.2.4. Breakdown Voltage	66
6.2.5. On-Resistance	67
6.2.6. On-State Drain Current	68
6.2.7. Capacitance.....	68
6.3. Walkthrough of LDMOS Fabrication.....	69
6.4. Final Device Characteristics and Comparisons.....	78
6.4.1. $I_d = (V_d, V_g)$ Characteristic.....	79
6.4.2. Transistion Potential vs V_g, V_d	80
6.4.3. C_{dd} vs V_d, V_g	80
6.5 Conclusion	81
7. BCD Fabrication Wafer.....	83
7.1. Problem Statement.....	83
7.2. Process Recipe.....	83
7.3. Strategies for maximizing Performance Parameters	85
7.3.3. Process Problems	86
7.4. Strategies For Improving Shrinking Device Geometry	86
7.4.1 VLSI technology shrinking Poly-Silicon Window.....	86
7.4.2. Trench gate structure.....	86
7.4.3. Materials.....	87
7.4.4. Tapered Oxide (TEOS).....	87
7.5. Conclusion.....	87
8. Project Summary and Future Work.....	88
Appendix A – References.....	90
Appendix C – PMOS Athena and Atlas Code.....	98
Appendix D – BJT Athena and Atlas Code.....	104
Appendix E – LDMOS Athena and Atlas Code.....	110

List of Figures

Figure 2-2 Atlas Coding Process	14
Figure 3-3 Rounded Oxide	17
Figure 3-4 Bird Beak Effect	18
Figure 3-5 Nitride Mask Layer	19
Figure 3-6 After Nitride Mask Layer	19
Figure 3-7 Implantation During Mask Step	20
Figure 3-11 Before Diffusion	25
Figure 3-12 After Diffusion	26
Figure 3-13 Juntion Lines	27
Figure 3-14Plated Aluminum Contacts	28
Figure 3-15 Etched Aluminum Contacts	28
Figure 4-1: Oxidation thickness versus time for wet and dry O ₂	32
Figure 4-2: CMOS Design flow chart	35
Figure 4-3: N-Channel MOSFET Device	37
Figure 4-4: P-Channel MOSFET Device	37
Figure 4-5: P-Type wafer with Arsenic Epitaxial Layer	38
Figure 4-6: Boron Well Drive	39
Figure 4-7: Upper surface of NMOS transistor	40
Figure 4-8: Implanted Arsenic and grown shielding oxide	41
Figure 4-9: NMOS transistor after Arsenic Diffusion	42
Figure 4-10: Completed NMOS transistor	43
Figure 4-11: NMOS Conductivity versus Gate Bias	45
Figure 4-12: I-V Curve for NMOS transistor	46
Figure 5-1: Ideal and Non-Ideal Gummel Plots (Pierret, p. 425)	50
Figure 5-2: Sample Ideal I-V characteristics for a PNP BJT (Pierret, p. 408)	51
Figure 5-3: BJT Process Recipe	52
Figure 5-4: Simplified BJT Structure	53
Figure 5-5: BJT after epitaxial growth	54
Figure 5-6: BJT post Boron Diffusion	55

Figure 5-7: BJT post Arsenic Implantation	56
Figure 5-8: BJT Post Arsenic Collector Implant	57
Figure 5-9: BJT Post Aluminum Deposition	58
Figure 5-10: Completed BJT Structure	58
Figure 5-11: Non-Ideal Gummel plot.....	59
Figure 5-12: Gummel Plot without SRH Model.....	60
Figure 5-13: BJT I-V Characteristics.....	61
Figure 6-7 LDMOS 2nd Oxide Layer	76
Figure 6-8 LDMOS P-Well Drive	77
Figure 6-9 Final LDMOS Device	78
Figure 6-11 V_{di} vs V_d , V_g	80
Figure 6-12 C_{gg} vs V_d	81

List of Tables

Table 2-1: device characteristics of BCD-I though BCD-V	4
Table 3-1: Threshold Voltage Symbol Explanation	33
Table 3-2: Saturation Current Symbol Explanation.....	34
Table 3-3: CMOS Masking Steps	36

Executive Summary

As the semiconductor industry continues to mature, technological advancements have allowed for the scaling down of BCD devices to submicron dimensions. As these devices decrease in size, their complexity increases and device issues such as leakage current, latch-up, isolation, and 2nd order transients all become more prevalent. In order to isolate these issues, and develop a fabrication process which minimizes their effect, software packages have been developed in order to simulate both the creation process and BCD device behavior.

Silvaco is one such software package that has been developed in order to provide a complete simulation tool for both the fabrication process as well as modeling completed device behavior. This project focused on the use of Athena and Atlas, which are part of the Silvaco suite of modeling applications, in order to create a 10 mask fabrication process encompassing all of the BCD devices. Additionally, research was conducted into the evolution of BCD technology, as well as many aspects of the fabrication process.

We researched the lithography process. A strong grasp of the fabrication process was necessary to perform the analysis that would occur later in the project. In addition, we researched the evolution of the transistor, past and future. We did so, in hopes that we could learn the direction of technology, so that we may more accurately apply it to our simulations.

The initial device which was modeled was an NMOS transistor. Research conducted on the theoretical behavior of an NMOS transistor would be the basis for which we measured our success in developing this device. As this was our first experience with using Athena to generate a device of any sort we began by modifying an existing example. Incremental changes were made between simulations, and by viewing their effects on the device's behavior and characteristics we were able to understand the coding language used by Athena and Atlas.

Athena is used to generate results for device behavior, and it was these results which were compared against the theoretical behaviors. In most cases, our NMOS transistor demonstrated acceptable behavior. An acceptable turn-on voltage, I-V characteristic, and oxide thickness were all obtained with the NMOS device.

The second of three devices which we were to simulate was a bipolar junction transistor (BJT). Rather than modify an existing example, this device was to be designed from scratch. Physical parameters were chosen so that the BJT would roughly correspond in size to the NMOS transistor, and the process flow was created so that it could be implemented alongside the process flow of the NMOS transistor. As BCD technology requires the simultaneous development of several different types of devices on the same wafer, it was necessary to make these size and process considerations.

During the process of modeling the BJT, we both refined and expanded our knowledge of Atlas and Athena, allowing for a much more rapid development process. Again, research into the theoretical behavior of a BJT would prove to be the basis for which we determined the success of our device. Careful consideration of the doping characteristics for the base, emitter and collector, as well as knowledge of the constraints placed on the geometry of the BJT allowed us to create a device that again demonstrated acceptable operating characteristics.

The final device we modeled was the LDMOS. We further learned how to simulate a device we had never even seen prior to this project. We used our step-by-step process to fabricate the LDMOS on the wafer. We learned of the double diffused transistor and the drift length.

The final step of the project involved placing all the devices on a single wafer. We thought of the strategies of changing p and n type dopants at the cost of BJT amplification or LDMOS on-resistance. We learned about the tradeoffs of high switching speeds for the CMOS and how that put the LDMOS at risk of punch through. We designed a single process recipe that accounted for accommodating all the needs of each individual device, only on a single wafer.

Through the research conducted into both the fabrication process as well as the evolution of BCD technology and its components, we were able to generate three devices which demonstrated acceptable operating characteristics. Our knowledge of semiconductor development, and the tradeoffs which must be considered when developing separate technologies on an individual silicon wafer has greatly increased. We achieved our goal of creating a ten-mask process for BCD technology, and in the

process learned how to program using one of the industry's most widely accepted software packages for semiconductor device modeling.

1. Introduction

As the semiconductor industry continues to mature, technological advancements have allowed for the scaling down of BCD devices to submicron dimensions. BCD is the name given to an integrated circuit (IC) composed of Bipolar Junction Transistors (Bipolar), Complimentary Metal-Oxide-Semiconductor Field-Effect Transistors (CMOS), and Lateral Double Diffused Metal Oxide Semiconductor Field-Effect Transistor (LDMOS). As these devices decrease in size, their complexity increases and device issues such as leakage current, punch-through, isolation, and 2nd order transients all become more prevalent.

In order to isolate these issues, and develop a fabrication process, which minimizes their effect, software packages have been developed in order to simulate both the creation process and BCD device behavior. The Silvaco suite of applications, including TonyPlot, Athena, and Atlas, is just one such software package that is commonly used in industry in order to simulate the BCD fabrication process. Silvaco has gained broad acceptance in the semiconductor industry as being a reliable and accurate simulation tool for the development of BCD devices.

Within Silvaco there are complex non-ideality models which account for such device behaviors as average minority carrier lifetime (Shockley-Read-Hall), or doping impurities arising during the annealing process. Silvaco allows designers to efficiently test a masking process, and then analyze the resulting device without having to physically create the device on a silicon wafer. This saves designers both time and money, and software packages like Silvaco have become an invaluable tool in the semiconductor industry.

The goal of this project is to use Silvaco to successfully simulate a 10 mask process corresponding to BCD III technology parameters, and then analyze the issues that would arise were we to attempt a BCD V device. We intend to simulate a CMOS transistor, BJT transistor, and LDMOS device, and although each of the devices is simulated independently to reduce the computational burden of the software package, each device will be treated as if it were fully integrated on the same silicon wafer. The processing steps must then be optimized to create the “best” devices while still adhering

to BCD III standards. There are numerous parameter tradeoffs between devices, such as diffusion depth, sheet resistance vs. turn on voltage, complexity vs. cost, breakdown voltages, and other device parameters that are dependent upon the doping profile.

In addition to the fabrication process, we will explore the expected, theoretical behavior of these BCD devices, and then use Silvaco to extract performance parameters, such as the sheet resistance, turn-on voltage, I-V curves, reverse breakdown voltage, and more. Comparisons can then be made between the expected behavior and the simulated behavior of the devices. Then, time can be spent to fine tune the doping profiles and physical geometry of the device in order to achieve optimal results.

This report is organized so that the reader will first acquire an understanding of the evolution of the BCD components. Then, an overview of the BCD fabrication process is presented, including the most common methodologies used. Once the background information has been concluded, a more in depth analysis of three separate BCD technologies is presented. Each analysis will begin with a description of the theoretical performance characteristics, followed by a description of the fabrication process, and then completed with a comparison between the generated results and the theoretical expectations.

2. Background

The need for higher power switching applications is increasing as technology advances. Power supplies, current sources, battery chargers, boost/buck converters, computer processors etc. are requiring more power switching and less silicon. The transistor has come along way since its creation. This chapter will discuss the evolution of the transistor and the means to fabricate it.

2.1. Evolution of the Transistor in BCD Technology

Until the eighties, BJT's were the main technology used for Power IC's. The BJT was the best transistor for his application because of its "amplification and matching properties". BJT I²L was used to implement the gate logic at that time. Soon, the high demand for gate logic led to the need for a better switching technology. The BJT I²L then became outdated because of its power consumption needs and complex design. At low frequencies, CMOS was the apparent choice for gate logic design. Power IC's expanded to include BJT and CMOS technology. BJT's reached a limit in delivering power to the load. The DMOS overcame these limitations. Virtually no DC driving current is required for the DMOS. With the addition of the DMOS to the BJT and CMOS, a new form of technology was created, BCD technology.¹

BCD technology itself has gone through multiple stages of change and evolution. As the demand of complex designs increased, so did cost. Eventually BCD technology had to take up less real estate, other wise its evolution would be coming to an end.

Instead of increasing the die size, the designers came up with an alternative solution to increase space; they would reduce the size requirement of the BCD technology from 4 μ to 2.5 μ . This allowed almost three times the density of transistors on the same size chip. Also, lower threshold voltages were obtained. BCD-I had a threshold of 1.3V while the new device, which had a smaller width, (named BCD II technology) boasted a threshold voltage of 1.1V. Now signal component density and power current density parameters were nearly doubled.²

¹ Smart Power IC's pg. 1

² Ibid pg. 2-8

But soon, the introduction of EEPROM would lead to the creation and need for BCD III technology or system oriented BCD generations. The new attainable device width parameter was around 1.2u, doubling the system oriented capacity. Now entire systems could be condensed onto a single chip. The power rating nearly doubled since BCD-I technology. Also, the gate oxide thickness shrank about 3 times to BCD-I allowing for less reaction to parasitic.

But, in order to incorporate flash memory, the BCD device would have to be shrunk down as low as 0.6u in width. This equated to BCD V technology. BCD V is the most current evolution of BCD technology. It can fit up to 15,000 transistors per square millimeter. Threshold voltages as low as .85 volts could be obtained. BCD-V seems to be reaching its limits as well. The gate oxide will soon reach its limitations. As a result, parasitic and 2nd order transients begin to affect device parameters to a great extent.³

	L-gate (μm)		Th _{ox} gate (nm)	V _{TH}	K _{LIN} (μA/V ²)		CMOS density (tr./mm ²)
	NMOS	PMOS			NMOS	PMOS	
BCD-I	4.00	7.00	85	1.30	27	10	650
BCD-II	3.00	4.00	60	1.10	40	15	1600
BCD-III	1.20	1.20	28	0.90	60	21	4000
BCD-V	0.8	0.9	20	0.85	85	28	15000

Table 2-1: device characteristics of BCD-I though BCD-V

Table 2-1 depicts the numerous families of BCD technology. Note how the CMOS densities double with each family transition. Also not how the threshold voltage values decrease as the devices get smaller. This is because the space between the devices is smaller, and there is more charge in less area. Therefore, it takes less charge to activate the switch because there is more charge there.

2.2. The Fabrication Process

The fabrication process is a complex thing. There are many variables to consider during each step of the process. Also, each step occurs many different times adding on to

³ Smart Power IC's pg. 9-17

further complexities. In this chapter each step of the fabrication process will be discussed in great detail.

2.2.1. Lithography

The term lithography equates to a term that analog designers and manufacturers know as a 'mask'. The number of masking steps in a given fabrication process acts as a rubric for determining both complexity and cost of that process.

The first step in the lithographical process is to clean the wafer. After it has been cleaned we can then deposit some barrier layer. This layer serves to protect the silicon from damage, when the layer is later stripped. The photo-resist is then put on top of the barrier metal. To ensure the photo-resist, the metal, and the silicon are bonded well, the wafer is soft-baked.

It is here that we begin our very precise masking steps. The masks are placed over the wafer in a specific manner to either mask away the area or mask around the area depending on the type of resist used. The resist is then exposed to high intensity ultra violet light leaving the desired part and etching away the unwanted material.⁴

2.2.2. Oxidation of Silicon

Heating silicon up to high temperatures in the presence of water vapor or oxygen results in the creation of silicon dioxide, a major component in the creation of BCD technology. The main factors in determining the growth of silicon have to do with the atmosphere in which the silicon is annealed, the time it is annealed, the temperature in which it is annealed, the crystal orientation, and the doping of the impurity atoms.

There are generally two types of growth processes that silicon can be grown in, a wet oxidation process and a dry oxidation process. The dry process involves an atmosphere of oxygen, and the wet involves the presence of water vapors. The dry process is usually reserved for slower growth rates, as used in MOS technology. The wet process is a much faster growth rate and is used more for making thick masking layers.

⁴ Introduction to Microelectronic Fabrication pg. 13-27

Time and temperature are large factors for the growth of oxidation. The longer time the silicon is heated, and the higher the temperature, the thicker the masking layer becomes.

The type of dopant of the impurity atoms has an affect on the oxidation growth as well. “Boron and gallium tend to be depleted from the surface, whereas phosphorus and arsenic... pile up at the surfaces”.⁵ “Mobility reaches a maximum value at low impurity concentrations; (in gallium arsenide and silicon) this corresponds to the lattice-scattering limitation. Both electron and hole motilities decrease with increasing impurity concentration and eventually approach a minimum value at high concentrations.”⁶ This means that the acceptors diffuse more quickly than the donors. However, the diffusion reaches its maximum more quickly.

Also, the number of times a silicon layer is heated affects the rate of growth. The more times, the thicker the layer becomes.

Silicon nitride is an effective substance to mask silicon dioxide.⁷

2.2.3. Diffusion and Ion Implantation

The process of diffusion has a great impact upon the size measurements of a given device. Diffusion controls junction distances, laterally and vertically, sheet resistance, which directly correlates to R_{on} of the LDMOS.

Diffusion is controlled once again by an annealing process. Diffusion annealment is done typically longer than oxidation growth. This is because its sole purpose to expand the region of concentration to create the proper junctions in a device, which influence the channel/well specifications.

The same factors exist throughout the process of diffusion as exist in growth oxidation.⁸

2.2.4. Ion Implantation

Ion implantation is used as a step in the fabrication process to place some impurity concentration projected at some range, into a layer of the device being made.

⁵ Introduction to Microelectronic Fabrication pg.38

⁶ Semi-conductor Devices Physics And Technology pg. 33

⁷ Introduction to Microelectronic Fabrication pg. 29-47

⁸ Semi-conductor Devices Physics And Technology pg. 49-83

The distance that the impurity concentration is spread into the material is based on a Gaussian distribution. The projected range that the ion implantation goes is based on the acceleration energy. Typically it is used for shallow PN junctions because of the Gaussian distribution. In reality, the curve is not exactly Gaussian; there are some deviations.⁹

2.2.5. Film Deposition

CVD forms a thin film on the surface by thermal decomposition. The desired material is then placed there directly from its gaseous form.

To apply the contacts to the device at hand, a step of film deposition is necessary. Chemical Vapor Deposition (CVD) is a common way to apply the contacts. A mask layer is applied, and then the contacts are plated onto the exposed areas of the device.

CVD is also a common way to apply the epitaxial layer, or the “seed” layer.¹⁰

2.3. BCD Masking Process

In this section of the report, the masking process of BCD fabrication will be discussed. This section is independent of simulations or the simulation process.

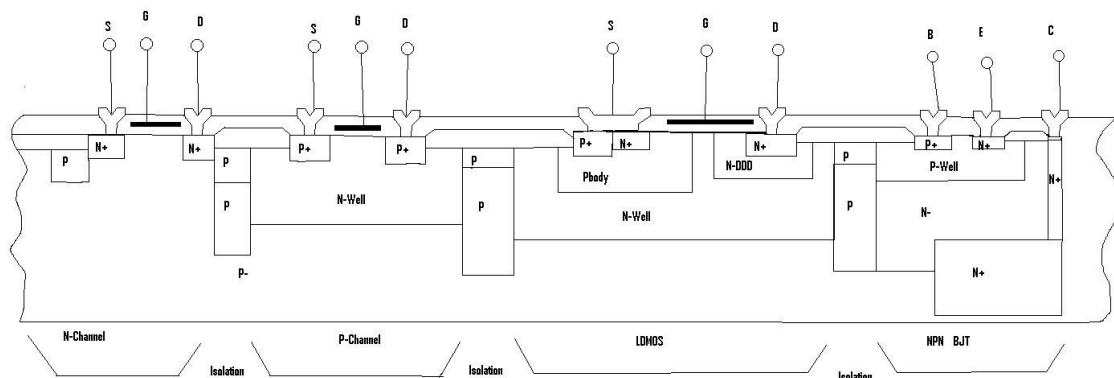


Figure 2-1 BCD Wafer Cross Section

Figure 2-1 shows an example of a cross section of a BCD wafer. This example uses junction isolation and lacks an epitaxial layer, so it is quite unlike the example in the report which uses LOCOS isolation and has an N-type epitaxial layer on all the devices

⁹ Semi-conductor Devices Physics And Technology pg. 89-105

¹⁰ Semi-conductor Devices Physics And Technology pg. 107-129

except for the N-channel MOSFET. In this figure, additional N-well's have been created in the absence of the epitaxial layer.

2.3.1. Locos Isolation

Device isolation is an important part of BCD technology. The affects of one device should not be felt by other devices on the same chip. That would result in flawed chips, and large unwanted expenses. To avoid this scenario, techniques of device isolation can be applied. There are three main types of device isolation. Trench isolation, junction isolation, and locos isolation.

Trench isolation involves physically cutting a small trench between two devices on a chip. In other words, there is actually a piece of silicon missing in-between the two devices. This method is somewhat complicated, and does not work well with very small devices for two reasons. First of all, the trench cutting machine can only cut so small. Secondly, as the devices gets smaller, the trench separating the devices also gets smaller. Thus, parasitic effects can begin to affect devices mutually.

Another type of isolation is called junction isolation. This method is preferred most of the time. It is cheap, quick and easy. This method involves separating two devices by creating a junction doped with the opposite impurity concentration as the devices it surrounds. In this manner, the junction effectively acts like a diode, not letting current pass to and from either device. The drawbacks of this method of isolation are more noticeable in BCD-V technology. As the device gets smaller, the junctions become closer together. Essentially, adding another junction may create an additional transistor or NPN junction where one is not wanted. Under certain conditions, that transistor can turn on, ruining the parameters of the original device.¹¹

The last type of isolation is known as LOCOS isolation. This method is easy to implement. This method of isolation involves growing an oxide layer between two devices. This way, the oxide isolates the two devices. The problem with LOCOS isolation is that it may require some maneuvering of masking steps, and may require an

¹¹ Power IC's pg.3-6

extra masking step in order to isolate that oxide from being improperly doped by an impurity concentration.¹²

¹² Characteristics of P-channel SOI

3. Silvaco Software Suite

Athena, Atlas, Tonyplot comprise the Silvaco Suite of applications. Each of them have their distinct uses and powerful applications. Athena is used for creating the fabrication design process. Atlas is used for modeling fabricated designs and extracting device parameters. Tonyplot is used for creating visual representations of the coded simulations. Together, they accurately allow a user to simulate and test devices of a production wafer fabrication process.

3.1. *How to Code with Athena*

Figure 3-1 is a representation of the coding process we learned to use out of necessity. Initially the project seems very overwhelming. However, after we created a goal relating to a general problem statement, an outline, and a step-by-step process, the project was finished soon. We held the same idea to coding with Athena. At first, coding an entire device seemed difficult. After going step-by-step, the project was fairly easy to finish.

3.1.1. Overview

Presented is a conceptual diagram and overview of the Athena coding process.

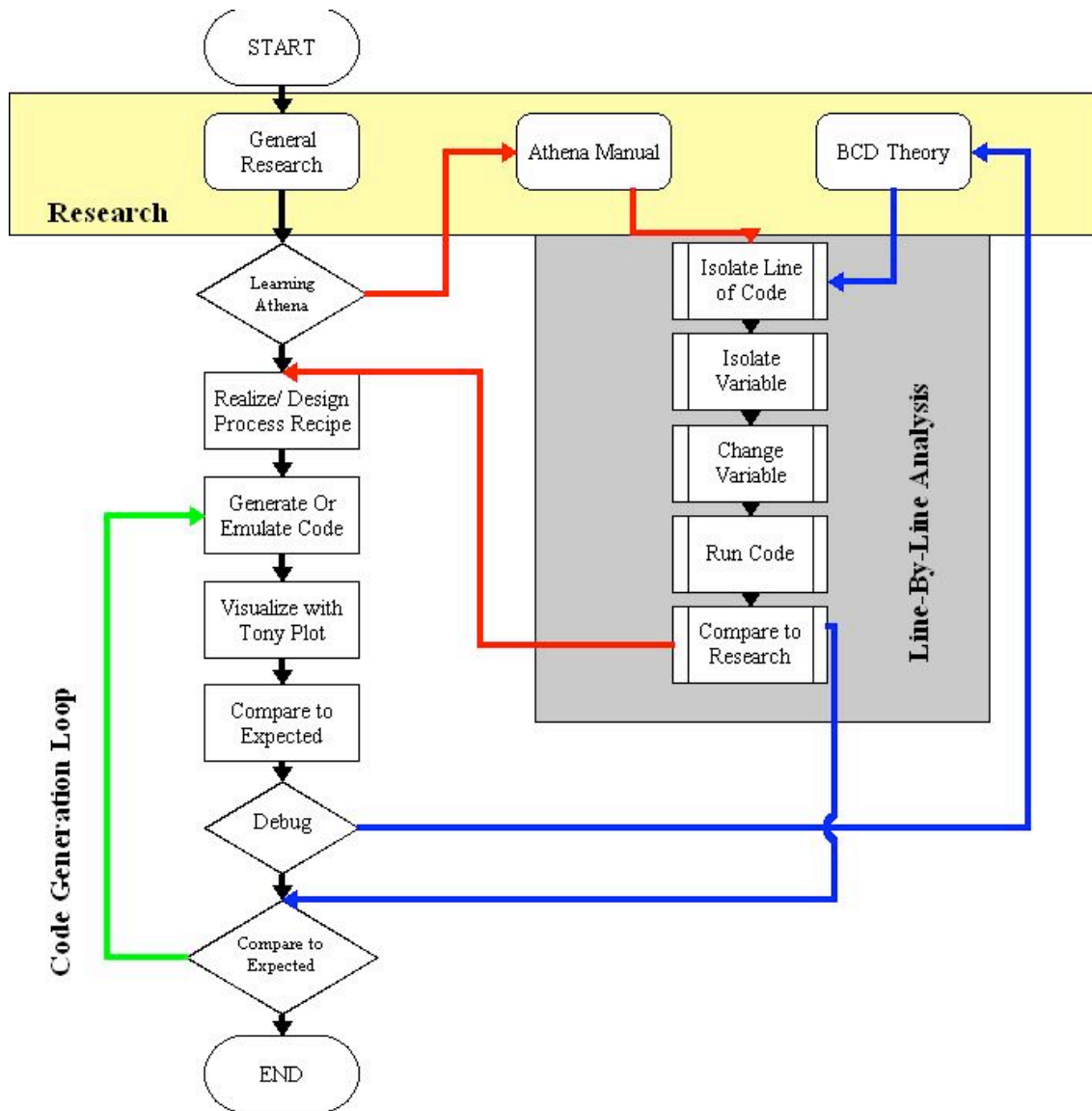


Figure 3-1Athena Coding Process

Figure 3-1 shows how to learn and generate code with Athena. In order to use Athena, the user needs to have done some general research. Then, the user can learn about Athena. The next step to learning Athena is looking at a sample piece of code, and comparing commands to the Athena user manual. This is the only way to understand what each command does; they are not always self-explanatory.

Next, the user must perform line-by-line analysis of the code. After grasping the sample piece of Athena code, the user should then figure out the process recipe on which the example was based. If the user is generating new code, then a process recipe is also

necessary. Once the process recipe has been created, the user can then generate (or emulate existing code). Next, the user must visualize the code and compare it to the expected results (from research).

At this point, the Athena code may possess errors or undesired results. If that is the case, the user has to debug the code. Doing this involves the same line-by-line process as learning Athena. Isolate the line of code and the variable (by commenting out the desired piece of code) and see how it affects the design. Once the bugs are out, the user must compare the results to what is expected and continue.

After one line of code has been generated, the user must continue generating the next line until all of the code is produced and works correctly. Then, the user is temporarily done using the Athena portion of Silvaco. It will be again after implementing Atlas.

3.1.2. Research

Some research must be accomplished prior to attempting to use Silvaco, let alone Athena. The user must know how to code with an application (in general). It may be helpful to navigate through a tutorial, or have a professor teach some of the syntax to user. Furthermore, the user should possess some background knowledge of wafer fabrication.

Especially during the learning process, it will be necessary for the user to refer to the Silvaco manual. At one point, the user will have to do some background research on the manual to learn basic commands and syntax. Then, the user will have to use the manual, not just study from it. There are two ways to use the manual. One way is to look up a specific command. The other is to look up keywords from the fabrication process and scan the digital version. This is useful because sometimes the user will not know the command, or he will need to learn a new command.

Most importantly, the user must know the theory of BCD. Drift, diffusion, band gap voltages, square law, and semi-conductor knowledge are crucial to the coding process. If the user has made a mistake, it must be compared back to the research. Sometimes a user is coding a device he has never seen, in that case, the user needs to fall back on the principles of BCD theory.

3.1.3. Line-By-Line Analysis

The user will have to perform a line-by-line analysis of code both when learning and when debugging code. This is the easiest way to piece together the project.

To perform this analysis, the user must view the entire sample code, isolate a single line, then isolate a single variable. The he then must change the variable and run the code. The user must then compare the results to what is expected. If the line of code makes sense, then the user should continue to the next step. The next step is fairly simple as well: isolate the next line of code and repeat the same process.

3.2 *How to Code with Atlas*

The same statement with Athena holds true for Atlas. A step-by-step process is necessary for completing the project. In this section, the user will learn how to code with Atlas.

3.2.1. Overview

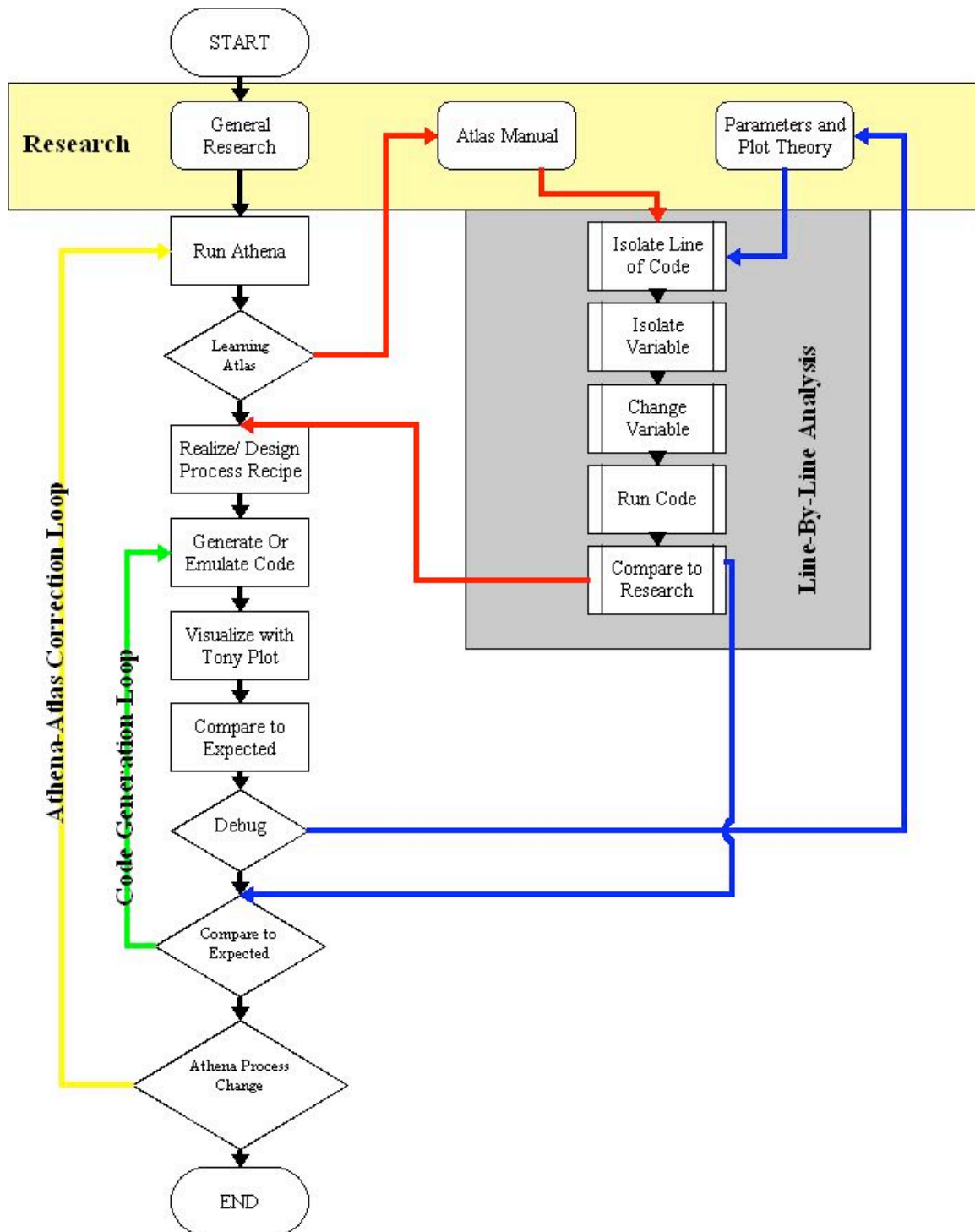


Figure 3-2 Atlas Coding Process

Figure 3-2 shows the Atlas coding process. It is very similar to the Athena coding process. Athena is used prior to Atlas chronologically. For this reason, the process flow

is different. The two applications are intertwined and jumping back and forth between the two is common for simulating wafer fabrication.

The same general research and background is applied to learning Atlas. Prior to running Atlas code, the user must have a working Athena sample of code. Then the user can run Atlas and begin understanding it.

Once again the user must familiarize himself with the Silvaco manual (Atlas this time). Then the user must start with the line-by-line analysis of a piece of sample Atlas code. Once he fully understands the code, he must reverse engineer and make a recipe of the sample, and begin generating code.

The visualizing, and comparing steps are the same as before, as is the debugging step. Even if the Atlas code is correct, there still may be problems with the simulation. If this is the case, then the user will have to check the Athena code again, and start the entire process over again.

3.2.2. Research

The same general background research will be necessary for Atlas as it was for Athena.

The most important things to know when coding with Atlas are equations. The user needs to know how variables are affected (inversely proportional, proportional etc.) by the code lines. He needs to know which equations are pertinent and which ones are being modeled in the simulation process.

The user must also understand the application of the device being fabricated (is it depletion, inversion etc.). It may affect the atlas code, and Athena in turn.

The user must also understand the numerous plots. Specifically the user must know IV curves, capacitance curves, bias vs conductivity, and Gummel plots. All of these curves are useful to know about prior to coding with Atlas.

3.3. *Deviance from Ideal Simulation Examples*

3.3.1. Mesh Lines

Mesh lines are important for modeling devices and extracting their parameters. Where mesh lines intersect, calculations occur. Important plots are based on hundreds and sometimes thousands of these intersecting lines.

When using Athena and simulating the fabrication process, the user needs to specify an initial mesh density. This is important because setting too many mesh points can create long calculation times, and setting too few can cause gaps in analysis (which may end up taking a lot of time in the long run). Typically, more mesh points occur in the channel region and along the surface of the device. The other points are then graduated to a lesser mesh density.

Whenever a new layer is deposited using Athena, a new mesh density must be added. This is because no mesh lines have been specified other than the original mesh. An entirely new layer is void of mesh formatting.

Calculation time can be reduced by using the “mirror” command within Athena. This allows the user to only have to make half as many calculations up until the point of mirroring. This is because there are half as many mesh calculation points. However, at times the user may encounter devices that are a-symmetrical and are not able to be mirrored. When that is the case, no time can be saved with the mirror command.

3.3.2. Oxidation

Growing oxides is an important step in the fabrication process. However, they grow in very specific ways. Certain processes can be undergone in order to manipulate the oxidation growth process, as talked about in chapter 2.

The oxide grows noticeable slower and thicker in a dry environment. In the wet environment, it tends to grow faster. Be careful when annealing oxides numerous times after being grown in a particular environment. It may negatively affect the outcome of the desired oxide shape and position.

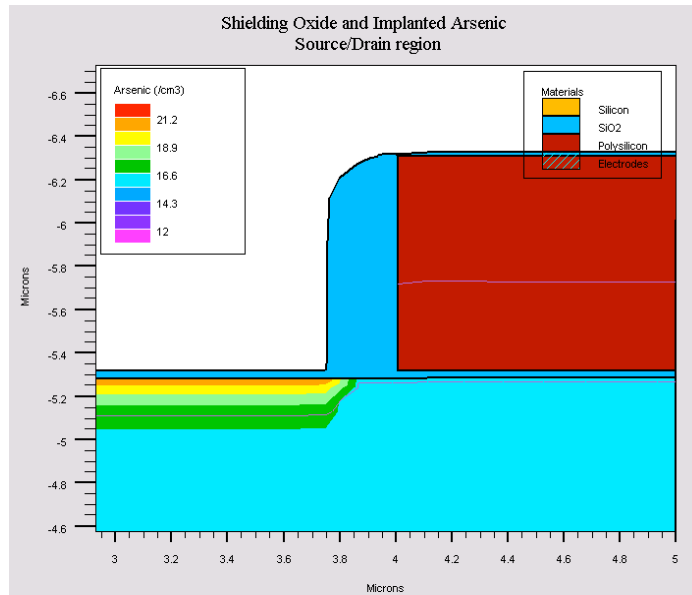


Figure 3-3 Rounded Oxide

Note how the Oxide grows with round edges in figure 3-3. This may adversely affect results if left unanticipated. Such a scenario may exist when performing LOCOS isolation. The user will want the oxide to grow a certain depth and width, however the rounded edges may cut the isolation area just short of the desired area.

Oxides can also be used to shield implantations of dopants. This will be discussed further in the masking section.

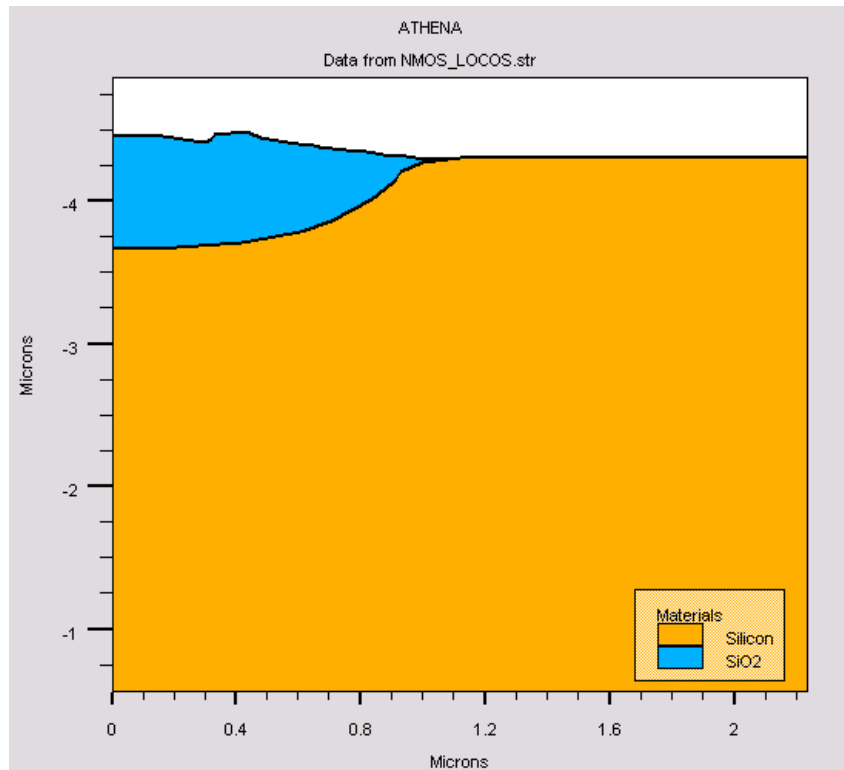


Figure 3-4 Bird Beak Effect

Figure 3-4 shows a picture of the bird beak effect. The uneven growth occurs when growing oxides in a wet atmosphere. This problem can be facilitated by growing the oxide in a nitrogen atmosphere. The picture above is grown in a nitrogen atmosphere. The bird beak effect could be far more significant. Also note that Oxides grow in a 45%-55% pattern. This is particular important when growing FOX or LOCOS isolation oxides. 55% of the oxide is below the surface and 45% of the oxide is above the surface. It is possible to grow the oxide too thick because of the unanticipated 55% growth below the surface.

3.3.3. Masking

Masking is a crucial part in the fabrication process. Here masking is simulated and depicted showing Tonyplots of Athena. It is important to specify the exact coordinates of the mask layer to ensure the proper placement of the new layer being created.

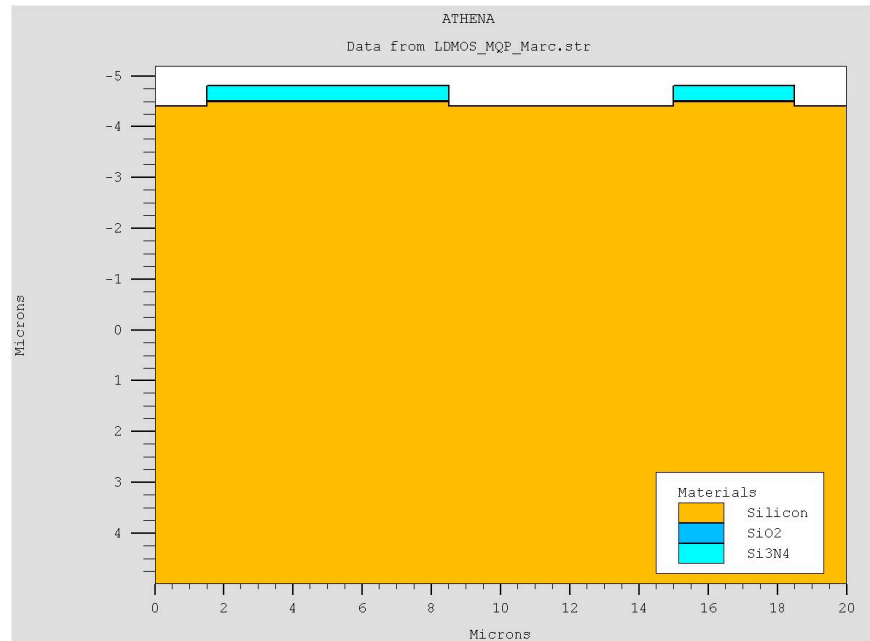


Figure 3-5 Nitride Mask Layer

Figure 3-5 shows a nitride mask layer. This will act as a photo-resist. Oxide will later be grown over the entire area, and later etched away.

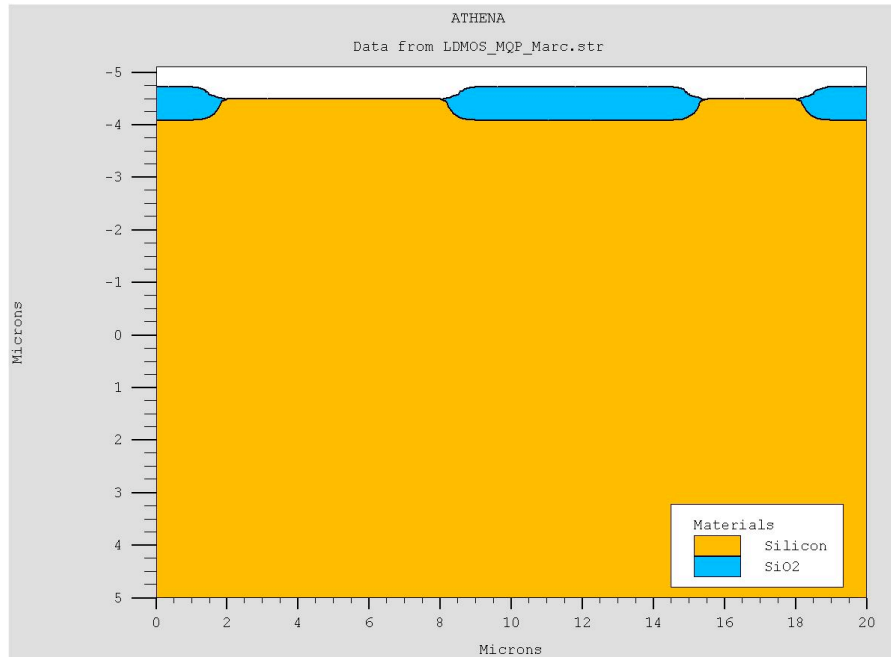


Figure 3-6 After Nitride Mask Layer

Figure 3-6 shows the oxide grown after the nitride mask layer has been produced and etched away. Note how the oxide has grown underneath where the nitride mask layer

was. This is important to note because it can effect placement of shielding oxides later used to place a channel of dopants. It can shrink the later diffusion of the dopants.

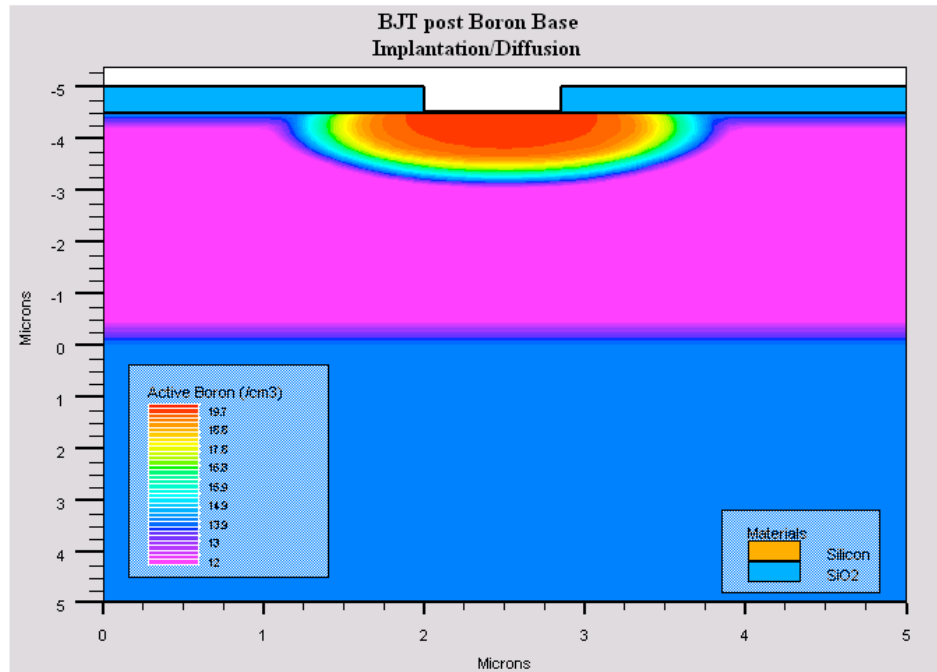


Figure 3-7 Implantation During Mask Step

Figure 3-7 shows boron being implanted during a masking step. Note how the diffusion pushes the surface concentration horizontally as well as vertically. It is important to make sure to take these into account when positioning the mask layer.

3.3.4. LOCOS Isolation process

The initial project goal focused on the isolated creation of a BCD Wafer. However, BCD fabrication adds an additional layer of complexity to the fabrication of devices, because each component needs to be isolated from the surrounding devices. Because of this, it was decided that LOCOS isolation be implemented into transistor fabrication process. The following steps detail the implementation of LOCOS isolation.

a) Process Flow Insertion

The initial decision when implementing LOCOS isolation is deciding where, in the existing process flow, the oxide layer will be grown. Through careful examination of

the process presented by McClay¹³, it was decided that the oxide layer be grown immediately after the epitaxial layer growth. The reason for this is that there are significant annealing steps that occur in order to grow the oxide to the desired depth and thickness. Were this process to be delayed until after the implantation of either the source/drain or channel dopants, then the diffusion depths and characteristics of any dopants would change dramatically. By performing the LOCOS process first, we were able to maintain the same process flow for the remainder of the device.

b) Barrier Layers, Silicon Etching, and Oxide Growth

As discussed earlier, when a layer of oxide is grown on top of silicon, it results in a slightly uneven dispersion of the oxide. This 55/45 (above/below) growth ratio will need to be taken into consideration so that the silicon is etched to the right depth before the wafer is annealed. However, before the silicon is etched, several layers are placed on top of the wafer, in order to protect those parts of the device that the designer wished to remain unchanged.

These layers consist of a thin layer of oxide (.01 μm), a thick layer of nitride (.3 μm) and a barrier layer (.1 μm). All of these layers serve to protect the silicon, however the nitride serves an additional purpose. The nitride layer is especially thick, because it helps inhibit the “bird beak” effect. This negative effect of oxide growth will cause the oxide to spread horizontally into the device. Once the barriers are in place, and the silicon etched, the device will resemble that of figure 3-8.

¹³ McClay

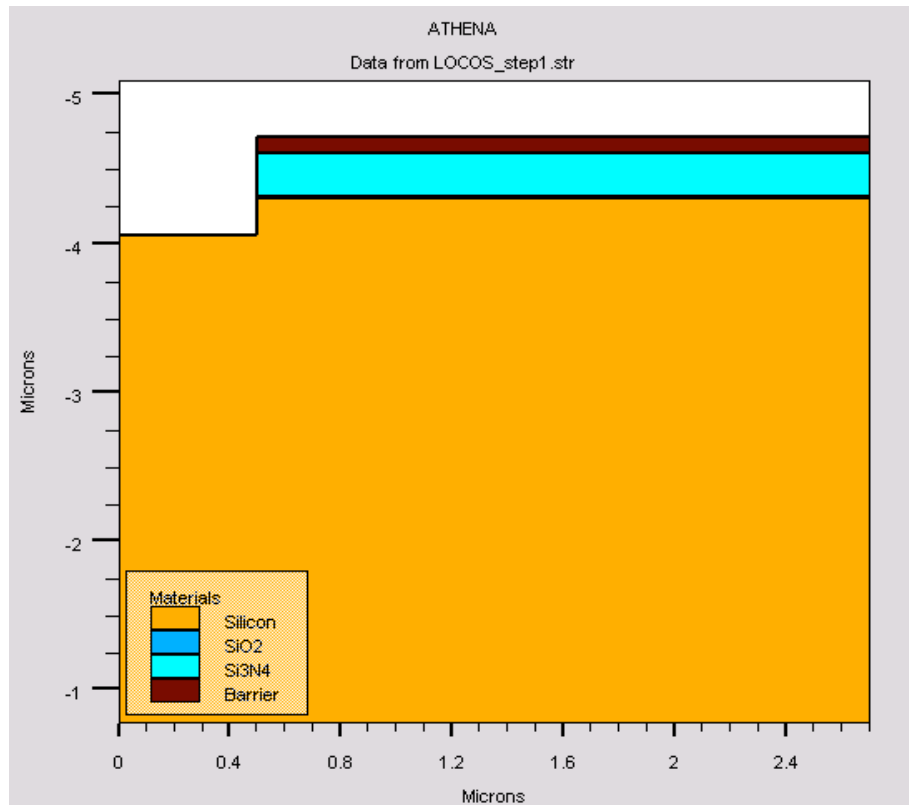


Figure 3-8 Silicon Wafer post Etching

Figure 3-8 shows the nitride layer and the barrier layer on top of the silicon wafer.

c) Oxide Growth and Final Device Geometry

The device is now annealed in a water vapor environment, at a temperature of 1200°C for a time of 60 minutes. According to figure 4-1, this should yield an oxide thickness of close to 1μm. Whether or not this is deep enough can only be determined once the device is completed, and the pn junction lines, as well as current flow can be modeled and examined. For now, the device looks like that of figure 3-9.

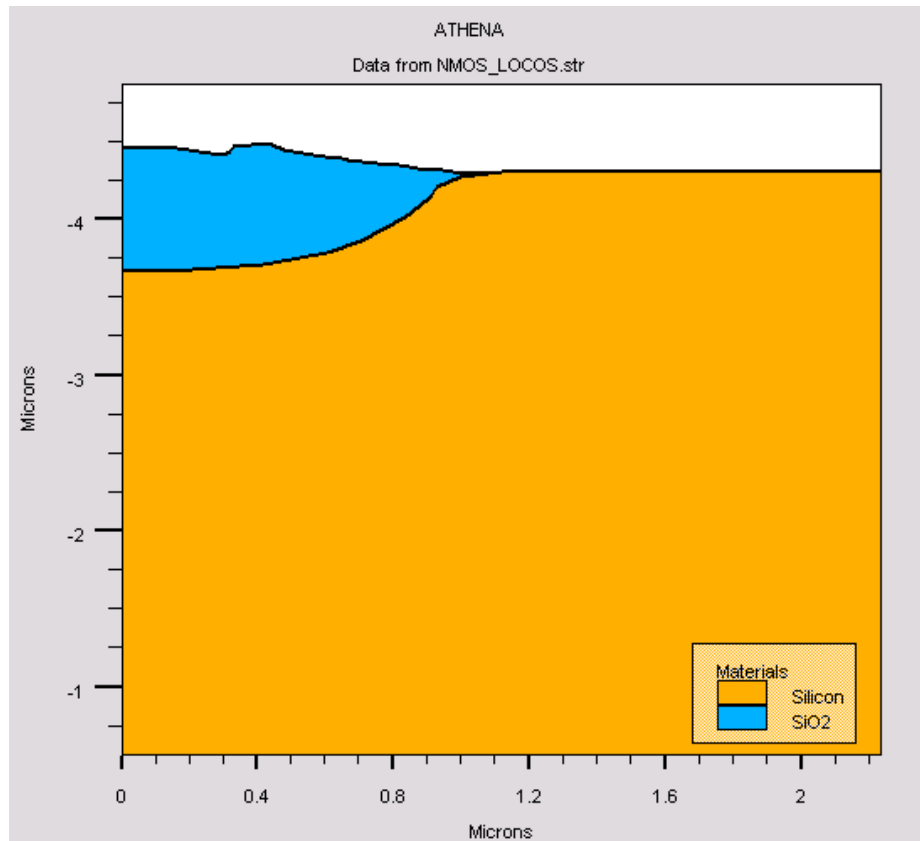


Figure 3-9 Wafer Post LOCOS Oxide Growth

Figure 3-9 shows a Tonyplot of a wafer after the LOCOS oxide growth. This step occurs after the silicon is introduced into the nitrogen atmosphere with the barrier layer.

Now that the LOCOS oxide layer is in place, the transistors can be completed following the same processing steps outlined in their respective chapters. The final devices should have all the same operating characteristics as before, however it is now isolated from any surrounding devices. Figure 3-10 shows the completed device, as well as the pn junction lines formed by the dopants in the device. As can be seen, the junction lines terminate in the oxide, meaning that any pn junction created has been successfully contained within the transistor.

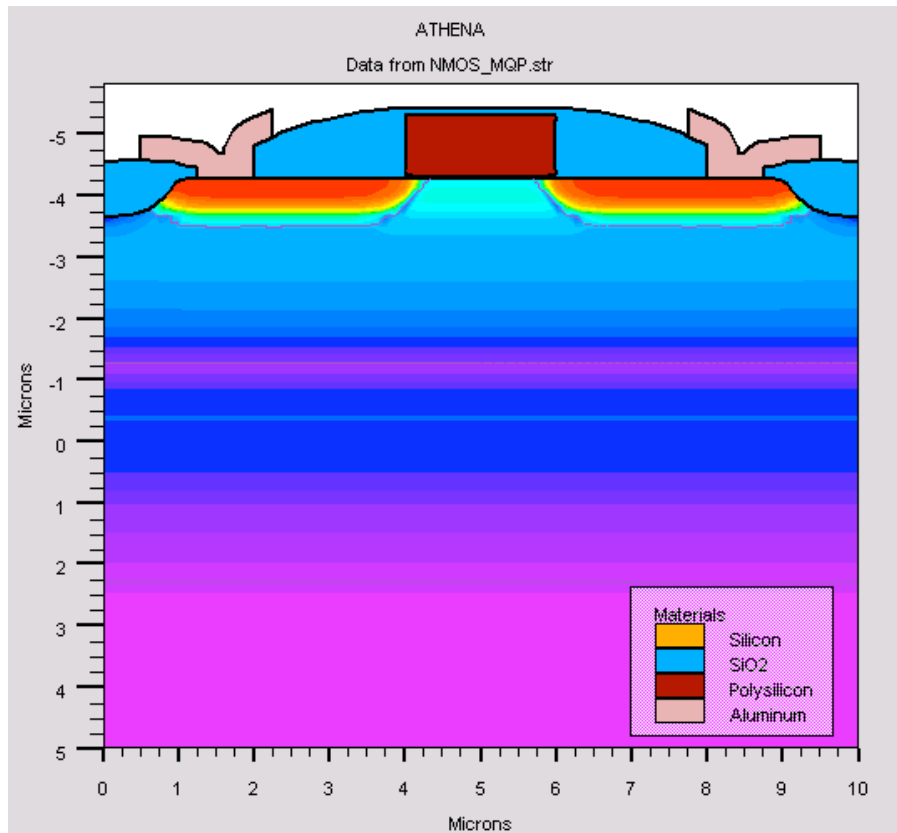


Figure 3-10 NMOS Transistor with LOCOS

Figure 3-10 is a sample of an NMOS transistor with LOCOS isolation. The junction lines terminate in the LOCOS oxide (the blue on the outside edges of the transistor). The junction lines are denoted by reddish-purple lines. They encompass both the drain and the source dopant regions.

3.3.5. Diffusion

Diffusing dopants is an important part of the fabrication process. Diffusion helps activate bonds, move surface charge, and move junction lines. When diffusing dopants, it is necessary to create a plan. Any diffusion step done early in the fabrication process can be affected by a diffusion step occurring later in the fabrication process. If an initial step is diffused to what is thought to be perfect, it may be diffused later and ruined completely.

Furthermore, when modeling an entire BCD wafer, the same precautions must be taken when compiling the individual devices. Certain diffusion steps may not exist when

modeling the individual devices. But when putting them all together, they may be additional diffusion steps that may affect the individual devices.

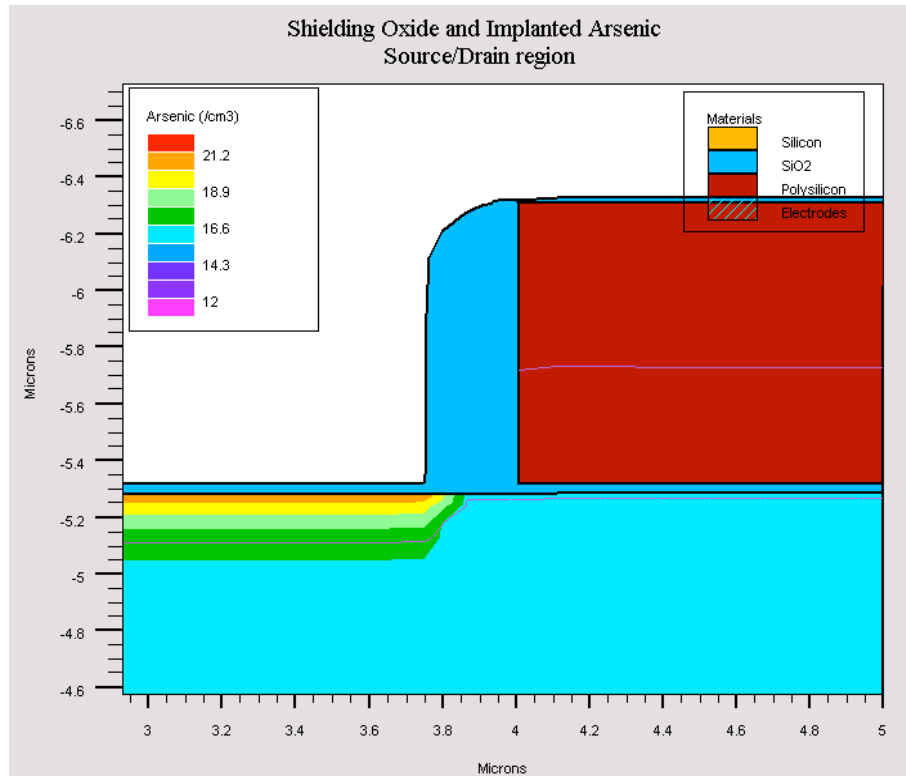


Figure 3-11 Before Diffusion

Figure 3-11 shows a MOSFET after the implantation step. Note how most of the carrier concentrations are at the surface in a tight formation.

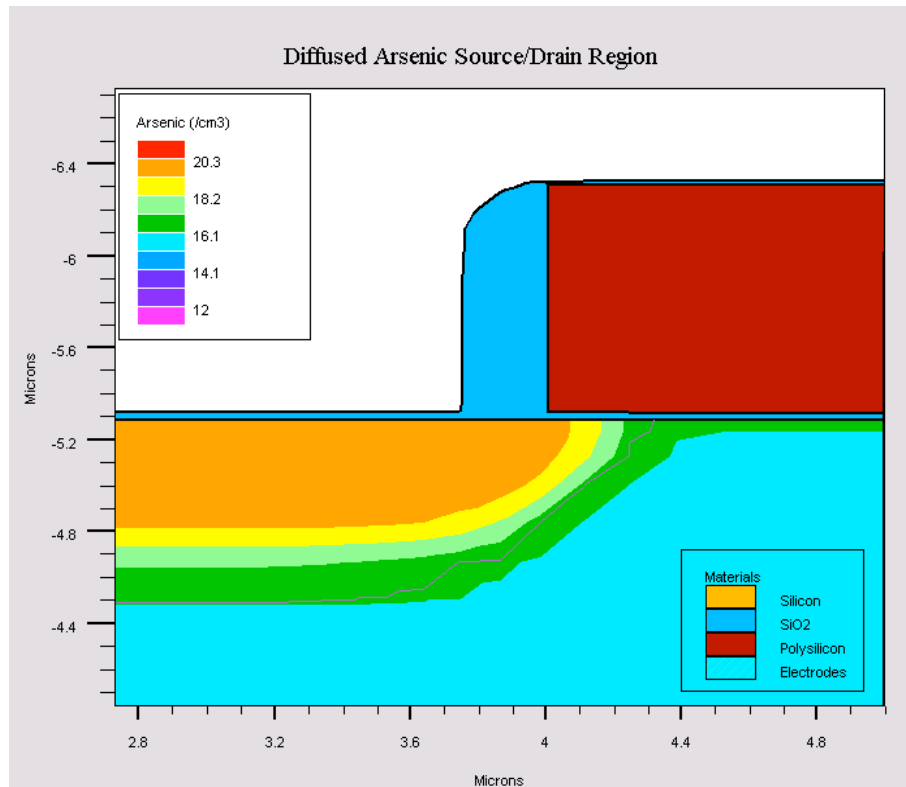


Figure 3-12 After Diffusion

Figure 3-12 shows the same picture after diffusion 3-11. Note how the surface concentrations have moved horizontally to underneath the position of the shielding oxide and the poly-silicon. Also note how the majority of the carrier concentration now lies halfway down the diffused area. Also note how the junction lines have moved. The junction lines are also less perfectly curved. This is because the junction line has been expanded and more imperfections show (much like blowing up a photograph). The dopants diffused in a gaussian distribution. It was annealed for 175 minutes 1000 degrees energy of 50 for the ion implantation. This baking process resulted in the expansion of the more than double its size.

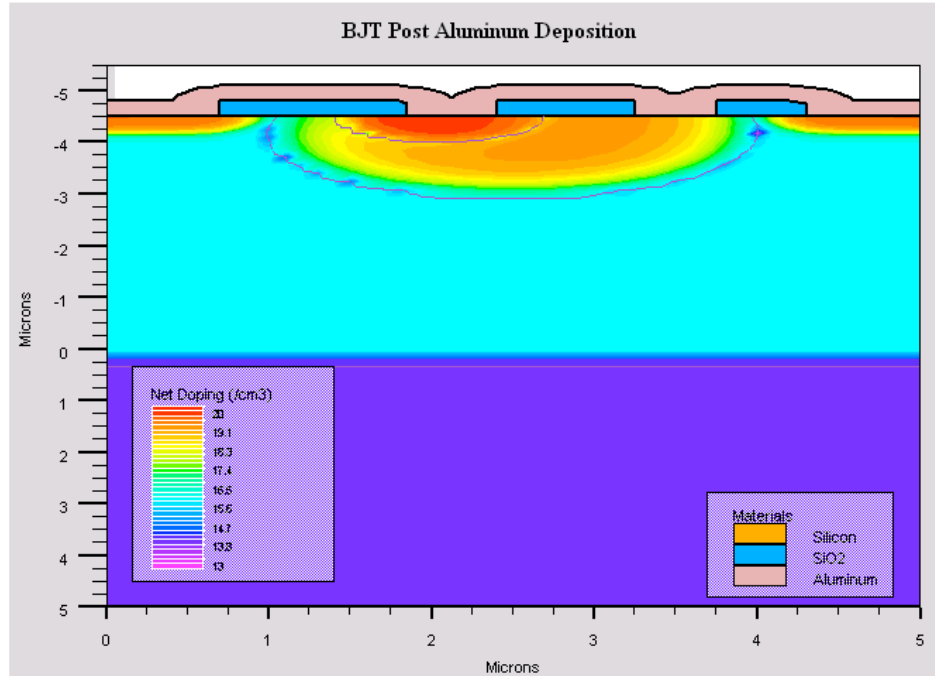


Figure 3-13 Junction Lines

This figure delineates clear junction lines. The red line going from the left oxide to the right oxide and the red line going from the left oxide to the middle oxide are both junction lines.

3.3.5. Contacts

The contacts represent the final step in the fabrication process. They are plated on top of the device and then etched away in a purposeful manner. The placement and width of aluminum contacts can have a large affect on the e-fields within the important aspects of the device. Further more, if the contacts are too short, then the device may not work at all.

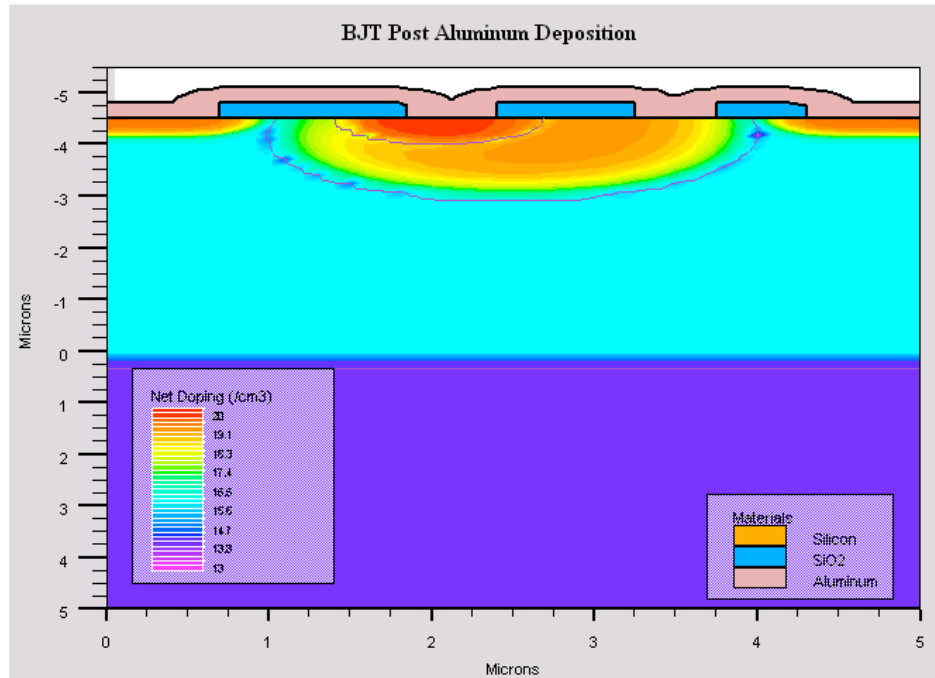


Figure 3-14 Plated Aluminum Contacts

Figure 3-14 shows how the aluminum contacts are plated at a uniform thickness over the top of the device.

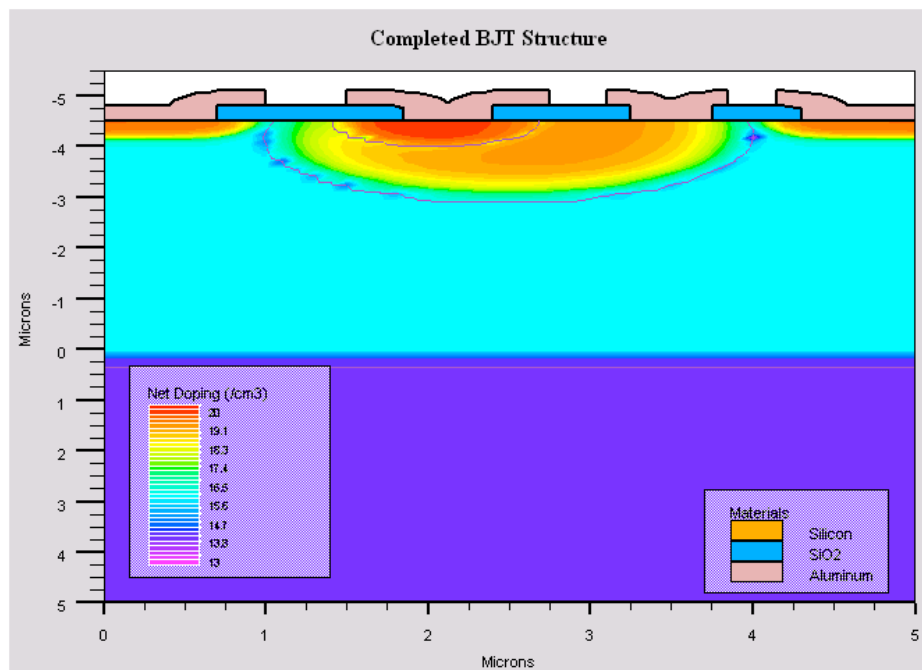


Figure 3-15 Etched Aluminum Contacts

Figure 3-15 shows the completed BJT after the aluminum contacts have been etched away. Note how the etched aluminum does not affect the other parts of the device.

3.4. Conclusion

Coding with Atlas and Athena can be a difficult process if a plan is not developed. Even with a plan, there may be some obstacles that get in the way. In the end coding with Athena and Atlas gets done by simply following a step-by-step process.

4. CMOS Transistor

The first phase of our project was to familiarize ourselves with the Silvaco software by analyzing and adapting an existing Atlas example of an NMOS transistor. By using an existing example, we were able to dissect functional code, and hopefully, rapidly increase our knowledge of how to use Silvaco for device modeling. Single changes could be made to the code, and their effects could be immediately seen through the output graphs. This allowed us to better understand the processing steps of creating a CMOS device, and in a much shorter amount of time than had we started with no example code.

Additionally, the reason a CMOS device was chosen as the first BCD device we would create was for its relative simplicity compared to an LDMOS transistor, as well as our current level of familiarity with CMOS transistors. This chapter is introduced by a concise problem statement, and then the theoretical performance characteristics. Then, a detailed process for the development of an NMOS transistor is presented. LOCOS isolation is then examined through its addition to the NMOS fabrication process. Lastly, the Atlas generated results are compared to the theoretical behavior as described in section 3.2.

4.1. *Problem Statement*

Our first goal was to modify the code so that the device would be scaled up to closer reflect the size of a BCD-III transistor. The NMOS transistor supplied in the Atlas example measured $1.2\mu\text{m}$ wide by $.8\mu\text{m}$ tall and had a gate oxide thickness of approximately $.01\mu\text{m}$. As Silvaco does not render devices in three dimensions, it is not possible to declare the desired width of the device. Rather, results that are dependant upon the width of the transistor are given as “per unit width”, typically per micrometer. Once the physical size of the device was modified, it would then be our goal to change enough of the processing steps, like ion implantation energy, diffusion lengths, oxide thicknesses, etc., until we achieved a transistor that exhibited real world operating characteristics. Both an NMOS and a PMOS transistor were to be attempted during the first stage of our project.

4.2. Theoretical Device Characteristics

In addition to the physical parameters taken from Jim McClay's¹⁴ research, it was important that we establish which family of BCD devices our transistor would belong to. After some thought, it was decided that the BCD-III family would be a good fit for our purposes, as it was physically large enough that issues such as sheet resistance and parasitic capacitances would not play a large adverse role in the functionality of our finished transistor.

Additionally, in order to obtain these characteristics, we spent time during our research focusing on the key equations and charts for parameters such as the threshold voltage, I-V curves, diffusion depths, and oxide thickness. This information would allow us to intelligently manipulate the Atlas example, and analyze our results to notice any deviancy from the ideal.

4.2.1. Oxide Thickness

As the following graph shows, the oxide thickness varies almost linearly over a logarithmic time versus thickness coordinate system. A dry oxygen environment will yield oxide growth at a slower rate than in the presence of water vapor, so the oxidation time should be adjusted accordingly.

¹⁴ McClay

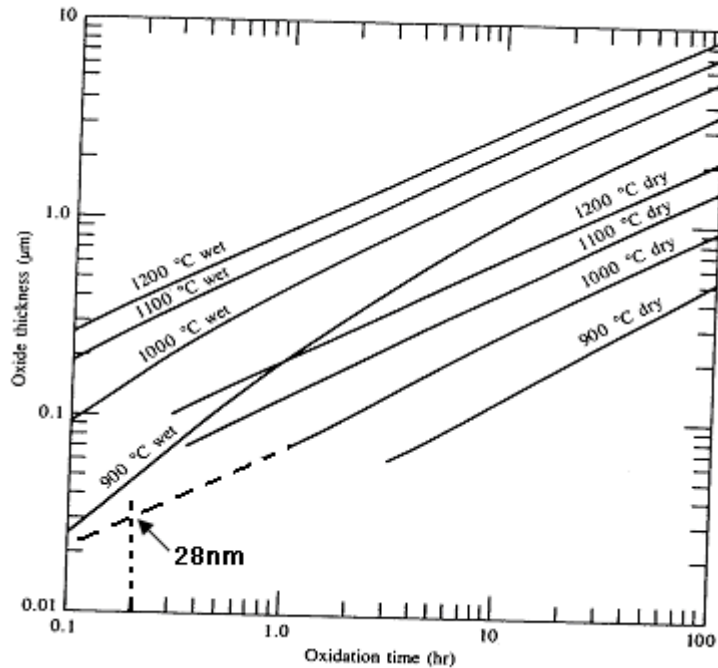


Figure 4-1: Oxidation thickness versus time for wet and dry O₂

Figure 4-1 shows an oxidation thickness versus time for annealing oxide in both a wet and dry process. Note where the dotted line of the 1000 °C line meets with the annealing time of 12 minutes.¹⁵

The BCD-III requirement of a 28 nm gate oxide means that if we were to use a dry oxygen environment, at a temperature of 1000 °C, then we would need to let the oxide grow for a total time of approximately 12 minutes.

4.2.2. Threshold Voltage

Having the correct gate oxide thickness is crucial, because it plays the largest role in the determination of the transistor's turn-on voltage. The capacitance induced by the gate oxide is what largely determines the amount of charge needed at the gate, in order to create the conductive channel to connect the drain and source. The equations controlling this behavior are:

$$\phi_f = -\frac{kT}{q} \ln\left(\frac{N_D}{n_i}\right) \quad \text{Equation 1}$$

¹⁵ Introduction to Microelectronic Fabrication pg 34.

$$V_T = 2\phi_F - \frac{K_S x_o}{K_O} \sqrt{\frac{4qN_D}{K_S \epsilon_0}} (-\phi_F) \quad \text{Equation 2}$$

Where $2\phi_F = \phi_S = \text{energy required for channel inversion}$

Description	Symbol	Value
Thermal voltage @ $T = 300K$	$\frac{kT}{q}$.0259 V
dielectric constant of Si	K_S	11.9
dielectric constant of SiO ₂	K_O	3.9
gate oxide thickness	x_0	28nm
donor concentration at surface of silicon	N_D	1×10^{18}
intrinsic carrier concentration	N_i	1×10^{10}
permittivity of free space	ϵ_0	8.85×10^{-14}

Table 4-1: Threshold Voltage Symbol Explanation

Table 4-1 explains the first two equations.

Based on these equations, if our final device has the same doping characteristics, than the turn-on voltage should be approximately .91 volts. In order to achieve this value, we must be careful to properly dope the source and drain regions so that the donor concentration is as close to $1 \times 10^{18}/\text{cm}^3$ as possible. These regions are shown in figure 3-3, on page14. Then, once the device is simulated, and the turn-on voltage observed, adjustments can be made.

4.2.3. I-V Characteristics

When fabricating a CMOS device, the drain current versus drain voltage relationship is an essential consideration. By fixing the gate voltage at separate voltage levels, and then swinging the drain voltage over a range of values, the drain current should increase asymptotically up to its saturation limit, I_{Dsat} . I_{Dsat} occurs when the drain voltage equals its saturation level, $V_{Dsat} = V_G - V_T$, and is given by the equation:

$$I_{Dsat} = \frac{Z \bar{\mu}_n C_0}{2L} (V_G - V_T)^2 \quad \text{Equation 3}$$

Description	Symbol
<i>Saturation Current</i>	I_{Dsat}
<i>Effective Carrier Mobility</i>	$\bar{\mu}_n$
<i>Capacitance per unit Area of the gate</i>	C_0
<i>Channel Width</i>	Z
<i>Channel Length</i>	L
<i>Threshold Voltage</i>	V_T
<i>Gate Voltage</i>	V_G

Table 4-2: Saturation Current Symbol Explanation

Table 4-2 explains the variable entailed in equation 3.

Ideally, this value would remain constant as V_D exceeds V_{Dsat} . However, due to device non-idealities, such as leakage current from the drain to the body, the actual drain current will slightly exceed the predicted saturation current for larger values of drain voltage, $V_D > V_{Dsat}$.

Additionally, for digital switching applications, designers would prefer that the increase in drain current vary linearly with the increase in gate voltage applied. That way, the drain voltage could be held constant, and the current varied linearly with the gate voltage. However, for long channel devices such as this, the behavior of the drain current is governed by the square law, $(V_G - V_T)^2$, and therefore this request cannot be met.¹⁶

4.3. Walkthrough of CMOS Fabrication

Now that the main operating characteristics of the CMOS device have been established it is time to use Silvaco to fabricate a device with operating characteristics as close to these as possible. Additionally, Silvaco will reveal to us how the device should actually behave, and we will be able to use these results and compare its actual operation,

¹⁶ Analog Integrated Circuit Design

to its predicted theoretical operation. The following procedures were used to create an NMOS transistor, using both Athena and Atlas software packages.

CMOS Design Flow Chart

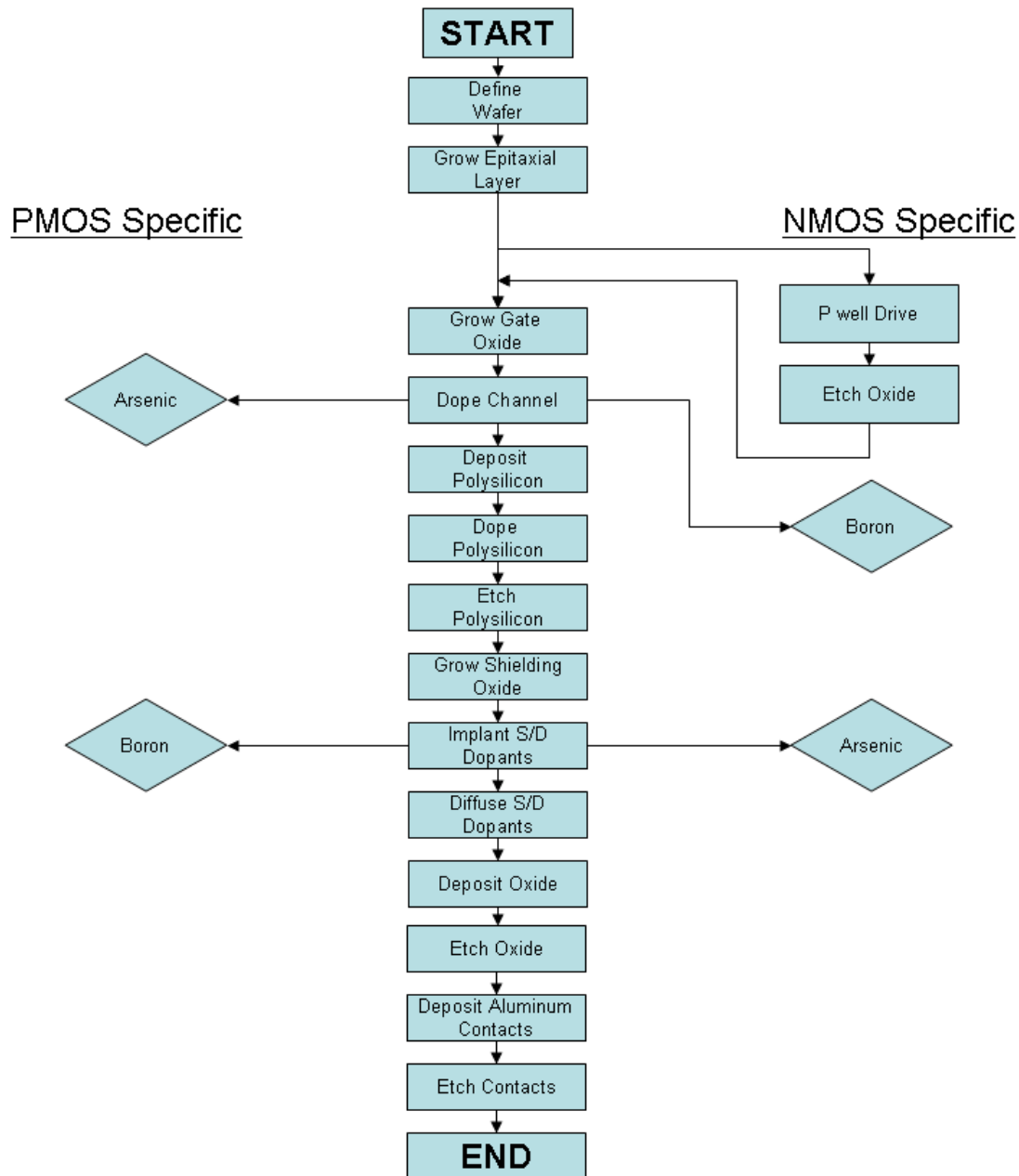


Figure 4-2: CMOS Design flow chart

Figure 4-2 shows the design recipe for the CMOS design. Both the PMOS and NMOS share similar steps. For the NMOS, there is an additional P-well drive added.

This is because of the n doped epitaxial layer. Also note that the arsenic and boron

doping stages of the NMOS and PMOS are switched. This is because each has a differently doped channel, and the other steps interfere with the order of processing steps.

4.3.1. PMOS Fabrication Summary

One of the goals of BCD fabrication is to simplify the processing of similar devices, and concurrently fabricate bipolar, CMOS, and DMOS devices. For this reason, the NMOS and PMOS transistors share almost exactly the same processing steps. This report will detail the fabrication of an NMOS transistor from the initial wafer, through to completion. The steps shown in Figure 4-7 through Figure 4-10 are representative of the development of both a PMOS and NMOS device. The difference between the NMOS and PMOS devices arise from the different dopants that are used throughout fabrication, and not the actual processing steps, or order thereof. Table 4-3: CMOS Masking Steps shows the main masking steps for the CMOS transistors, and Figure 4-3 and Figure 4-4 show simplified versions of the NMOS and PMOS transistors.

Steps	Name	Dopant Type	Type	Concentration	
1.	Wafer	Boron	P-Type	$1e14/cm^3$	Substrate
2.	Epitaxy	Arsenic	N-Type	$1e16/cm^3$	Grown Region
3.	PWell	Boron	P-Type	$8e12/cmA^3$	Implant
4.	Device	Oxide			Grown/Active Region
5.	Poly Silicon	Phosphorous	N-Type	$3e13/cm^3$	
6.	P-plus	Boron	P-Type	$1e20$ surface conc. @ $5e15$ dose	Implant
7.	N-plus	Arsenic	N-Type	$1e20$ surface conc. @ $5e15$ dose	Implant
8.	Contact	Aluminum(99%) Silicon(1%)			Deposited
9.	Metal	Aluminum(99%) Silicon(1%)			Deposited

Table 4-3: CMOS Masking Steps

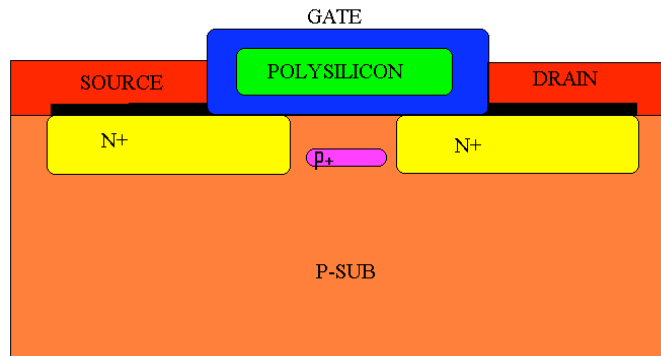


Figure 4-3: N-Channel MOSFET Device

Figure 4-3 is a color coded representation of the NMOS transistor. Each color of the device correlates to a processing step from table 4-3.

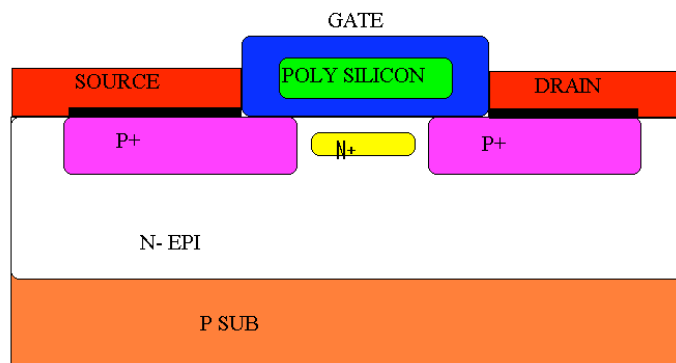


Figure 4-4: P-Channel MOSFET Device

Figure 4-4 is a color coded representation of the PMOS transistor. Each color of the device correlates to a processing step from table 4-3.

4.3.2. NMOS Device Process

Figure 4-4 and 4-5 show the NMOS and PMOS processing steps. The two devices share many of the same processing steps, however they have complementary doping profiles. Additionally, the PMOS transistor lacks the P-well drive that is present in the NMOS fabrication process. The initial fabrication step is declaring the type of

silicon wafer on which the BCD devices will be produced. Our BCD wafer is of P-Type silicon, with a Boron concentration of $1 \times 10^{14}/\text{cm}^3$. Next, an N-Type epitaxial layer is grown on top of the silicon. Arsenic is used as the N-Type dopant for this layer, with a concentration of $1 \times 10^{16}/\text{cm}^3$.

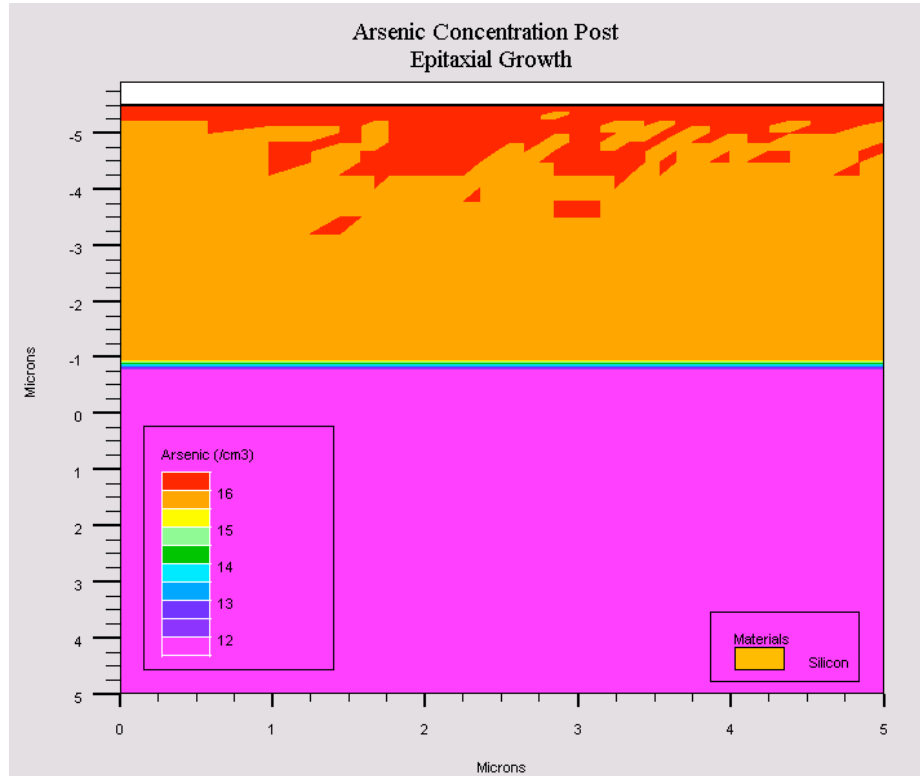


Figure 4-5: P-Type wafer with Arsenic Epitaxial Layer

Figure 4-5 shows the epitaxial layer of the N channel MOSFET.

As this will be an NMOS device, the channel will need to be of a P-type majority, so that the proper NPN device structure can be achieved. Boron will be diffused into the epitaxial layer, using a two step process of implantation and then diffusion. Ion implantation is used to generate a large amount of charge close to the surface of the wafer, and then a near eight hour diffusion step, at temperatures ranging from 950 °C to 1200 °C, will diffuse the boron down throughout the device. This will change the wafer from N-type to P-type, and allow for the creation of an NMOS transistor.

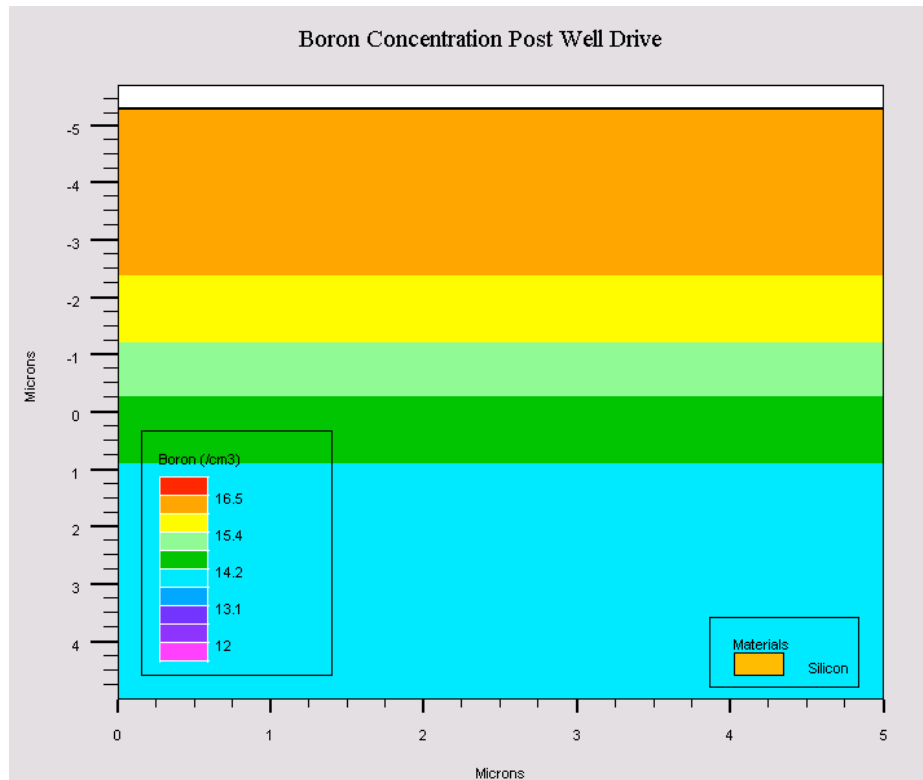


Figure 4-6: Boron Well Drive

Figure 4-6 shows the addition of a boron well drive into the NMOS. This step occurs after the epitaxial layer is deposited.

The next processing step is to grow the thin gate oxide across the top of the silicon. Our device uses an oxidation time of 10 minutes, and a temperature of 1035 °C. Then, in order to concentrate the flow of current through the channel, a high concentration of Boron is implanted near the surface of the device. Once the n^+ regions are diffused into the transistor this p-channel should help prevent the leakage of current out the substrate of the transistor. Ion implantation is used to deposit the Boron near the surface of the wafer, and in this case, there will be no explicit diffusion step. Instead, the diffusion time and temperature of the n^+ regions will be used to diffuse the Boron. This will ensure that the Boron layer is as concentrated as possible in the channel.

Next, the polysilicon gate can be deposited on top of the gate oxide. Based on the dimensions of the NMOS transistor in Jim McClay's research, a polysilicon of 1 μm tall and 2 μm wide was created. In order to achieve this, a 1 μm thick polysilicon is deposited across the entire surface of the silicon. As is common practice, the polysilicon is doped with phosphorous in order to assist its conductance. A $3 \times 10^{13}/\text{cm}^3$ dose of phosphorous is used to achieve the polysilicon doping. Additionally, it is best to dope the polysilicon before it is etched away, as this will prevent the implantation of undesired dopants into the n^+ regions. Once doped, the polysilicon is etched away everywhere except for above the eventual device channel. Figure 4-7 shows what the device looks like after the gate oxide has been grown, and the polysilicon deposited (*Note: because the NMOS transistor is a symmetric device, only half of the device is simulated and the device is then mirrored across the y-axis.*):

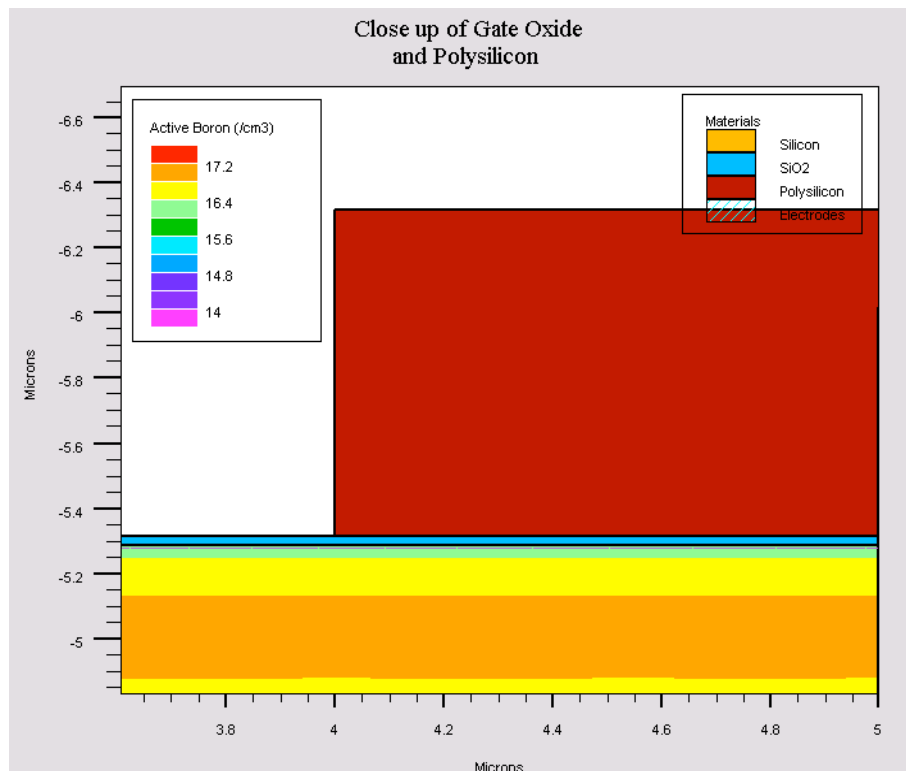


Figure 4-7: Upper surface of NMOS transistor

Figure 4-7 shows the surface of the NMOS after the application of the first gate oxide as well as the deposition of the poly-silicon layer.

As diffusion has the unwanted effect of spreading dopants laterally across the device, it is necessary to control where the Arsenic is implanted. This will be accomplished through the deposition of an SiO₂ layer on either side of the polysilicon (Figure 4-8). This will provide a buffer between the channel region, and the implanted Arsenic, so that when the diffusion step occurs, the lateral diffusion will not carry Arsenic too deeply into the channel. As BCD-III devices require a channel length of 1.2 μm , it will be important to deposit the proper size oxide in order to achieve the desired channel length.

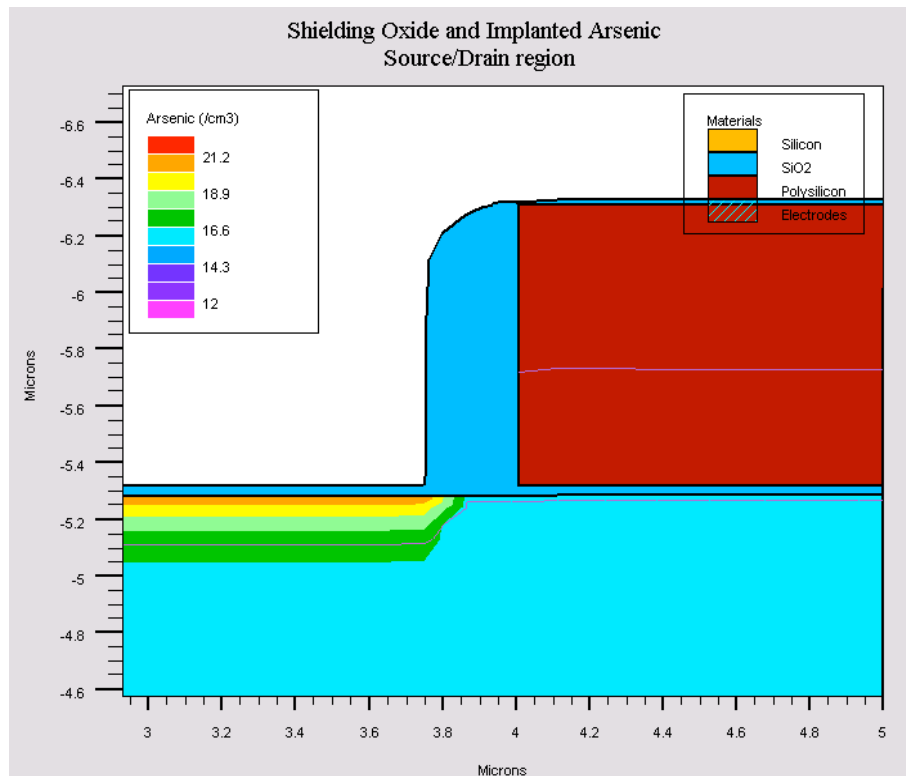


Figure 4-8: Implanted Arsenic and grown shielding oxide

Figure 4-8 shows the deposition of the 2nd gate oxide layer. More importantly, it shows the arsenic donor concentration of the source.

Once this “shielding oxide” has been deposited, the next stage of the process is to deposit the n⁺ regions into the silicon. Arsenic will be used and ion implantation as well as diffusion will be used to deposit the carriers at the surface of the silicon. As ion implantation results in a Gaussian distribution of dopant ions, it is important that the peak concentration be at the surface of the silicon. An energy of 50 keV combined with a dose of $5 \times 10^{15}/\text{cm}^3$ will deposit more than enough electrons at the surface of the wafer.

Once the ions have been implanted, a diffusion step of 175 minutes at a temperature of 1000 °C will activate the bonds between the arsenic ions and the silicon crystal, as well as diffuse the arsenic deeper into the device.

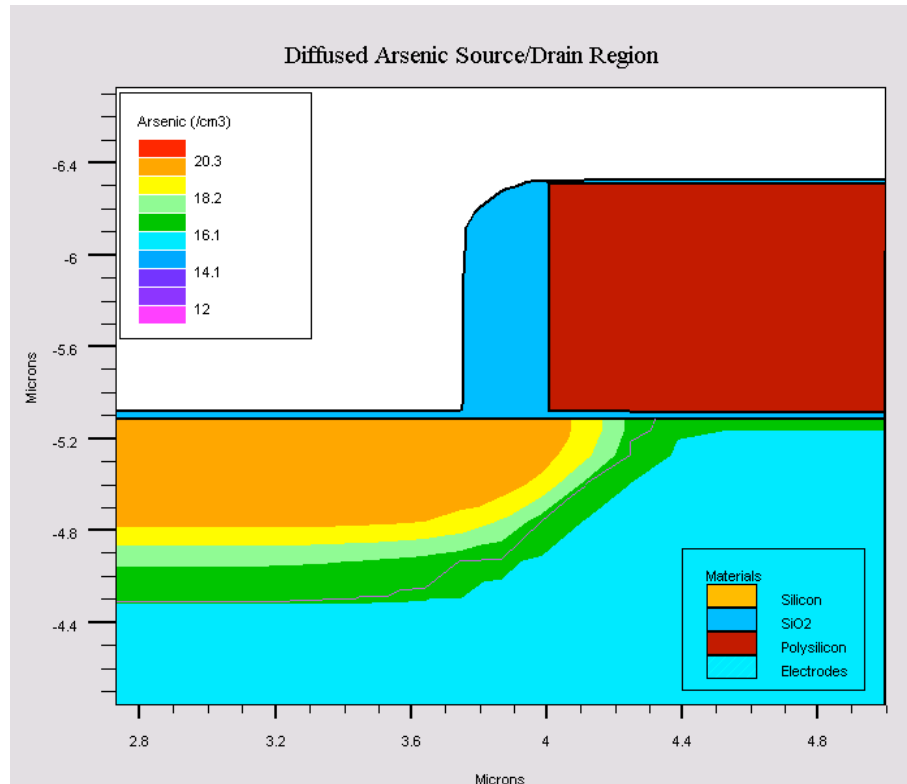


Figure 4-9: NMOS transistor after Arsenic Diffusion

Figure 4-9 shows the near complete NMOS transistor. The n^+ region has been deposited beneath the exposed silicon, and is awaiting the diffusion step described above. Once completed, a protective oxide will be deposited over the remainder of the transistor. An etching step then removes the oxide from the far sides of the transistor, in order to make room for the aluminum contacts. The contacts are deposited in much the same way. Aluminum is deposited over the entirety of the surface of the transistor, and then is etched away everywhere except for where it is desired. In order to prevent any kind of excess capacitance between the source/drain and the channel, the contacts are kept far away from the channel, and only need be big enough to supply a connection to the source and drain.

Figure 4-10 shows the completed, and mirrored, NMOS transistor. At this point the physical construction of the device is complete, and Athena need no longer be used.

Atlas will be used from here on out, in order to obtain device characteristics, such as those described in sections 4.2.1 through 4.2.3.

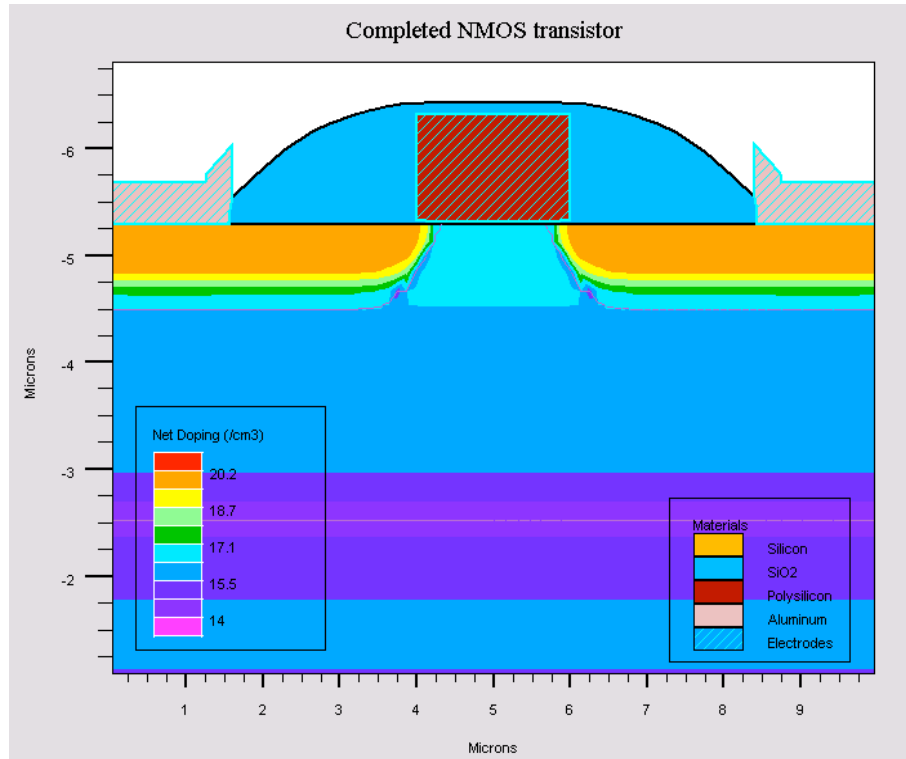


Figure 4-10: Completed NMOS transistor

Figure 4-10 shows the completed NMOS transistor. The slashed lines denote the electrodes of the device.

4.4. Final Device Characteristics and Comparison

Before the NMOS is considered to be complete, we must first use Atlas to analyze and characterize its behavior. Atlas is an extremely powerful tool that allows for the extraction of device parameters, as well as the ability to apply potentials to the source, drain, and gate and measure their corresponding impact on the device.

4.4.1. Gate Oxide

As stated in section 4.3.2, to achieve the proper size gate oxide, we performed an oxidation step at a temperature of 1035 °C for a time of 10 minutes. Using the graphs generated in TonyPlot, we were able to determine that the resulting oxide thickness was very close to 29 nanometers. This is reassuring, as it matches up nicely with the desired oxide thickness of a BCD-III family device. Unfortunately, at 1000°C, the reference of

Figure 4-1: Oxidation thickness versus time for wet and dry O₂, does not provide a defined line for an annealing time of 10 minutes. However, by extrapolating, it can be determined that the predicted oxide thickness should be approximately 30-35 nm.¹⁷ This value correlates quite nicely with the value we obtained through the Athena simulation software.

4.4.2. Threshold Voltage

In order to establish what the turn-on voltage of the transistor is, the gate bias versus conductivity was plotted. Based on the graph it was possible to determine at which voltage the transistor would turn on, and begin conducting current. Figure 4-11 shows the conductivity versus bias relationship that we attained with the device, and it can be determined that the transistor will turn on at approximately .8 V. More specifically, equations 1 and 2 can be used to calculate the predicted turn-on voltage.

Our final device had n⁺ regions doped with a donor concentration of approximately $1 \times 10^{20}/\text{cm}^3$ near the surface of the wafer. Additionally, our oxide thickness is 29 nm. By plugging these numbers into the two equations, we get a predicted turn-on voltage of .8 volts. This number is very close to our graphical approximation, and that similarity is encouraging to see.

¹⁷ Introduction to Microelectronic Fabrication pg. 34

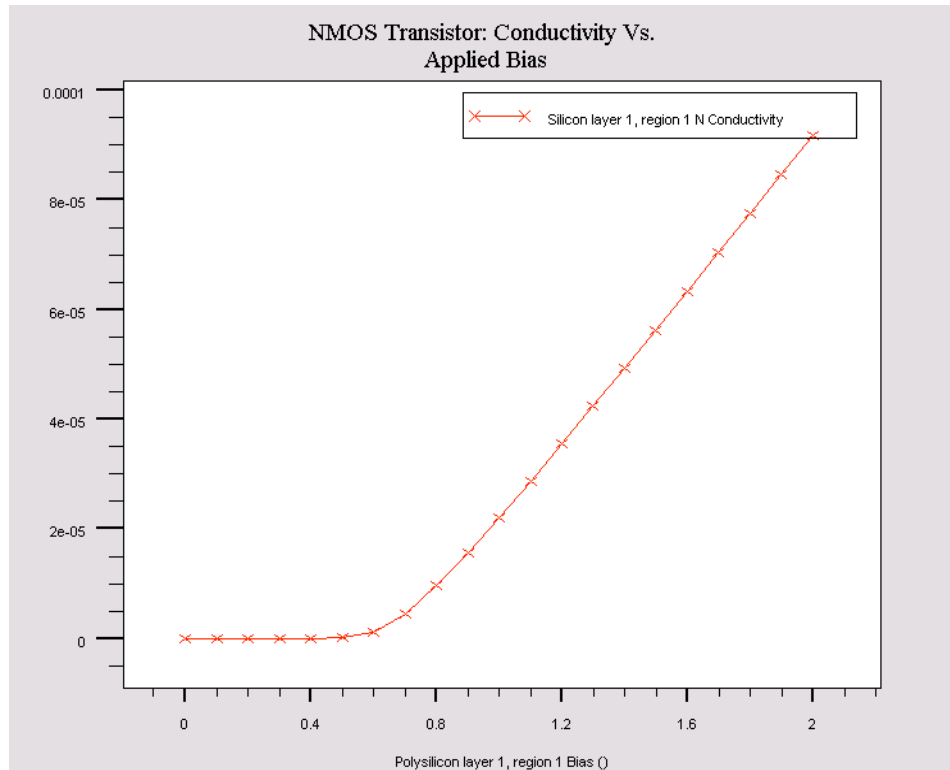


Figure 4-11: NMOS Conductivity versus Gate Bias

Figure 4-11 shows the conductivity versus bias curve for the NMOS transistor. Note the turn on voltage of around .8 volts.

4.4.3. I-V Relationship

The I-V curves obtained from the NMOS transistor give a good indication of the performance of the device. Figure 4-12 shows the I-V curves that were obtained from our device. Gate voltages of 1.5 V, 2.5 V, and 3.5 V were applied to the transistor, and the drain current was graphed as a function of the applied drain voltage. The generated curves resemble theoretical I-V curves, and the drain current increases up to its saturation point, however, device non-idealities allow the drain current to keep increasing, rather than asymptotically approach I_{Dsat} .

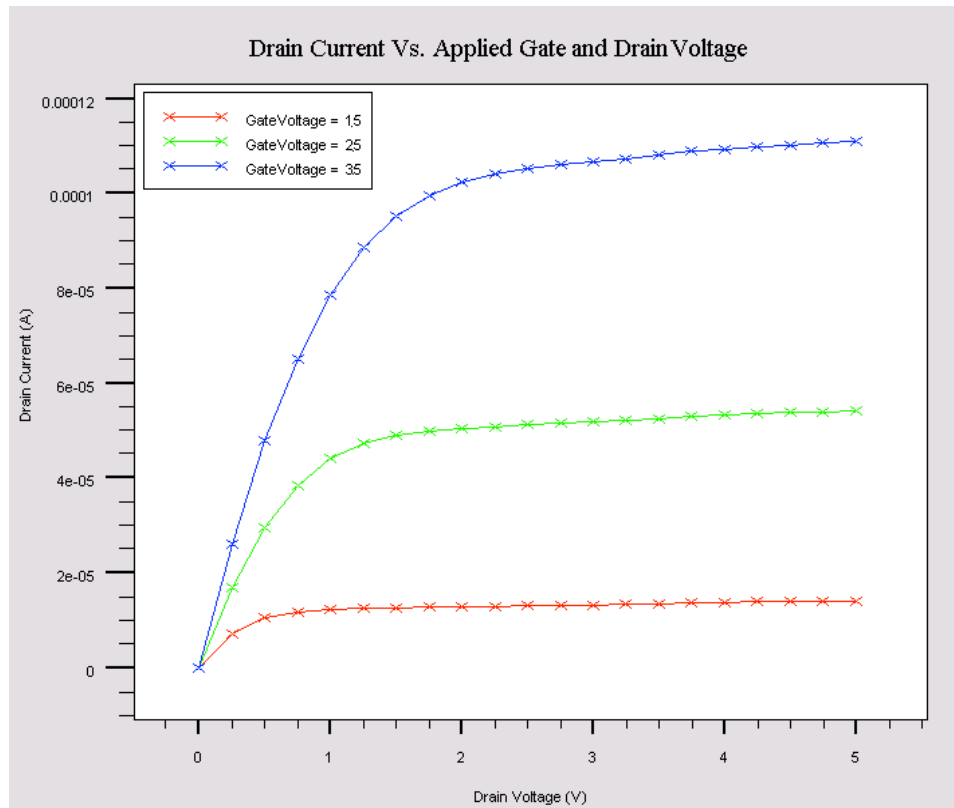


Figure 4-12: I-V Curve for NMOS transistor

Figure 4-12 shows the I-V curves for the NMOS transistor at applied gate voltages of 1.5V, 2.5V, and 3.5V respectively. Notice the non-zero linear slope as the in the active region. This is created because of pinch-off, a common characteristic of MOSFET's.

4.5. Conclusion

Performing the software development of an NMOS transistor has allowed us to gain valuable insight into the real world problems that must be considered, such as the ideal order in which the processing steps should be conducted. Silvaco proved to be a challenging, but not overwhelming software package, and it is extremely powerful in its ability to extract numerous device characteristics. With more practice, we will soon have completed a PMOS device, BJT, and LDMOS.

Additionally, we found that the NMOS device characteristics matched their theoretical prediction quite nicely. Both the threshold voltage and gate oxide were within acceptable margins of error from their predicted values, 15%. After speaking with professionals in the semiconductor industry, we have learned that the models created by

Silvaco should very accurately match their physical counterparts, and it can serve to highlight the discrepancies that arise between the theoretical and the actual.

5. Bipolar Junction Transistor

After the completion of the CMOS device fabrication, the focus of the project shifted to creating a bipolar junction transistor (BJT). While Silvaco offered several BJT examples from which we could model this device, none of them represented the lateral BJT structure which we intended to create. Being unable to adapt an existing model, our Silvaco abilities were greatly tested with the creation of a wholly new device. We were unable to perform slight code modifications and observe their effects, as was done for the CMOS transistor, so knowledge of the BJT device geometry played an important role in the fabrication of this device. An example was used as a guide for the fabrication process.¹⁸

This chapter is presented in much the same way as chapter 4. A detailed problem statement is given, followed by theoretical device behavior and the fabrication process. Lastly, the generated results are compared to the theoretical behavior of the device, as presented in section 4.4.

5.1. Problem Statement

The problem presented by the BJT was much the same as that of the CMOS transistor: Create a functional device that performs to the specifications of the BCD-III family of devices. The main difference for this device, however, was our inability to modify an existing example, so careful device planning was performed.

During the initial planning of the device, it was decided that the BJT would measure $5\mu\text{m}$ wide by $9.5\mu\text{m}$ tall. Again, Silvaco does not explicitly declare the width of the device, rather, it gives results in a “per unit area” manner. These dimensions were chosen for the following reasons. The width of the device was selected so that it would be half the size of the CMOS transistor. The relative simplicity of a BJT allowed for the physical size to be reduced without incident. Additionally, at a size of $5\mu\text{m}$ (relatively large for modern devices), there would not be any issues, such as latch-up, that would

¹⁸ Zambuto pg 335

need to be considered. 9.5 μ m represents the approximate height of the devices presented in Jim McClay's report.¹⁹

5.2. Theoretical Device Characteristics

Much the same as the CMOS transistor, the BJT must conform to the characteristics of the BCD-III family of devices, as defined in Table 2-1. Additionally, measurements such as the Gummel plot, as well as the I-V characteristics were used to ensure that the device was working properly, with as little deviation from the theoretical as possible. Silvaco is equipped with many different models that recreate real life device imperfections, so their effects are observable through the simulations that are generated.

5.2.1. Gummel Plot

The Gummel plot is used to represent the “simultaneous semi log plot of I_B and I_C as a function of the input voltage V_{EB} ”.²⁰ The value of this plot is that it will showcase the current characteristics of the BJT over a range of voltages. The figure below shows a Gummel plot with both actual and theoretical behaviors represented. Additionally, this graph will allow the extraction of key values such as the β_{dc} .

¹⁹ McClay

²⁰ Pierret pg. 424

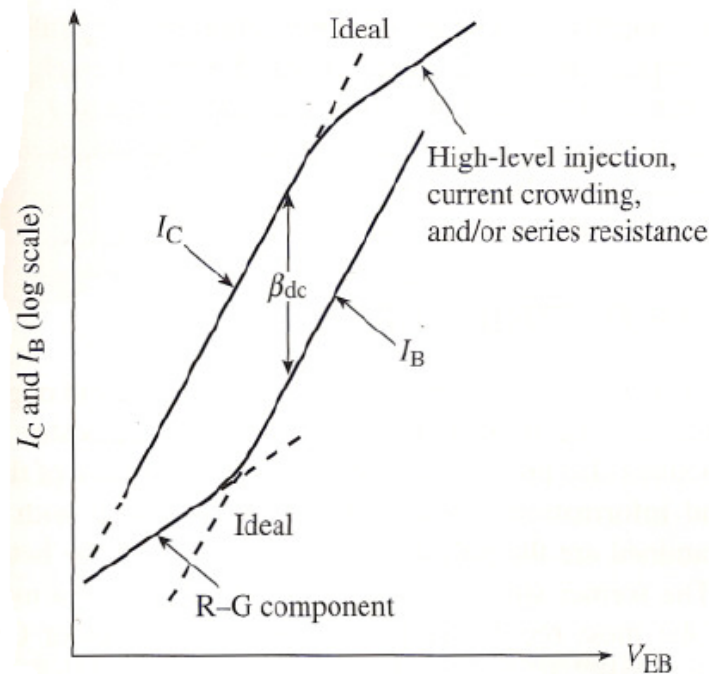


Figure 5-1: Ideal and Non-Ideal Gummel Plots

Figure 5-1 shows an ideal and non-ideal gummel plot. This is a common way to illustrate beneficial characteristics of a BJT.²¹

For a device to be considered useful in modern circuitry, the β_{dc} will need to be at least a magnitude of 10.²² This value can be easily extracted from the Gummel plot, as the y-axis represents a logarithmic scale of the current. For example, if the I_C was 1×10^{-14} mA and the I_B was 3×10^{-13} mA, then the β_{dc} is easily calculated as a magnitude of 30. Additionally, the effects of recombination-generation can be seen at low input voltages.

5.2.2. I-V Characteristics

Much like the NMOS transistor, it is desirable to generate distinct values of collector current for increasing values of the collector bias. This property can be used to generate voltage thresholds that will not significantly fluctuate with changes in V_C . By fixing the base current, and ramping the collector voltage, the device's collector current can be monitored. By repeating this for several fixed values of I_B it is possible to

²¹ Pierret, pg. 425

²² Neudeck and Pierret pg. 202

determine the characteristics over a wide range of values. Figure 5-2 shows a sample I-V characteristic for a PNP transistor.

For fast switching applications, it is ideal for the collector current to ramp up to its asymptotical limit as quickly as possible, and tradeoffs can be made for the devices performance for increasing values of collector voltage. However, for high power applications, it is vital that the collector current suffer only slight variations from its ideal value as the collector voltages continue to ramp up. For the purposes of this project, we will try to achieve a device that has good performance in both categories, however does not necessary specialize in either. Suggestions will be made that would improve the device's performance for either higher power, or fast switching applications.

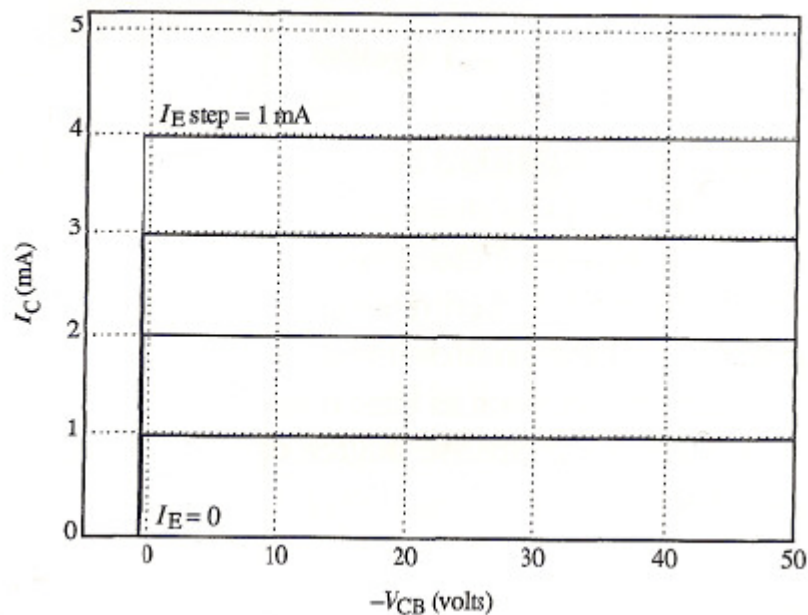


Figure 5-2: Sample Ideal I-V characteristics for a PNP BJT

Figure 5-2 shows the ideal I-V characteristic of a BJT (PNP). Note how the idea curve is a step function.²³

5.3. Walkthrough of BJT Fabrication

While the NMOS and PMOS transistors were able to use almost the same processing steps, the BJT requires several different processing steps, as well as the exclusion of many of the CMOS steps. The BJT transistor does not need the application

²³ Pierret pg. 408

of a polysilicon layer, nor does it require the growth of a gate oxide, due to the behavioral differences of a BJT. Figure 5-3 provides a recipe for the creation of a BJT device. For this section, we will examine the fabrication of a dedicated lateral BJT, and will delay its integration into a full BCD process procedure until satisfactory behavior can be achieved.

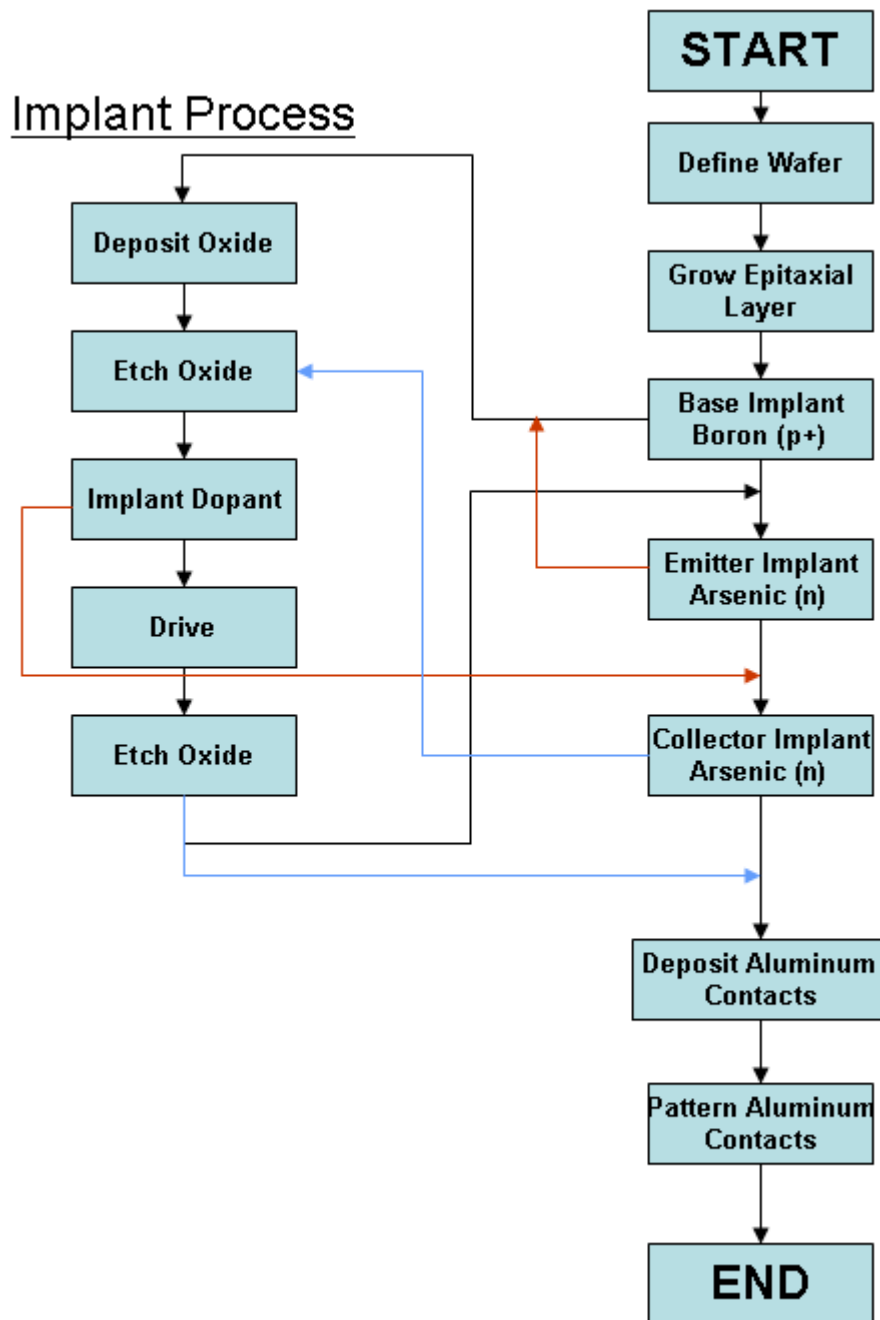


Figure 5-3: BJT Process Recipe

Figure 5-3 shows the process recipe for the BJT. Note how the subroutine of the implant process occurs every time a masking layer is needed to implant a concentration of doped silicon.

Figure 5-4, below, shows a simplified version of the bipolar junction transistor that is to be fabricated. While commonly described as a vertical structure, most BJTs created as part of a BCD process are lateral structures. This allows for a simpler integration into the BCD process as a whole, and their behavior will be very similar to their vertical counterparts. The doping will be controlled in such a way that $N_E > N_B > N_C$. Additionally, no P-well formation is required for the BJT, however, a highly doped N^+ region will need to be embedded within a highly doped P region.

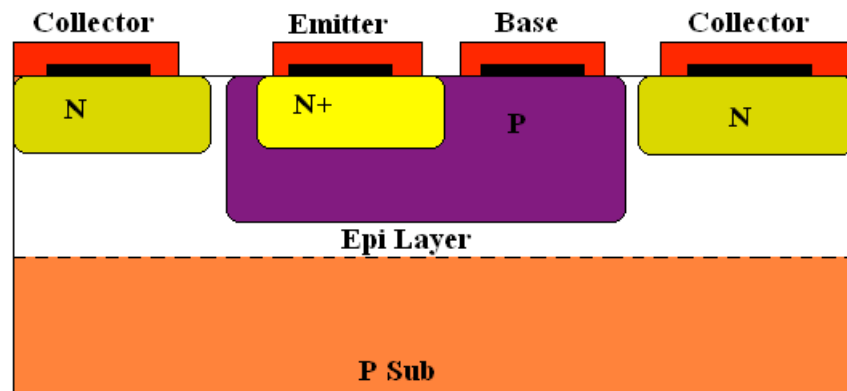


Figure 5-4: Simplified BJT Structure

Figure 5-4 shows a color coded BJT structure. Each aspect of the BJT corresponds to a process step from a process table.

5.3.1. BJT Device Process

As with the CMOS transistors, the initial step in creating the BJT transistor is to define the wafer. In order to begin to align the processing steps between the BJT and CMOS transistors, a p-type wafer was used. The wafer is moderately doped with Boron, at a concentration of $1e14/cm^3$. Next, the epitaxial layer was grown. Once again, the same profile layer was used for the BJT. The epitaxial layer is $4.5\ \mu m$ thick, and doped with arsenic, at a concentration of $1e16/cm^3$. Next, a thick layer of silicon dioxide is deposited upon the epitaxial layer. The figure below shows what the transistor looks like after these initial processing steps.

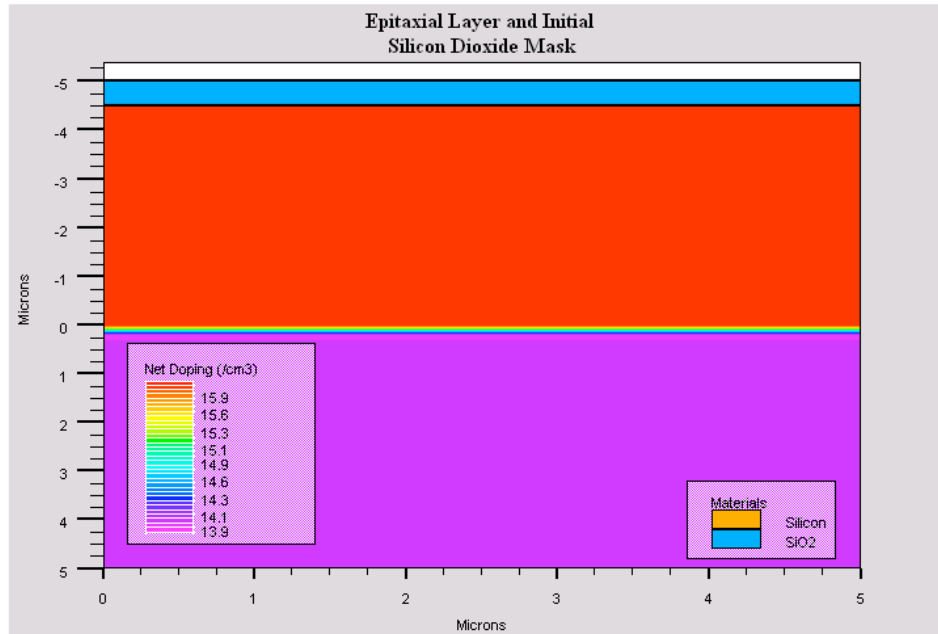


Figure 5-5: BJT after epitaxial growth

Figure 5-5 shows the BJT after the initial epitaxial growth. An oxide layer is then deposited and grown on top of the wafer.

A section of the poly-silicon can now be etched away to allow the base dopant to be implanted. Boron is used to achieve the proper p-type doping profile. As mentioned above, the desired doping profile should have $N_E > N_B > N_C$ so a dose of $5 \times 10^{15}/\text{cm}^3$ is selected. This is the same dose that was used with the PMOS transistor, in order to achieve a source/drain doping near $1 \times 10^{20}/\text{cm}^3$, however the extended annealing process required in the BJT will yield a doping lower than that of the PMOS transistor, because the boron will diffuse deeper into the device. The figure below shows the BJT after the boron has been implanted into the device and partially diffused. The reason behind the partial diffusion of the Boron is because there are annealing steps related to the emitter and collector that have not yet occurred. Because each annealing step will cause the dopants to diffuse throughout the device, the future processing steps must be taken into consideration.

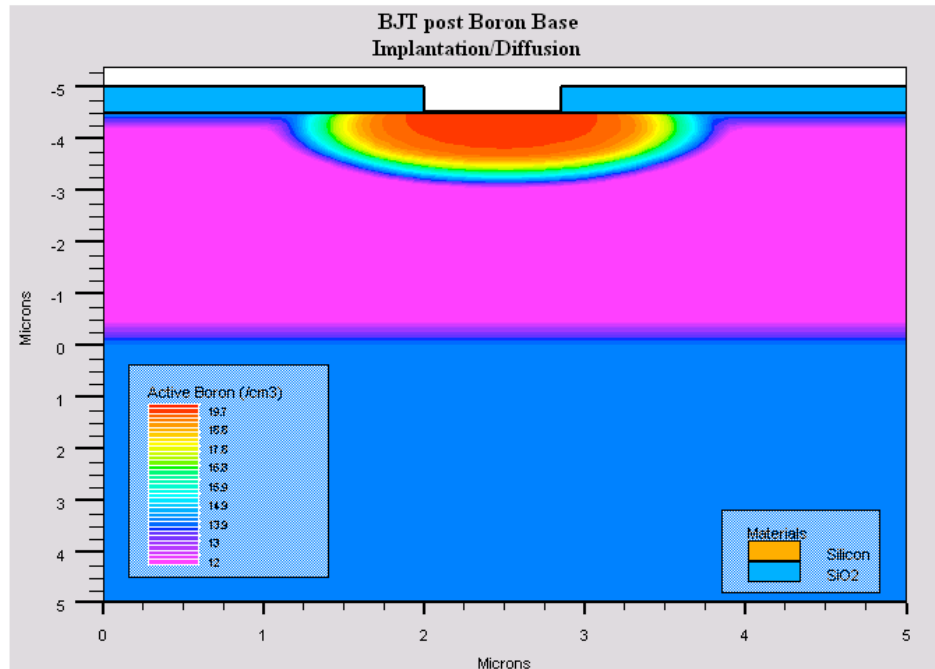


Figure 5-6: BJT post Boron Diffusion

Figure 5-6 shows a BJT after diffusing boron into the base-emitter region.

Next, the existing layer of silicon dioxide is etched away, and a new layer is added. This layer will serve to mask the appropriate sections of the BJT while the collector and emitter regions are created. As the emitter is to be the most highly doped region of the BJT, it will be created first. A section of the silicon dioxide is etched away, and arsenic is implanted at a dose of $5 \times 10^{15}/\text{cm}^3$. The reason this dose is chosen is because it yields a surface concentration near $1 \times 10^{20}/\text{cm}^3$ when moderately diffused, as demonstrated through the CMOS transistor. Normally, the next step would be to anneal the device, thereby diffusing the arsenic, however, this step will be delayed until the collector has been implanted. The reason for this is that both the emitter and collector will need to undergo similar diffusion steps, so, in order to save time in the physical construction of the device and prevent unwanted diffusion of the base, this step is combined with the collector diffusion. Figure 5-7 shows a close-up of the emitter region of the BJT. Notice that the current surface concentration is approximately $1 \times 10^{22}/\text{cm}^3$, however as the region diffuses, this concentration will decrease to its appropriate value.

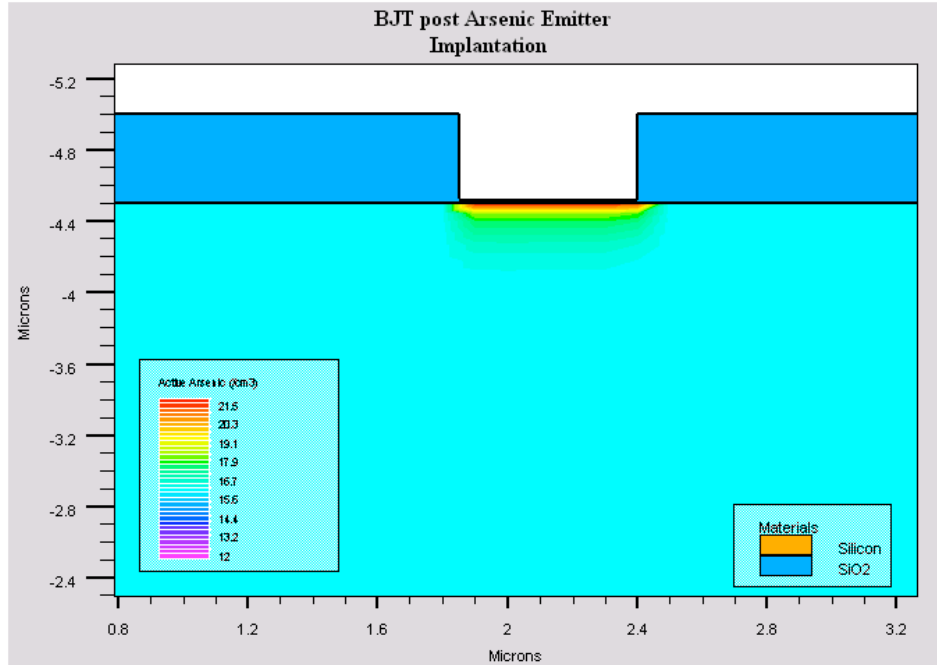


Figure 5-7: BJT post Arsenic Implantation

Figure 5-7 shows a BJT after the arsenic implantation in the emitter region.

Now that the emitter has been implanted, the collector regions can be created. Because the collector regions will be the lightest doped regions of the device, approximately ten times lighter than the emitter, a new mask need not be created. Rather, the sections of the previous silicon dioxide mask corresponding to the collector can be etched away, and the arsenic implantation step can be repeated. The collector implantation will be at a dose of $5 \times 10^{14}/\text{cm}^3$, to try and ensure that it is lighter doped than the base. The added arsenic in the emitter will not greatly increase the surface concentration, and will only help ensure that $N_E > N_B > N_C$.

Once the collector and emitter regions have been implanted, they can be diffused into the device. The BJT is annealed at a temperature of 1000°C and for a time of 180 minutes. This step occurs in a nitrogen environment, in order to prevent the growth of any unwanted silicon dioxide.

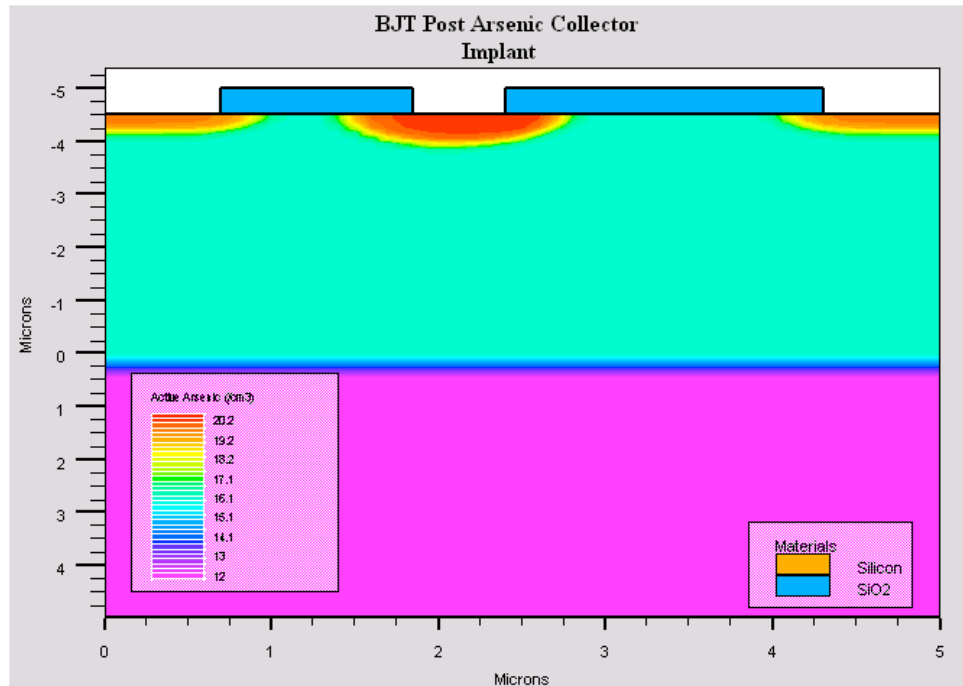


Figure 5-8: BJT Post Arsenic Collector Implant

Figure 5-8 shows a BJT after the implantation of arsenic in the collector region.

Once the annealing step is complete one final section of the silicon dioxide is etched away, in order to provide a contact to the base region. A layer of aluminum is then deposited, and the device resembles Figure 5-9. Additionally, lines denoting the device's pn junctions have been added to illustrate its NPN characteristic.

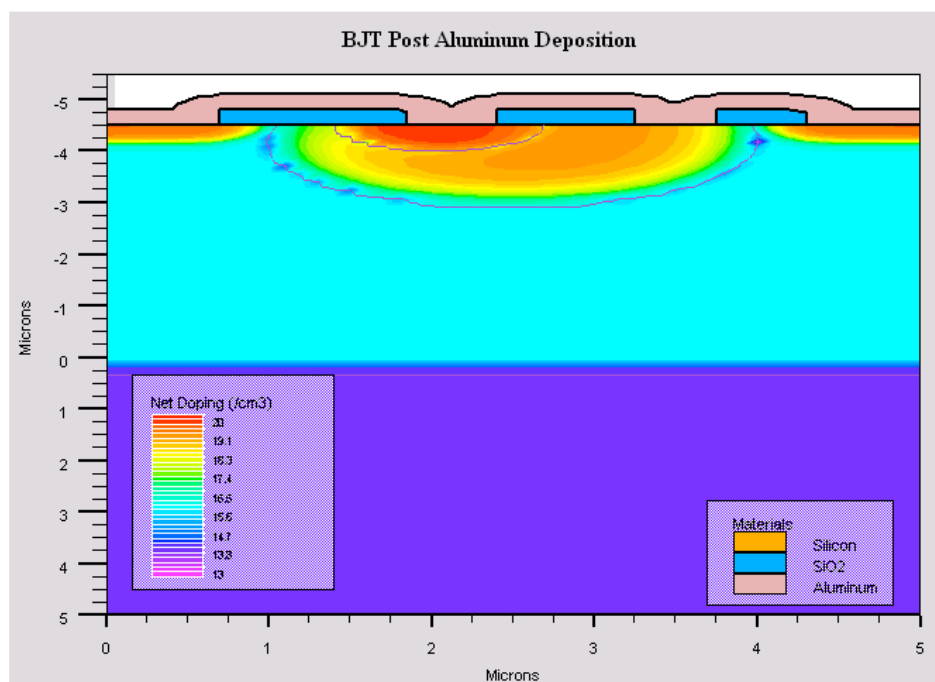


Figure 5-9: BJT Post Aluminum Deposition

Figure 5-9 shows a BJT after the aluminum has been deposited.

The final processing step is to etch away sections of the aluminum, thereby creating the separate base, collector, and emitter. The completed BJT is represented in Figure 5-10, and it can now be analyzed using Atlas, so that such curves as the Gummel Plot and collector voltage vs. current can be extracted. These curves will be crucial in ensuring the proper operation of the BJT, and will be compared to their theoretical equivalents, as discussed in the previous section.

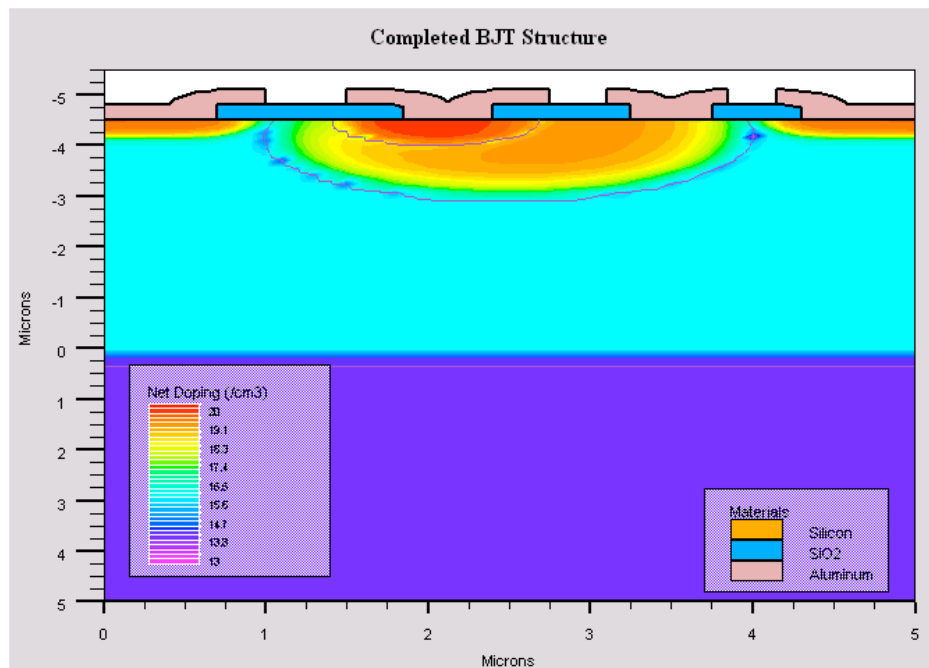


Figure 5-10: Completed BJT Structure

Figure 5-10 shows the completed BJT structure. The aluminum has been etched away.

5.4. Final Device Characteristics and Comparison

Now that the device has been constructing using Athena, it is possible to once again extract its performance parameters using the Atlas software package. With the ability to apply potentials to any of the aluminum contacts, as well as monitor the response characteristics, it is possible to determine the performance of the device.

5.4.1. Gummel Plot

As Figure 5-11 shows, the device demonstrates acceptable operational characteristics for the range of values, V_B . For small values of V_B , $V_B < .5$, the base current deviates from the ideal q/kT slope as a result of the Recombination-Generation effects. These effects are controlled in Atlas by the declaration of the Shockley-Read-Hall model. This model has become the most widely accepted method of modeling the real world effects of minority carrier recombination and generation.

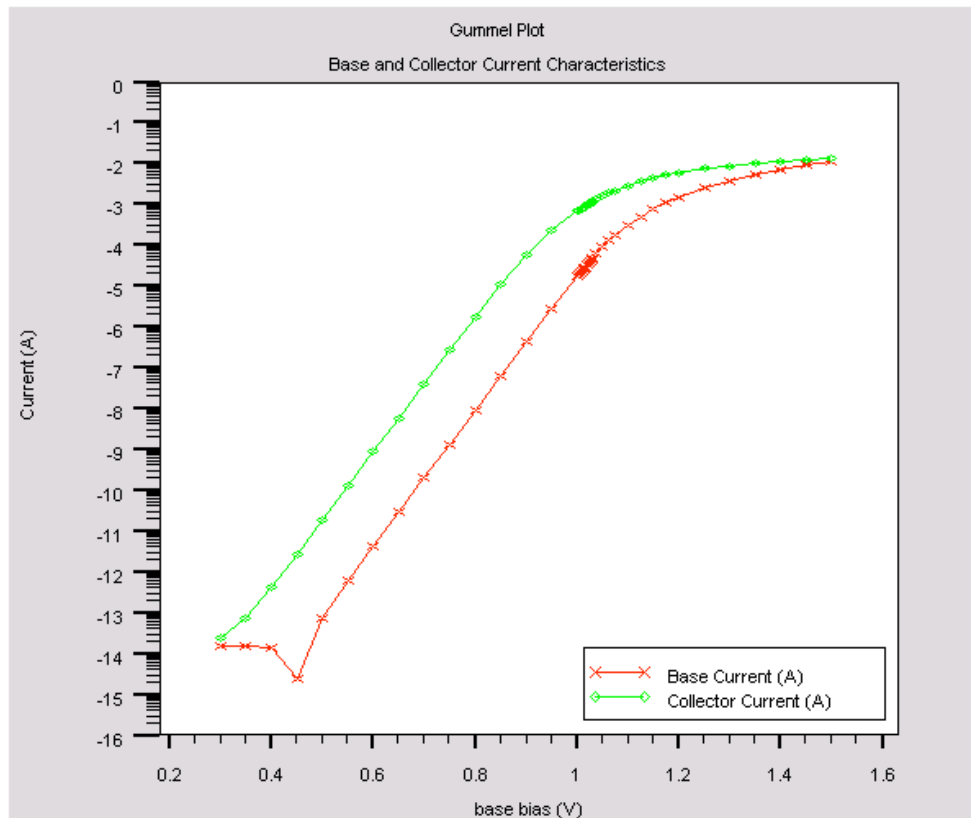


Figure 5-11: Non-Ideal Gummel plot

Figure 5-11 shows the Gummel plot of the BJT. Compare figure 5-11 to figure 5-1.

Essentially, when a bias is applied to the transistor, electrons begin to flow from the collector, through the base, and then out the emitter. However, due to the NPN structure of the transistor, as the electrons pass through the collector and enter the base, they become the minority carrier, and as such are governed by the average minority carrier lifetime. This lifetime determines the average minority carrier diffusion length, which is the distance through which a minority carrier can travel before it recombines

with the doped silicon. At weak bias levels, the majority of electrons are lost due to recombination, and as a result, the I_B line deviates from the q/kT slope.

Additionally, for larger values of V_B ($V_B > 1$) both the collector and base currents begin to slope over. This behavior can be attributed to “high level injection, possibly aggravated by current crowding”²⁴, as well as the series resistance between the collector and base. The figure below demonstrates how the device behaves once the Shockley-Read-Hall model is removed from the Atlas programming code. As can be seen, the non-idealities that occurred at low base voltage levels have not been accounted for, so the

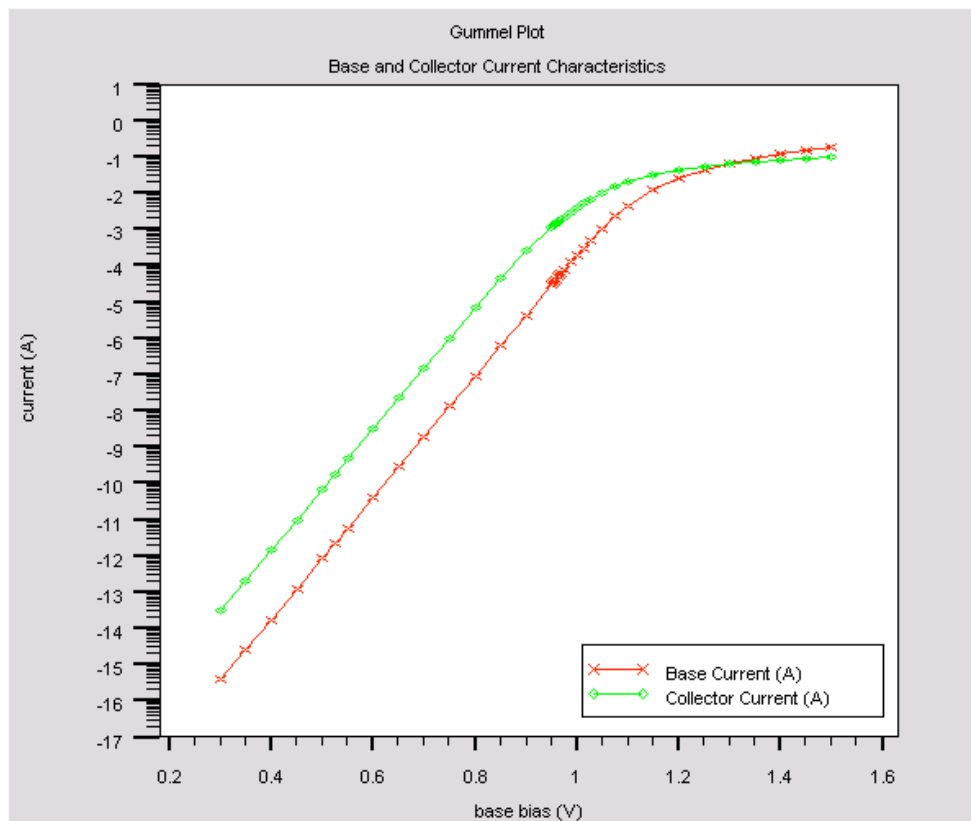


Figure 5-12: Gummel Plot without SRH Model

Figure 5-12 shows the Gummel plot of the BJT without the Shockley Read-Hall recombination effect. Compare figures 5-1, 5-11, and 5-12.

Lastly, by comparing values of the collector and base currents at a fixed V_B , it is possible to determine the β_{dc} of the device. As stated previously, for the device to be

²⁴ Pierret pg. 424

considered effective in modern applications, it needs to have a β_{dc} of at least 10. Based on our results, the β_{dc} of our BJT can be measured to be approximately 100, well above the required minimum.

5.4.2. I-V Characteristics

As can be seen in Figure 5-13, the BJT exhibits excellent performance characteristics. The device was fixed at five separate levels of base current, and the collector current was monitored as the collector voltage was increased. It can be observed that the current quickly ramps up to its asymptotical limit, only requiring approximately .6 volts of collector voltage. Beyond .6 volts, the collector current shows only slight deviations from its ideal level, most likely due to carrier recombination/generation throughout the device, as well as leakage effects throughout the device.

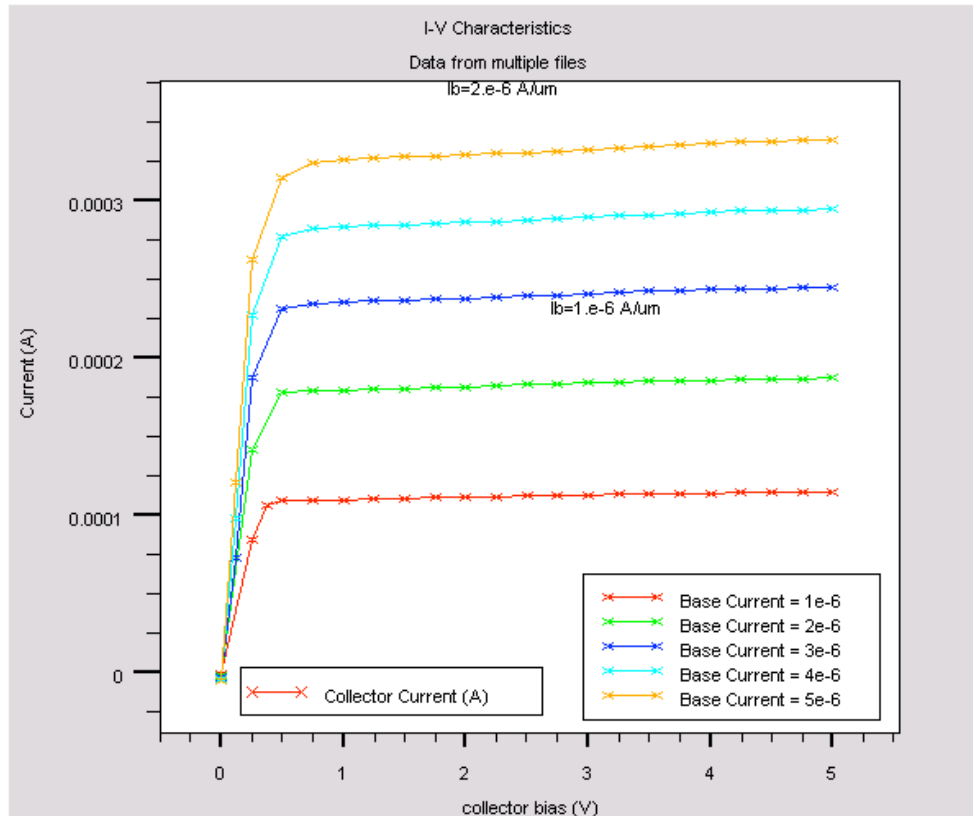


Figure 5-13: BJT I-V Characteristics

Figure 5-13 shows the I-V characteristics of the BJT at different applied base currents. Note the non-zero slope once again.

5.5. Conclusion

Similar to the construction of the NMOS transistor, the creation of the BJT gave us valuable insight into the design challenges of fabricating a BJT. Most importantly was the modulation of the base width, which proved to have the biggest effect on the performance of the device. While having a thick base is ideal for large reverse breakdown voltages, it also increases the threshold voltage of the device. Additionally, the minority carrier lifetime must be taken into consideration, as demonstrated in Figures 1-11 and 1-12. Once the time for a minority carrier to travel through the base exceeds the average lifetime, the device will exhibit poor operating characteristics at low voltages, and much of the current will be lost.

6. LDMOS Transistor

The final device left to create in the project was the LDMOS transistor. We had already had the practice of creating the CMOS transistor, from sample Silvaco structures, and creating the lateral BJT, modeling it after a different form of BJT. Next, we had to create the most difficult device of all three, the LDMOS. The LDMOS was an unfamiliar device to us. Furthermore, there were no Silvaco examples to facilitate the coding process. Therefore, we had to code the entire device from beginning to end, using our knowledge from previous experience.

6.1. Problem Statement

Create a functional LDMOS that performs to BCD-III standards. With no samples of an LDMOS simulation at hand, we took our time and came up with a logical design process recipe to ensure the efficiency of masking steps.

The LDMOS' dimensions would be 20 μm wide and 12.5 μm tall. This device was the largest device simulated yet. Moreover, it was unlike either of the previous structures in that it is a-symmetrical. In combination, the large size, and the inability to “mirror” the device, created large computational times. Thus, it was difficult to simulate.

The dimensions of the structure were chosen because of the characteristics of the device. A deep channel, and an additional oxide layer are both necessary to obtain

necessary high power device parameters such as an acceptable breakdown voltage. The parameters are based on Jim McClay's report.²⁵

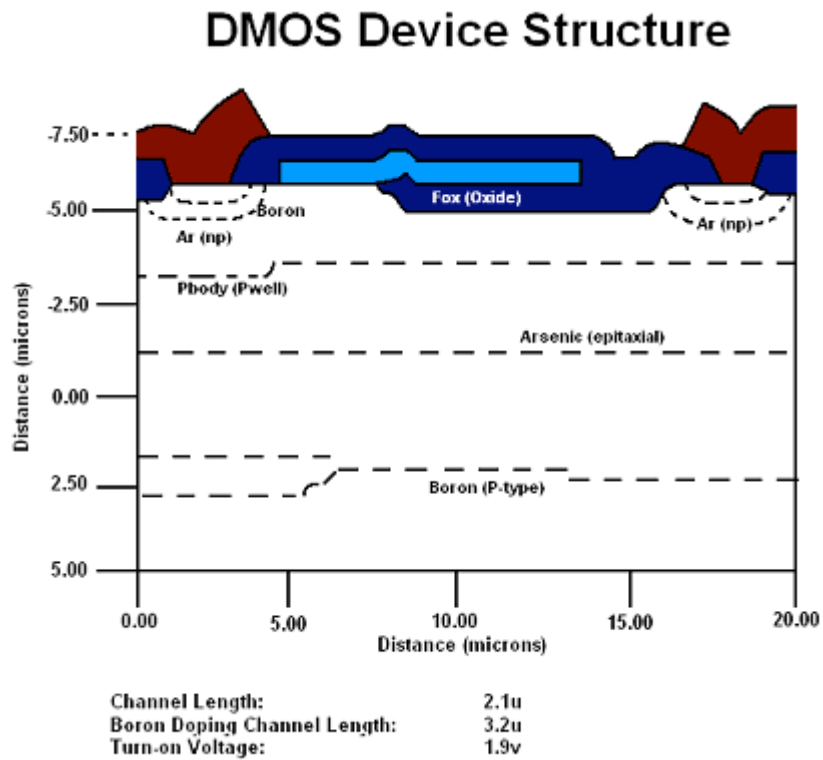


Figure 6-1 LDMOS (BCD-III Characteristics)

Figure 6-1 is our representation of the problem statement. It contains the double diffused sections, the FOX oxide, and the necessary dimensions to make a smart power IC LDMOS. Listed are also the channel length of 2.1 μm , the boron doping channel length of 3.2 μm , and the turn-on voltage of 1.9 volts. Our device actually uses a combination of arsenic, boron, and phosphorous dopants, even though the figure only shows the use of arsenic and boron.

6.2. Theoretical Device Characteristics

Although we did not complete the simulation of the device parameters for the LDMOS, we did some research about the theoretical values. Some theoretical device characteristics are common to all MOSFETS, and some are particularly important for the LDMOS. In this section, we have included all the important characteristics of

²⁵ McClay

MOSFETs, and theoretical analysis for the relevant ones. All of the issues are discussed even if they are not very important to the LDMOS. Some of these issues came during the simulation process. For example, if leakage current is not expected to be a problem in the device, but it is during simulation, then it may be encouraging to understand how leakage current works. All though we have not applied all of the theoretical values, we have given many theoretical equations and other applied research.

6.2.1. Threshold Voltage

$$\phi_f = -\frac{kT}{q} \ln\left(\frac{N_D}{n_i}\right) \quad \text{Equation 4}$$

$$V_T = 2\phi_F - \frac{K_S x_o}{K_O} \sqrt{\frac{4qN_D}{K_S \epsilon_0}} (-\phi_F) \quad \text{Equation 5}$$

Using the same threshold voltage equations apply to the LDMOS. The threshold is based on temperature, the doping of the device, some constants, and the device parameters. This measurement is taken by shorting the drain and the gate, and finding a value for which a specific drain current occurs at the threshold voltage level.²⁶ This is a common characteristic of any MOSFET device. Plugging in our numbers for the doping profile and the device parameters, we obtain a turn-on voltage of 1.8V.

6.2.2. Leakage Current

This is a common characteristic of any MOSFET. This characteristic is particularly unimportant for the LDMOS device. Leakage current is generally not an issue with most DMOS circuits. Common gate to body leakage currents are around a picoampere.²⁷

This characteristic is dependant upon the doping profile of the wafer, epitaxial layer and the drain. It is also dependant upon the depth of the device. In the case of the LDMOS, it is desired to have the epitaxial layer far enough away from the drain to not alter the junction lines of the device. The LDMOS device for BCD-III standards is fairly

²⁶ Supertex pg. 3.1

²⁷ Supertex pg. 3.1

deep. This increases the resistance along the path and does not allow for a large leakage current.²⁸

Leakage current is dependent upon temperature. As heat builds on the LDMOS, leakage current also increases.²⁹

Leakage current is governed by the following equations:

$$I_{lk} = (qA_j n_i / 2\tau_0)(x_d)$$

Equation 6 Leakage Current

Where, A_j = junction area

N_i = intrinsic carrier concentration

τ_0 = intrinsic carrier concentration

x_d = thickness of depletion region³⁰

$$\tau_0 = (\tau_n + \tau_p)/2$$

Equation 7 Intrinsic Carrier Concentration

Where, τ_0 = intrinsic carrier concentration

T_n = donor carrier concentration

T_p = acceptor carrier concentration³¹

6.2.3. Off-State Leakage Current

The off-state leakage current occurs in transistors when there are zero volts from gate to source, but a voltage from drain to source is applied. The current escapes from the body of the transistor that forms a reverse bias diode. Losses are common to diffusion. Once again, this characteristic is not crucial to the LDMOS.³²

The off-state leakage current is also greatly affected by the depth of the device. Once again, the 5 μ m deep device should offer enough protection against off-state leakage current.³³

Off-state leakage current is governed by the same equations as on-state leakage current.

²⁸ Supertex pg. 3.1

²⁹ Analog Integrated Circuit Design pg. 42

³⁰ Ibid pg. 42

³¹ Ibid pg. 42

³² Supertex pg. 3.1

³³ Ibid pg. 3.1

6.2.4. Breakdown Voltage

This characteristic is particularly important for the LDMOS device. A high breakdown voltage is the main characteristic that separates it from other MOS devices. It is the reason why BCD technology has been called “smart power”.

Breakdown voltage is measured by applying a current through the drain and the source, and measuring the voltage across the channel (the channel has some on-resistance). This parameter is likely to degrade over multiple uses of the device because of thermal reasons.³⁴

The double diffusion plays a major role in the breakdown voltage characteristic of an LDMOS transistor. Together, the two oppositely doped regions within the deep p-well drive act as diodes opposing each other. The dopings are variable, and they offer high voltage blocking characteristics.

Also, the breakdown voltage is highly dependent upon the depth of the channel within the device. The longer channel drift length, the larger the breakdown voltage can be.³⁵

The breakdown voltage is also dependent upon the doping concentration and positioning of the epitaxial layer (or the substrate if there is no epitaxial layer). A much higher voltage is able to be applied in the case of lower doped/ thinner epitaxial layer. The reason for this is because the field at the surface is below critical field due to the change in charge distribution.³⁶

The breakdown voltage is dependent upon the shape/ position of the contacts. They affect the curvature of the electric field lines. The affects due to the contacts are more prominent in smaller devices.³⁷ More importantly, the curvature of the junction depicts a change in the breakdown voltage (which is affected by the contacts).³⁸ Small Signal Transconductance

$$g_m = (V_{GS} - V_{GS(TH)})(\mu_{off} Z \xi_{ox}) / (L t_{ox})$$

Equation 8 Small Signal Transconductance

³⁴ Supertex pg. 3.1-2

³⁵ Chang Mf pg. 1996

³⁶ Appels pg. 238

³⁷ Ibid pg. 238

³⁸ Chang Mf pg. 1992

Where, Z/L = source perimeter/Channel length

μ_{off} = Effective carrier mobility

ϵ_{ox} = Gate Dielectric constant

t_{ox} = Gate Oxide Thickness

Small signal transconductance is considered to be the ratio of the change in current through the drain and the change in gate to source voltage.³⁹

This can be a crucial characteristic in determining the current gain of an LDMOS.

More equations that govern small signal transconductance are as follows:

$$g_m = 2I_D/V_{\text{eff}}$$

Equation 9 Small Signal Transconductance (I_D and V_{eff})

$$g_m = (2\mu_n C_{\text{ox}}(W/L)I_D)^{1/2}$$

Equation 10 Small Signal Transconductance (C_{ox} and I_D)

$$g_m = \mu_n C_{\text{ox}} (W/L) V_{\text{eff}}$$

Equation 11 Small Signal Transconductance (C_{ox} and V_{eff})⁴⁰

6.2.5. On-Resistance

This characteristic is particularly important for the LDMOS device. It is dependent upon temperature (as the temperature of a MOSFET increases, carrier mobility decreases, thereby reducing "...current for a given voltage")⁴¹, diffusion length, and the material. It is measured by dividing a given drain to source voltage by a given drain current. Typical on-resistances for LDMOS structures range between $0.5\Omega - 2\Omega$ for high power devices and $2\Omega - 5\Omega$ for low voltage applications.⁴²

³⁹ Supertex pg. 3.1-2

⁴⁰ Analog Integrated Circuit Design pg. 29-30

⁴¹ Supertex pg. 3.3

⁴² Ibid pg 3.3

The leading source of problems for on-resistance of MOSFET's stems from the area around the drain region. For the LDMOS all of the resistance occurs at the channel length, which is from the drain to the junction of the p-well.⁴³

Resistance increases due to a longer current path.⁴⁴

Channel length is controlled by adjusting the depth of the pn regions.⁴⁵

Highly dependent upon device layout.⁴⁶

6.2.6. On-State Drain Current

The on-state drain current is "...proportional to source perimeter and total chip area". It also affects temperature and on-resistance negatively over long periods of time.
⁴⁷

Here are some equations governing the on-state drain current:

$$I_{DS} = (B_V)(V_{DS})(V_{gst})$$

Equation 12 On-State Drain Current

$$I_D = (\mu_n C_{ox}/2)(W/L)(V_{GS} - V_{tn})^2$$

Equation 13 Ideal Square Law⁴⁸

6.2.7. Capacitance

This characteristic is particularly important for the LDMOS device. Although, it is also very important for fast switching low-voltage applications (CMOS).

The capacitance affects switching time. Doping profiles and device geometries directly affect the capacitances. If more charge is added to a region, it can change the standing capacitance. If an area's geometry is altered, it may affect the way one capacitance interacts with another one. For example if the gate is shifted to the right, then the gate capacitance is moved to the right, charge is redistributed to the left side, then the drain to source capacitance will be affected.

⁴³ Supertex pg. 3.3

⁴⁴ Kim SOI pg. 22

⁴⁵ Baliga pg. 1569

⁴⁶ Kim SOI pg. 22

⁴⁷ Supertex pg. 3.3

⁴⁸ Analog Integrated Circuit Design pg. 24-25

These are the three main capacitances in MOSFET's. They can be calculated by finding other values of capacitances.⁴⁹

$$C_{ISS} = C_{GS} + C_{DG}$$

Equation 14 Input Capacitance

$$C_{RSS} = C_{DG}$$

Equation 15 Common source capacitance

$$C_{OSS} = C_{DS} + C_{DG}$$

Equation 16 Reverse transfer capacitance

Here are the remaining equations to obtain the values for the above equations:

$$C_{ox} = K_{ox} \epsilon_o / t_{ox}$$

Equation 17 Oxide Capacitance

$$C_{gs(\text{approximately})} = 2/3 W L C_{ox}$$

Equation 18 Gate Capacitance

$$C_{DG} = C_{ox} W L_{ov}$$

Equation 19 Drain to Gate Capacitance

$$C_{GD} = W L C_{ox} / 2$$

Equation 20 Gate to Drain Capacitance⁵⁰

6.3. Walkthrough of LDMOS Fabrication

Provided is a walkthrough of the simulation of the fabrication process for the LDMOS.

⁴⁹ Supertex pg. 3.3

⁵⁰ Analog Integrated Circuit Design pg. 21

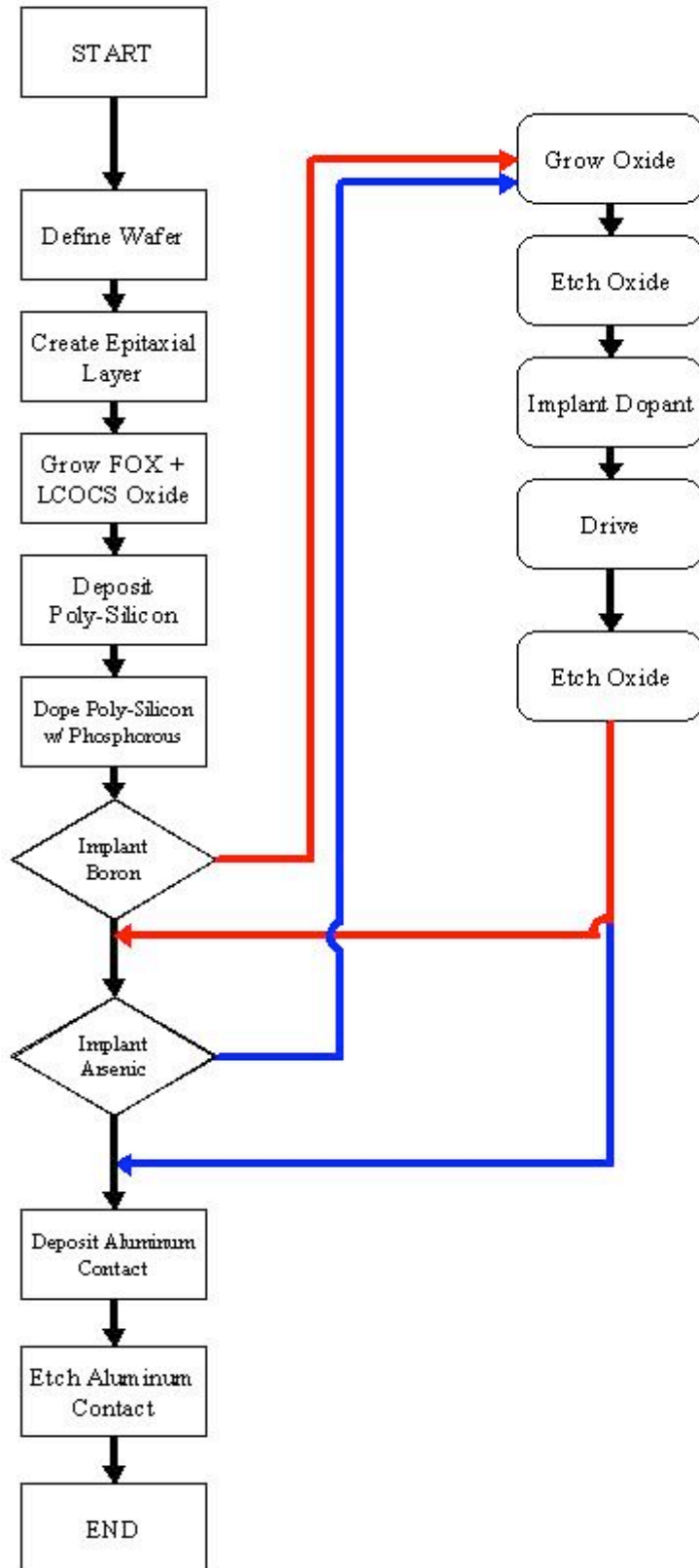


Figure 6-1 LDMOS Process Recipe

Figure 6-1 shows the process recipe for the LDMOS transistor. The first three steps are similar to the previous devices steps. First the wafer is defined, then the epitaxial layer is deposited. After that, the LOCOS isolation is done. In addition to this, the FOX enhancement is also done. Once the FOX enhancement is done, the poly-silicon is deposited and doped. Then the P drive is implanted, and then the N drive. Finally the aluminum contacts are added to complete the device.

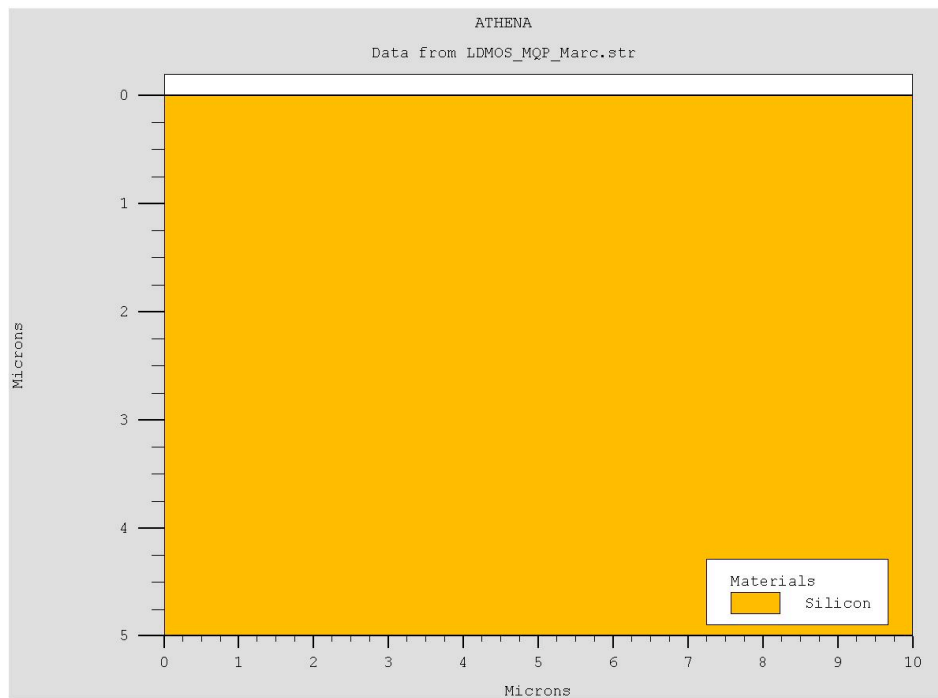


Figure 6-2 LDMOS Wafer

This figure (6-2) shows the initial wafer, which is the same wafer the other devices begin with as well. It is doped with a donor concentration of boron $1e14/cm^3$. It represents the left half of our LDMOS device, measuring $10\mu m$ wide and $5\mu m$ tall. The final device will be $20\mu m$ wide and $5\mu m$ tall. Although we were unable to mirror the LDMOS in the later stages because it is not a symmetrical device, we kept the device un-mirrored for as long as possible to reduce the total number of calculations.

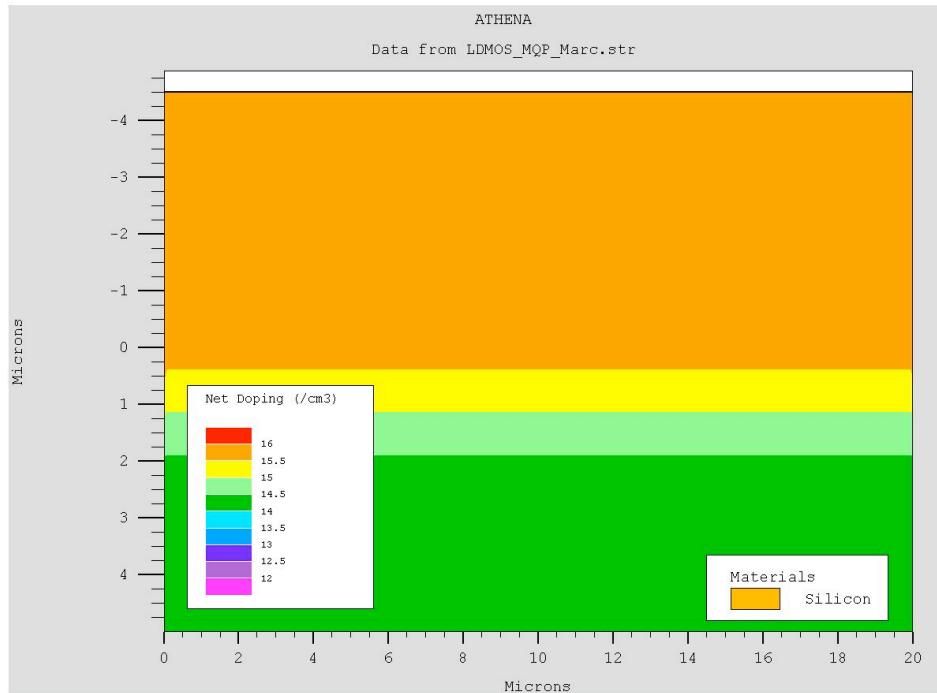


Figure 6-3 LDMOS Epitaxial Layer

Figure 6-3 shows the wafer after it is annealed for a time of 45 minutes with an initial temperature of 900°F and a final temperature of 1000°F. During the annealment process, a $1 \times 10^{16}/\text{cm}^3$ acceptor concentration of arsenic was added. After the epitaxial layer is diffused and bonded with the wafer, the device is then mirrored. The next steps in creating the LDMOS will involve a-symmetry, so it is important to mirror the device now.

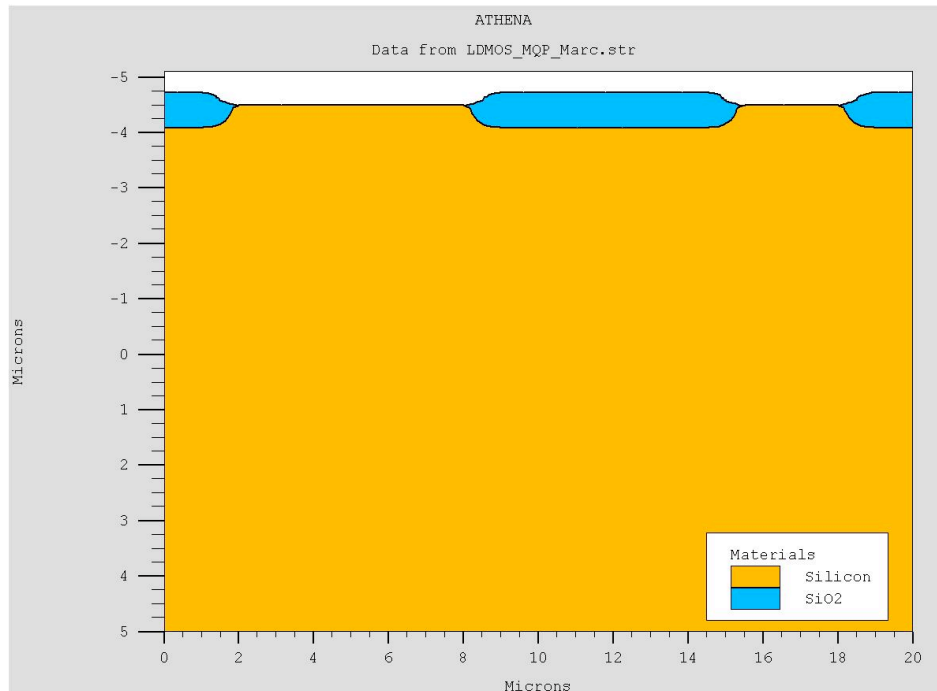


Figure 6-4 FOX Enhancement and LOCOS Isolation

Figure 6-4 shows the completion of the next masking step. We want to apply the nitride mask in the proper places to put the oxide layer exactly where we want it to be. The oxide will be used for both the LOCOS isolation (see section 3.3.4) and the FOX enhancement. Both of these types of oxidation need to occur early in the design process to allow time for them to grow in other annealing steps. The oxides are grown and diffused for a time of 60 minutes and for a temperature of 1100°F using a wet oxidation process.

FOX enhancement is a layer of oxidation beneath the poly-silicon and gate oxide that serves to boost performance parameters. It creates a deeper channel for current to travel, while still minimizing the length of the channel. The depth of the channel greatly affects the break down voltage of the device. For a power IC device, a high breakdown voltage is desired. A short channel length greatly reduces the on-resistance of the device. A minimal on-resistance is desired, it will allow for much higher current applications. FOX enhancement provides a solution to the breakdown voltage and on-resistance trade-off issue.⁵¹

⁵¹ McClay

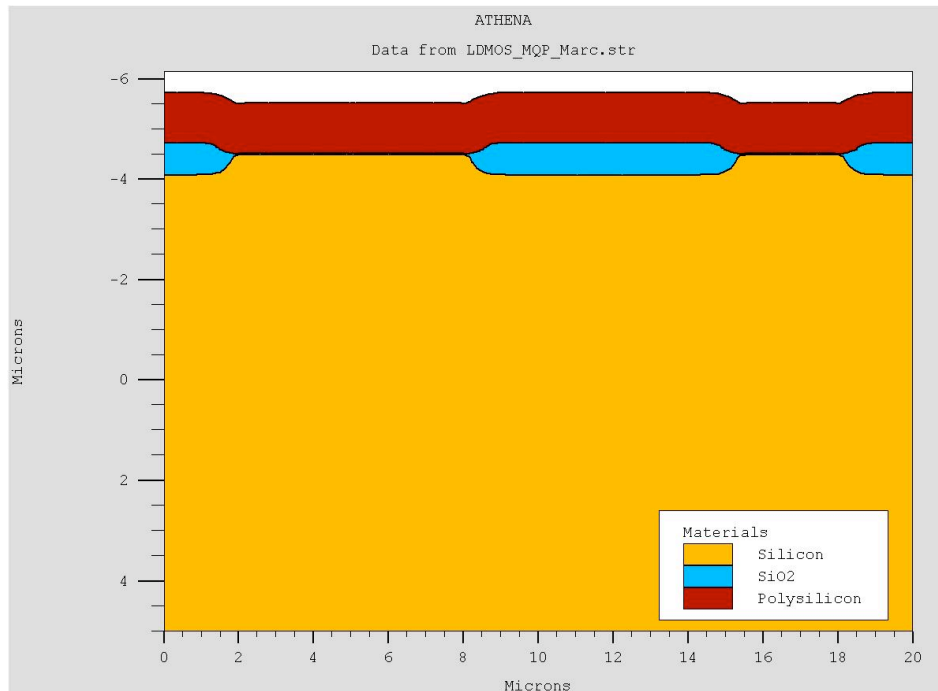


Figure 6-5 LDMOS with Poly-silicon

Figure 6-5 shows the poly-silicon layer after it has been deposited on the surface of the device. Prior to the deposition layer of poly-silicon, the wafer was diffused for 10 minutes at a temperature of 1035°F in a dry atmosphere. This allowed for the bonding of the existing layer, and for the separation of it from the new poly-silicon layer.

During this step, the doping profile has also changed. Although it is not visible with this figure, one can see the doping profile in the next figure (6-6). During this process step, ion implantation of a donor concentration of $3 \times 10^{13}/\text{cm}^3$ was added using an energy of 20 keV. The poly-silicon takes on a new doping profile of $3 \times 10^{13} \text{ cm}^{-3}$.

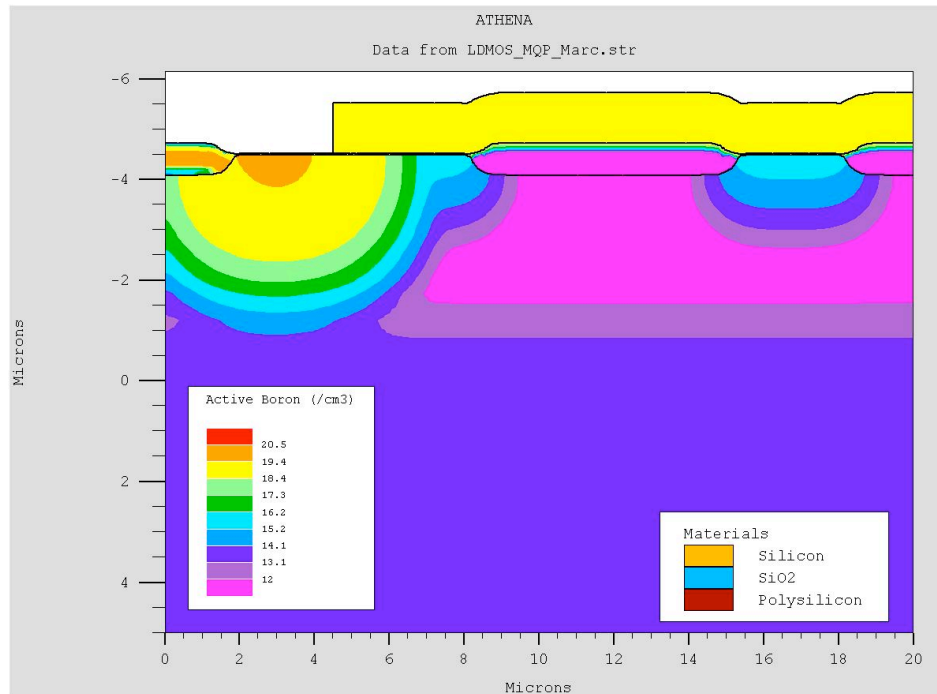


Figure 6-6 LDMOS Active Boron Dose

The next masking step involved the implantation of the boron n-type donor concentration into the device. Here the poly-silicon was unaffected by the implantation regardless of the color of the poly-silicon. Since ion implantation is used, essentially hitting anything on the surface with the boron dose is avoidable. The poly-silicon was etched away on the left side to allow a higher concentration of boron at the surface on that side. The boron was implanted at a concentration of $5 \times 10^{15}/\text{cm}^3$ at an energy of 100 keV. The wafer was diffused for a time of 150 minutes at a temperature of 1100°F in a nitrogen atmosphere. (As shown in figure 6-6).

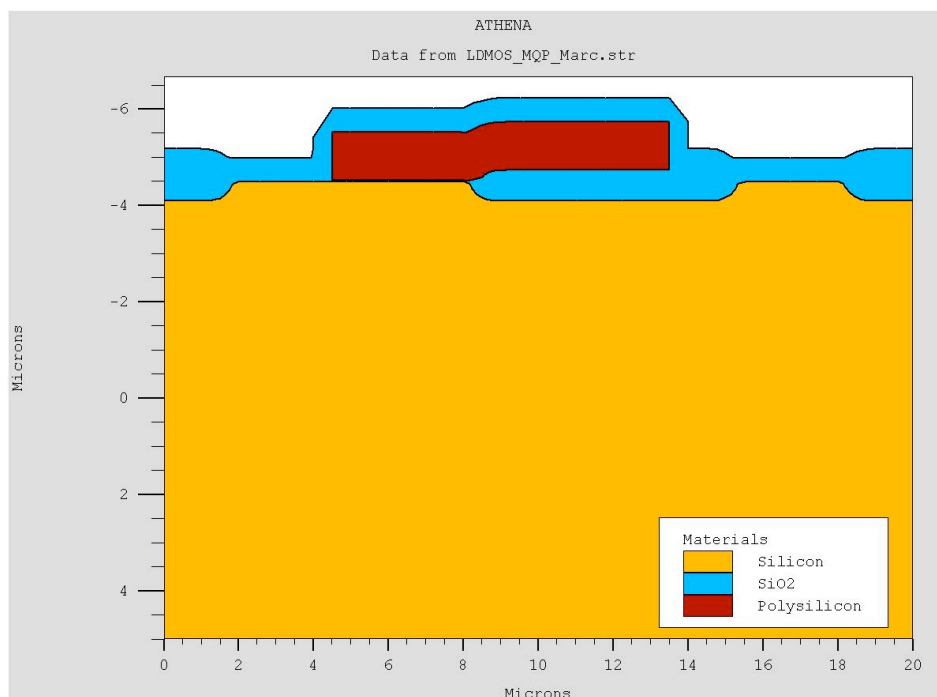


Figure 6-7 LDMOS 2nd Oxide Layer

The next figure (figure 6-7) shows the LDMOS device prior to the masking of the p-well drive (see figure 6-8). To prepare for the next ion implantation step the polysilicon was etched away on the right side. In addition, a small surface of oxide ($0.05\mu\text{m}$) was also etched. This ensures that, when the new gate oxide layer is grown, it surrounds the channel in the proper areas isolating junctions and leakage currents. After it was etched, the new gate oxide was then grown at a thickness of $0.5\mu\text{m}$. This oxide layer also serves as a mask for the upcoming p-well drive process step.

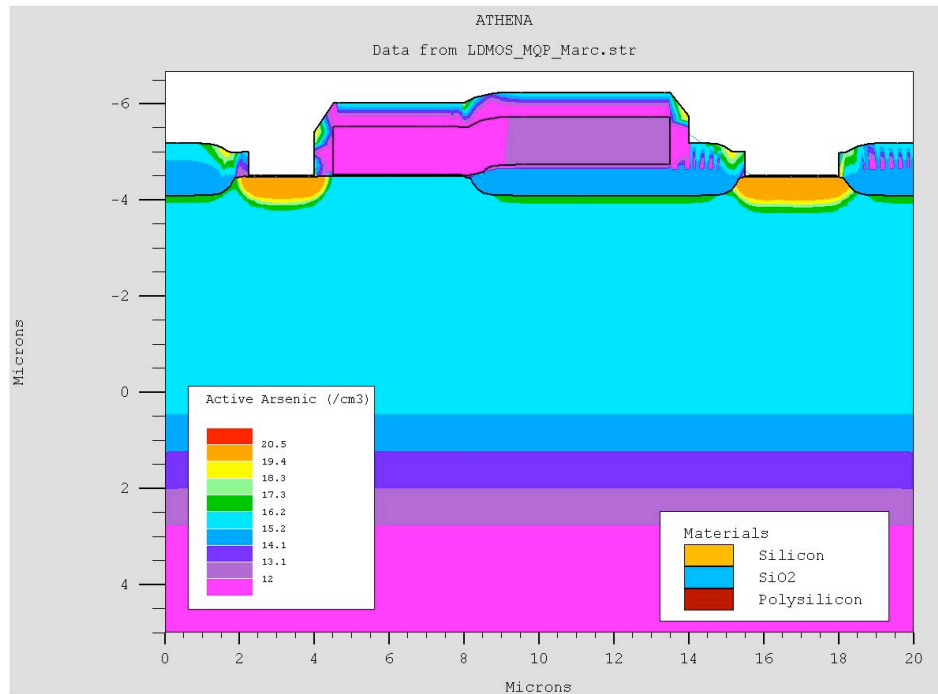


Figure 6-8 LDMOS P-Well Drive

After the gate oxide was grown, the oxide was then etched away at key points comprising the future channel of the LDMOS (see figure 6-8). The oxide was annealed at a time of 10 minutes at a temperature of 1035°F in a dry environment. This allowed the oxide to grow to its desired dimensions. Next, the p-type arsenic was implanted into the device at a concentration of $5 \times 10^{15}/\text{cm}^3$ and was diffused for a time of 180 minutes at a temperature of 1000°F in a nitrogen atmosphere.

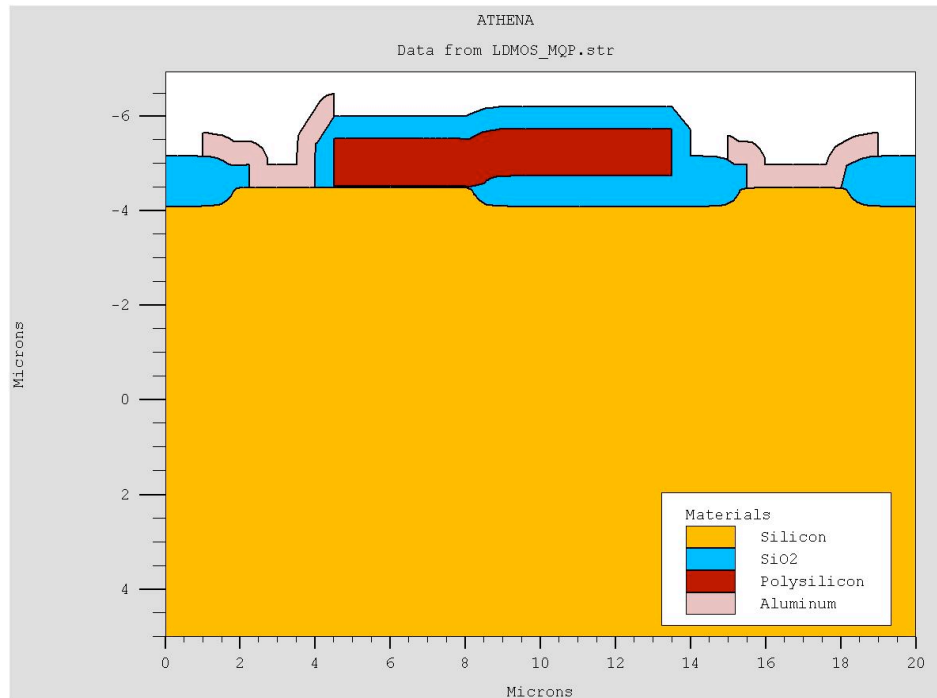


Figure 6-9 Final LDMOS Device

Figure 6-9 represents the final LDMOS structure. The transformation of figure 6-8 to figure 6-9 occurred because of the following steps. A thin layer of oxide was etched ($0.03\mu\text{m}$). Then, a layer of aluminum $0.5\mu\text{m}$ thick was deposited onto the device. Lastly, the aluminum was etched away to provide contacts wide enough for use on an IC. Now the device is completed to the required dimensions.

6.4. Final Device Characteristics and Comparisons

We were unable to commence atlas simulations for the project. The LDMOS device is large and requires numerous mesh calculation points. As a result, using Athena alone to simulate the LDMOS structure consumed much time.

Another problem that we faced involved figuring out exactly what to plot using Athena. We were familiar with both the CMOS and the BJT, but the LDMOS was a new device to us. Furthermore, there were no examples of the LDMOS in the Silvaco package. Therefore, we had to do some research to procure useful plots that may be used later to simulate with Athena.

6.4.1. $I_d = (V_d, V_g)$ Characteristic

We obtained the following figure from the Silvaco webpage.⁵² It shows certain characteristics of an LDMOS transistor.

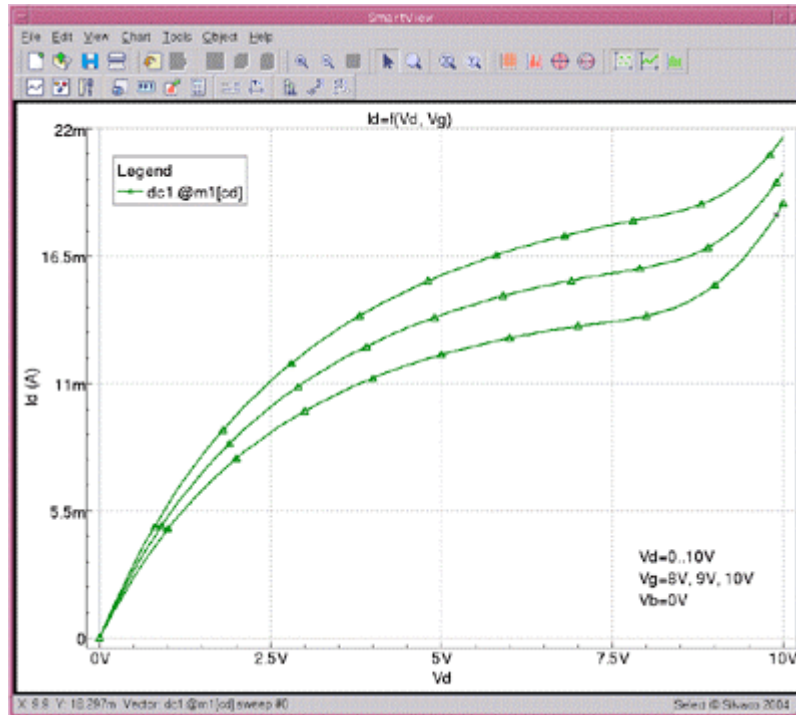


Figure 6-10 I_d vs V_d, V_g

The following figure (figure 6-10) was taken from the Silvaco webpage.⁵³ It demonstrates the on-state drain current versus the drain voltage of an LDMOS at various applied gate voltages. Ideally, the curve would rise rapidly, and then level off at a constant current. However, due to the “weak-avalanche of current”, otherwise known as impact ionization, the curve continues to slope upward. As more current ramps through the device, the LDMOS then heats up. Since the current of the device is proportional to temperature, the current continues ramping upward. Eventually, the device fails at some power dissipation spike or some power dissipation average maximum. This curve gives us useful information about the devices operating region, which is crucial to simulating a smart power device.

⁵² Silvaco Webpage np

⁵³ Ibid np

6.4.2. Transistion Potential vs V_g , V_d

We obtained the following figure from the Silvaco webpage.⁵⁴ It shows certain characteristics of an LDMOS transistor.

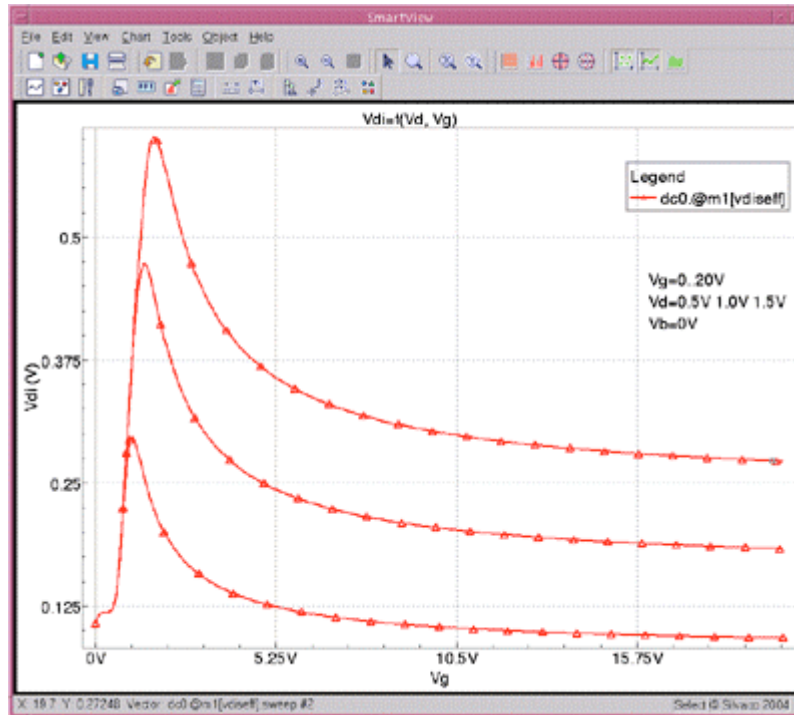


Figure 6-11 V_{di} vs V_d , V_g

The following figure represents the potential at the transition between channel and drift regions versus V_d and V_g . In other words, this figure represents the following situation. Given a cross sectional view of an LDMOS (see example 6-9), draw a line such that it crosses at a transition between the channel the drift region; now plot the potential of V_d and V_g . This graph demonstrates where the potential transition occurs as one varies the V_{di} .

6.4.3. C_{dd} vs V_d , V_g

We obtained the following figure from the Silvaco webpage.⁵⁵ It shows certain characteristics of an LDMOS transistor.

⁵⁴ Silvaco webpage np

⁵⁵ Ibid np

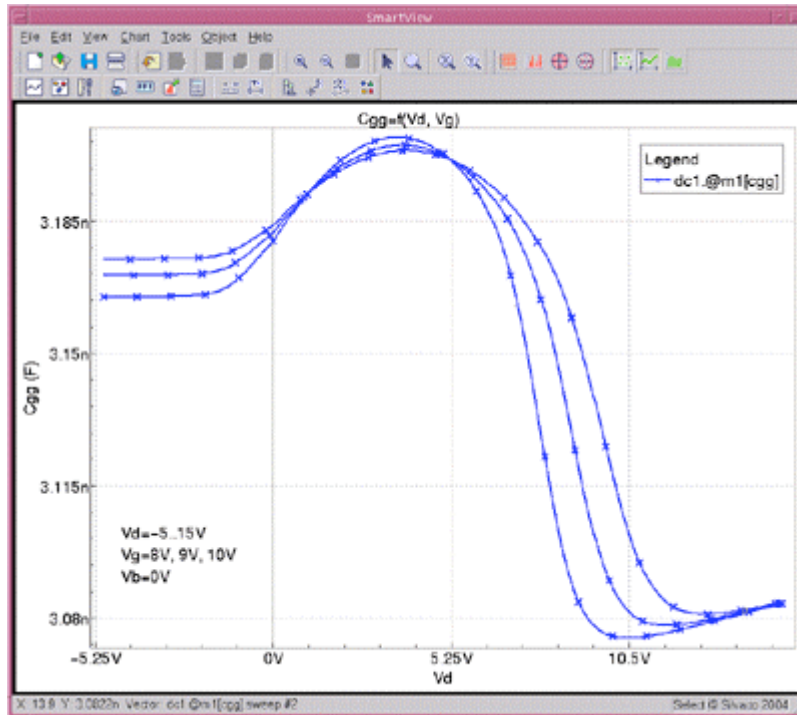


Figure 6-12 C_{gg} vs V_d

Figure 6-12 shows the on-state gate capacitance versus the drain voltage given three different applied V_g 's. This figure is important, because it shows how the gate capacitance is affected by a change in the drain voltage. This occurs because the gate-source voltage is measured diagonally on the device and the drain-voltage is measured horizontally. The two voltages affect each other, which in turn, affects the gate capacitance. Gate capacitance is important because it changes the time constant of the LDMOS, which affects the switching time. In essence, we can see at what applied voltages switching times will be affected. Tweaking this parameter can help increase the operating range of the device.

6.5 Conclusion

In order to simulate a working LDMOS, the simulated curves must match up similarly to the Silvaco website curves. They will be different, and perhaps not maintain the same shape or ideal properties, however, that is the nature of simulation. The curves may be reworked to make more ideal. In addition, the breakdown voltage, on-resistance, threshold voltage, and drain current parameters must be extracted. The capacitance curves should tell enough about the device. It is therefore not necessary to extract any

capacitances other than the value gate capacitance. These are the parameters and curves that best describe the LDMOS transistor.

7. BCD Fabrication Wafer

A single device is easy enough to simulate and achieve stellar results for a relatively inexpensive amount of money. The problem arises when multiple devices are produced on a single wafer. This section discusses in detail the problems that arise when creating a wafer with multiple devices. In addition, shrinking device parameters will also be discussed.

7.1. *Problem Statement*

The initial problem statement was to simulate combining the CMOS, BJT, and LDMOS devices onto a single wafer while conforming to BCD-III standards. Due to time constraints we could not simulate the optimization of the three devices onto a single wafer.

The new problem statement was to research strategies for optimization and analyze the fabrication of the three devices on a single wafer. Also, part of the new problem statement was to analyze problems that might arise when taking a BCD-III wafer and shrinking it down to BCD-V standards.

7.2. *Process Recipe*

In order to solve the problem, a process recipe had to be created in order to analyze the effect of changing a single process step on the fabrication process as a whole. A walkthrough of the recipe is given in this section.

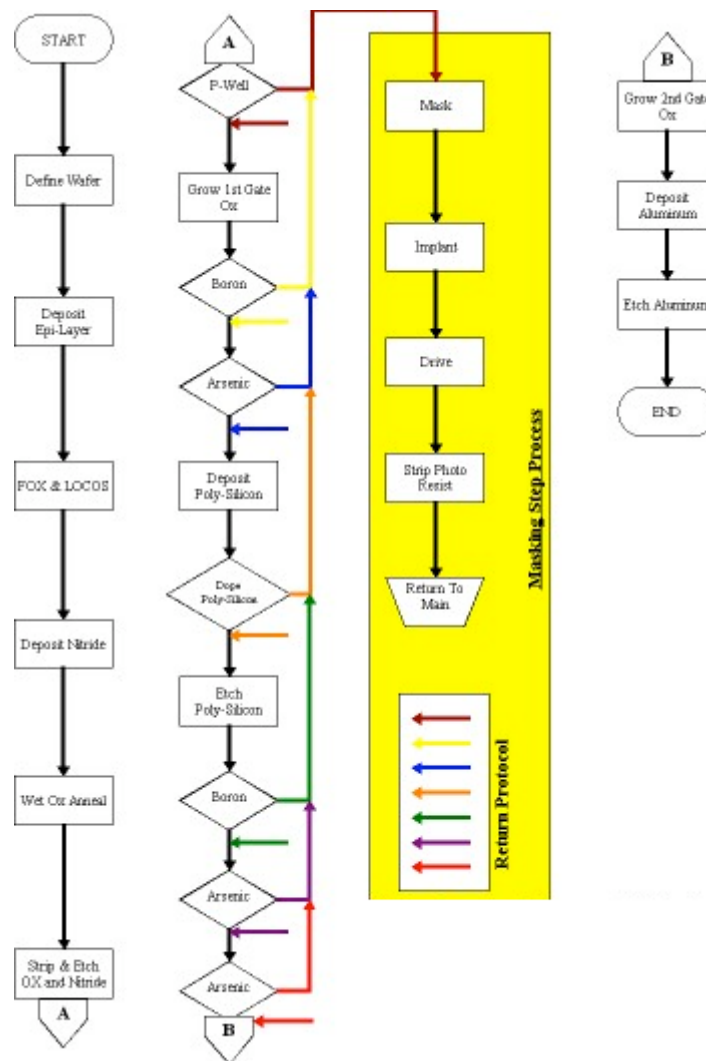


Figure 7-1 BCD Design Process Recipe

Figure 7-1 shows the process recipe of CMOS, BJT, and the LDMOS devices when all treated on the same wafer. The strand on the left is the same for all devices. It flows downward to the bottom of the page and is marked with a letter A. It then flows to the top of the next strand and picks up again at the letter A at the top of the page.

The middle section represents the implantation and masking step processes. For every diamond shaped box, a masking process occurs. The return protocol then shows the user where to return back in the main using a sequence of color coded arrows. The user is to enter the masking subroutine and exit based on the arrow of the same color.

The section on the right represents the final touches that all the devices go through during fabrication. Follow the implantation string to the bottom of the page where the letter B flows to. That letter B connects to the letter B in the process string on the top of the page all the way to the right.

7.3. *Strategies for maximizing Performance Parameters*

LDMOS accounts for 30%-70% of total BCD die surface area. Therefore it is important to maximize the performance of the LDMOS parameters, more so than the other devices. There are additional tradeoffs that occur with other devices as well.

7.3.1. Capacitance

The LDMOS has a high switching speed and high input impedance.⁵⁶ So compromising this factor may be to the advantage of the user. Characteristically, doping the substrate more highly can increase the gate capacitance. This will lower the switching time. However, this also increases the amount of charge at the junction, thereby allowing the breakdown voltage to increase

Problems with this are quite apparent. If the substrate or epitaxial layer are more highly doped, then the BJT may not have the same amplifying properties that it should have. Furthermore, if the capacitances of the CMOS transistors are increased, then their switching speeds too are greatly reduced. For the purposes of BCD technology, this is not acceptable.

If the substrate is too lightly doped (for optimized CMOS) then the LDMOS can suffer from punch through. That occurs when the pinched off current sneaks around the desired channel. It is not desirable.

7.3.2. Surface Field Reduction

High electric field at the surface is undesirable. It lowers the breakdown voltage and influences the on-resistance, the two most valuable parameters that affect the LDMOS. Limitations are being reached by using FOX enhancement (one way of reducing the surface field).

⁵⁶ Rossel Advanced pg. 119

One way to alter this is to change the junction of the double diffused region. If this parameter can be optimized (shank to its minimal functional size), then the LDMOS will have great characteristics. A problem with this is that the CMOS source and drain regions may not extend far enough down. This will cause the pinch-off factor to be increase greatly along with short channel effects.

7.3.3. Process Problems

Even if the devices are simulated exactly how you want them individually, the process parameters that occur later in the recipe can affect them. For example, if the CMOS is correctly diffused the right amount downward into the wafer, later it may expand too far due to later annealment steps. This can present many problems.

7.4. *Strategies For Improving Shrinking Device Geometry*

There are multiple strategies for improving the BCD devices. Much of the strategies are geared toward the LDMOS. Furthermore, certain methods are starting to reach their limits, and new technology needs to be developed in order to overcome shrinking issues.

7.4.1 VLSI technology shrinking Poly-Silicon Window

Using VLSI for improving many of the LDMOS's parameters is out of the question. It is too difficult. However, using VLSI technology can be used to shrink the poly-silicon window. The result is improved current distribution within the cell.⁵⁷ Using this method, on-resistance can be reduced by a factor of 2X.⁵⁸ However, that is approaching the theoretical limit 0.15 ohms. Therefore other forms of technology are also necessary.

7.4.2. Trench gate structure

One form of trench gate synthesis is using the LUDMOS. It is a trench in the drift region under the gate to reduce electric field at the surface. Now, breakdown voltage is governed by trench depth instead of charge at the surface. Now the drain can be placed close to the trench. The trench can be partially filled with poly-silicon, which helps with conduction. Now the epitaxial layer can be doped

⁵⁷ Baliga 1569

⁵⁸ Baliga pg. 1569

more highly without worrying about punch-through. The result is an increase in active area and a much lower on-resistance.⁵⁹

7.4.3. Materials

One Example of a different material other than silicon is the use of Gallium arsenide. Currently it is very costly. However, as production increases, the price of GaAs is dramatically decreasing, and it may soon become available more readily. It is beneficial to BCD technology because it is 3-5 times smaller module size. Also, it has better diffusion properties when doped.

Another example is Silicon carbide. It can reduce on resistance by over 100 times.⁶⁰

7.4.4. Tapered Oxide (TEOS)

Another way to reduce the field oxide and optimize BCS technology is by tapering the field oxide. It is more difficult to grow this type of oxide, which may be a cost design issue. With it, Boron in the drift region in particular performs better, and current distribution is very good.⁶¹ Furthermore the “boron out diffusion and reduced current path” are improved.⁶²

7.5. Conclusion

There are many ways of improving BCD technology currently. There are ways to optimize the devices and there are new forms of technology being introduced to aid the BCD characteristics. BCD technology needs to be implemented and simulated on even smaller level. Better BCD technology is in our grasp.

⁵⁹ Rossel Advanced pg. 119

⁶⁰ Baliga pg. 1569

⁶¹ Kim SOI pg. 25

⁶² Ibid pg. 21

8. Project Summary and Future Work

When we began our MQP, it was decided that this project would be, more than anything, a chance to learn. Rather than focus on endlessly tweaking the Athena code in pursuit of incremental performance gains of the BCD components, we felt it was significantly more important to pursue the knowledge, skills, and abilities that the field of semiconductor device design requires. This project was an opportunity to learn about both the BCD fabrication process, as well as the Silvaco suite of modeling applications, which are used throughout the semiconductor industry to model the behavior of BCD devices. Now that the project is complete, we recognize that we have learned an extensive amount about both the fabrication process, as well as the real world issues confronting component designers. In this respect, we feel that our project has been a success.

We started this project with little more than an Atlas example showing the fabrication of a 1.2 micron NPN transistor. Since then, we have become much more proficient with Silvaco. We have improved our abilities to the point where we no longer require an example of a device in order to create a functional BCD component. Through the use of Athena and Atlas, we are now able to design and test all manner of devices. Using formulas and equations from our research to supplement our calculations we were able to create working BCD devices with parameters close to those of the BCD-III family of ICs.

Our research has also come a long way, as we both know significantly more about the fabrication process than we did at the beginning of the project. We've learned the fundamentals, such as applying a photo resist in order to protect areas of the wafer during the etching process, using ion implantation to deposit ions below the surface of silicon, and how ion implantation results in a near Gaussian distribution of the ions within the silicon. We have also devoted research efforts to learning about more advanced techniques, like trench isolation, LOCOS, and RESURF.

While it is true that we have come a long way over the course of this project, we recognize that there is still more that can be done. The BCD devices that we have created demonstrate acceptable, however not production-worthy, performance characteristics. As

our focus was on acquiring the skills and knowledge to create the devices, we did not feel it was as important to strive for a commercially viable fabrication process. Additionally, information regarding the LDMOS has been sparse, so we recognize that further efforts can be devoted to the design and testing of this component. We were able to achieve an LDMOS model, however it remains as of yet, untested.

Appendix A – References

- 1) Appels JA and Vaes HMJ (1979) High-Voltage Thin-Layer Devices (RESURF Devices), IEDM Tech Dig, pp 238-241
- 2) Baliga, B. Jayant, IEEE Transactions on Electron Devices, Vol. 38. No. 7: *An Overview of Smart Power Technology*, July 1991.
- 3) Chang MF, Piefer G, Yilmaz H, Wildi EJ, Hodgins RG, Owyang K and Adler MS (1986) IEEE Trans Electron Devices vol ED-33, pp 1992-2001
- 4) Jaeger, Richard C., Modular Series On Solid State Devices Volume V: *Introduction to Microelectronic Fabrication*. Addison-Wesley Publishing Company, 1988
- 5) Johns, David A., Martin, Ken, *Analog Integrated Circuit Design*, John Wiley and Sons Inc., New York, 1997
- 6) Kim, Jongdae, ETRI Journal Volume 21, Number 3: *Characteristics of P-channel SOI LDMOS Transistor with Tapered Field Oxides*, September 1999
- 7) Mauro, Zambuto, *Semiconductor Devices*, McGraw Hill Book Company, New York, 1989
- 8) McClay, James M. *Personnel Communication*.
- 9) Moreau, Wayne M., *Semiconductor Lithography: Principles , Practices, and Materials*. Plenum Press: New York, 1988.
- 10) Murari, B. Bertotti, F. Vignola, G.A. (Eds.), *Smart Power IC's: Technologies and Applications*, Springer: Berlin, 2002.

- 11) Pierret, Robert F., *Semiconductor Device Fundamentals*, Addison-Wesley Publishing Company, 1996
- 12) RF Micro Devices, Augustine, Paul J., *Trends and Opportunities for Gallium Arsenide Semiconductors in Handsets*, 2005
- 13) Rossel, P., Proc 22nd International Conference on Microelectronics Vol. 1: *Advanced Concepts in Smart Power Integrated Circuits*, May 2000
- 14) Roulston, David J., *Bipolar Semiconductor Devices*, McGraw Hill Book Company, New York, 1990
- 15) Supertex Inc., Databook 1993-1994: High Voltage Integrated Circuits and DMOS Transistors, Supertex, 1993
- 16) Sze, S.M., *Semiconductor Devices: Physics and Technology*, AT&T Bell Laboratories: New York, 1985.
- 17) Warner Jr., R. M., Grung, B. L., *Semiconductor-Device Electronics*, Saunders College Publishing, 1991
- 18) Webmaster@silvaco.com., Silvaco Inc: Webpage,
<https://src.silvaco.com/ResourceCenter/en/SimulationStandard/showArticle.jsp?year=2004&article=a2&month=jan>, 2006
- 19) Yang, Edward S., *Fundamentals of Semiconductor Devices*, McGraw Hill Book Company, New York, 1978
- 20) Yuan, T., Ning, T. H., *Fundamentals of Modern VLSI Devices*, Cambridge University Press, New York, 1998

Appendix B – NMOS Athena and Atlas Code

```
go athena
```

```
#This initial step is used to define the mesh for the BCD structure. The mesh is
#important in determining on how many points of the device Athena will perform
#calculations. A mesh that is not dense enough will yield incorrect results, however a
#mesh that is too dense will require too many calculations and will make it impossible to
#run multiple simulations and quickly analyze results.
```

```
line x loc=0.0 spac=0.1
line x loc=1.66666 spac=0.05
line x loc=3.333333 spac=0.05
line x loc=5.0 spac=0.085
line y loc=0 spac=0.035
line y loc=1 spac=0.85
line y loc=5.0 spac=2.5
```

```
#The following line denotes the type of wafer on which the device is going to be
#constructed. For the CMOS devices, we will be using a silicon wafer, in a <100>
#orientation and doped with a boron level of 1e14
```

```
init orientation=100 c.boron=1e14 space.mul=2 TWO.D
```

```
#Here is where the arsenic epitaxial layer will be grown. Arsenic is chosen to create
#an n-type layer upon which the device will be constructed. The divisions parameter
#specifies the amount of new mesh layers to be applied to the newly grown epitaxial
#layer. The thickness is specified to be 4.5 micrometers (the default unit of length
#in Athena.
```

```
epitaxy time = 45 temp = 900 t.final = 1000 c.arsenic=1e16 \
thickness = 4.5 divisions = 20 dy = .05 ydy = 0.00
```

```
#P-well Implant - This step creates the P-type channel region for the NPN transistor.
#The energy level is chosen so that the peak doping will be at the surface of the device.
```

```
implant boron dose=8e12 energy=100 pears
diffus temp=950 time=100 weto2 hcl=3
```

```
#This next step further diffuses the Pwell into the device, creating a near uniform
#concentration gradient of the boron (especially near the surface of the device)
```

```
diffus time=50 temp=1000 t.rate=4.000 dryo2 press=0.10 hcl=3
diffus time=220 temp=1200 nitro press=1
diffus time=90 temp=1200 t.rate=-4.444 nitro press=1
etch oxide all
```

```
#sacrificial "cleaning" oxide
```

```

diffus time=20 temp=1000 dryo2 press=1 hcl=3
etch oxide all

##### LOCOS here #####

#As discussed in the report, LOCal Oxidation of Silicon is an effective technique
#for isolating the separate devices that are created on the wafer. This process
#grows a thick layer of Silicon Dioxide between neighboring devices, so that the
#performance of one device is not influenced by the operation of another.

#The following step creates the necessary mask to shield the device during the LOCOS
#process, and then etches away the area that is to be exposed to the growth of the Oxide.
#A thick layer of nitride is applied to not only serve as a barrier, but to
#also help diminish the "bird beak" effect that is common to the growth of an oxide
#layer.

    deposit oxide thick = .01 div = 1
    deposit nitride thick = .3 div = 6
    deposit barrier thick = .1 div = 1
    etch barrier left pl.x = .5
    etch nitride thick = .35
    etch oxide thick = .02
    etch silicon dry thick = .25

#The 'barrier' layer is now removed, and the device is annealed in a water vapor
#environment so that rapid oxide growth can be achieved.

    strip
    method grid.ox = .075
    diffuse temp = 1200 time = 60 weto2 hcl.pc=3

#The remaining deposited layers are now etched away, and the device has been
#successfully isolated.

    etch nitride all
    etch oxide thick = .05

#####

#The gate oxide is now grown on the device. Time and temperature are chosen
#to create a gate oxide of to the BCD-III spec of 28nm

    diffus time=10 temp=1035 dryo2 press=1.00 hcl=3

# Extract a design parameter

```

```

extract name="gateox" thickness oxide mat.occno=1 x.val=0.05

#In order to concentrate the current flow through the channel of the device,
#thereby helping reduce the leakage current, an additional boron implantation is
#performed.

implant boron dose=2.5e12 energy=100 pearson

#The polysilicon gate is then deposited on the device

depo poly thick=1 divi=10

#The polysilicon is lightly doped with phosphor

implant phosphor dose=3.0e13 energy=20 pearson

#this step etches away the sides of the polysilicon, and then performs a brief
#annealing step which will grow an oxide around the polysilicon in order to protect
#it from acquiring any further doping characteristics

etch poly left pl.x=4
method fermi compress
diffuse time=3 temp=900 weto2 press=1.0
depo oxide thick=0.235 divisions=8
etch oxide dry thick=0.235

#The n-type wells (source and drain)are then implanted into the device, and then
#diffused to the appropriate depth, as controlled by the time and temperature of
#diffusion

implant arsenic dose=5e15 energy=50 pearson
method fermi compress
diffuse time=175 temp=1000 nitro press=1.0

#A final oxide is grown to protect the device

depo oxide thick=3.5 divisions=8
etch oxide dry thick=3.4

# This step etches away the oxide in specific places so that aluminum contacts
# can be added to the source and drain wells.

etch oxide start x=2 y = -5.25
etch cont x = 2 y = -4.25
etch cont x = 1.25 y = -4.25
etch done x = 1.25 y = -5.25
deposit alumin thick=0.4 divi=2

```

```

    etch alumin right p1.x = 2.25
    etch alumin left p1.x = .5

#The final steps are to mirror the device (because the CMOS transistor is a symmetric
#device, only half of it was created during this process, the structure can now merely be
#mirrored to attain the full device.

    structure mirror right

#Lastly, the aluminum contacts are defined as electrodes, which will allow Atlas to
#perform computations. X and Y coordinates intersecting the appropriate contact are
#chosen, and a name is given to the contact at the point of intersection.

    electrode name=gate x=5 y=-5.5
    electrode name=source x=1
    electrode name=drain x=9
    electrode name=substrate backside

#This step saves the created structure, and then calls the tonyplot software package
#in order to provide a picture of the created device.

    structure outfile=NMOS_MQP.str
    tonyplot NMOS_MQP.str

# extract a curve of conductance versus bias. This curve will allow us to see the
# turnon voltage of the created transistor.

    extract start material="Polysilicon" mat.occno=1 bias=0.0 \
        bias.step=0.1 bias.stop=2 x.val=4.5
    extract done name="sheet cond v bias" \
        curve(bias,1dn.conduct material="Silicon" mat.occno=1 \
            region.occno=1)
    outfile="NMOS_CvsBias.dat"
    tonyplot NMOS_CvsBias.dat

##### Vt Test : Returns Vt, Beta and Theta #####
go atlas

# set material models. These models introduce real-world imperfections into the device
#and allow Atlas to generate answers that more accurately reflect the results of a
#physical device.

models cvt srh print

#the polysilicon is defined as a contact, although there is no direct connection with the

```

```

#aluminum contacts. Then, the device is solved for its initial condition state (no bias
#state)

contact name=gate n.poly
method newton
solve init

#Because Silvaco cannot accurately solve for large bias intervals, the device must be
#ramped up to an appropriate voltage on which calculations are to be performed

solve vdrain=0.1 vstep=0.2 vfinal=2.0 name=drain

#The output command generates a structure file similar to that obtained from Athena,
#however many more conditions have been solved for, and are available to be viewed in
#tonyplot.

output
structure outfile=NMOS_OUTPUT.str
tonyplot NMOS_OUTPUT.str

# Ramp the gate. This step will monitor the device as the applied gate voltage is
# ramped from 0 volts to 5 volts and then generate a structure file using the results
# of the calculations. This will allow us to observe some of the V-I characteristics

log outf=AtlasMQP.log master
solve vgate=0 vstep=0.25 vfinal=5.0 name=gate
save outf=AtlasMQP.str
tonyplot AtlasMQP.log -set moslex01_1_log.set

#Device parameters can be extracted, and then referenced later.

extract name="nvt" (xintercept(maxslope(curve(abs(v."gate"),abs(i."drain")))) \
- abs(ave(v."drain"))/2.0)
extract name="nbeta" slope(maxslope(curve(abs(v."gate"),abs(i."drain")))) \
* (1.0/abs(ave(v."drain")))
extract name="ntheta" ((max(abs(v."drain"))) * $"nbeta")/max(abs(i."drain"))) \
- (1.0 / (max(abs(v."gate"))) - ($"nvt"))

#these steps will act to adjust the current voltage levels of the device at which
#Atlas is making calculations.

solve vdrain=0.0
solve vgate=0.0 vstep=-0.5 vfinal=-5.0 name=gate

#This step will ramp the gate voltage of the device, and monitor the capacitance of the
#device. This C-V curve will show us if our device is exhibiting acceptable capacitance
#characteristics.

```

```

log outfile=mos2ex15_CV19_3.log
solve vgate=-5.0 vstep=0.1 vfinal=5.0 name=gate ac freq=1e0 previous
tonyplot mos2ex15_CV19_3.log -set mos2ex15_CV.set

#The following process will acquire three separate curves from the behavior of
#the device, and then plot them all on the same axes. The curves that we are
#generating are the drain current vs. drain voltage characteristics at three distinct
#gate voltage biases.

# set gate biases with Vds=0.0

solve vgate=1.5 outf=solve_tmp1
solve vgate=2.5 outf=solve_tmp2
solve vgate=3.5 outf=solve_tmp3

#load in temporary files and ramp Vds

load infile=solve_tmp1
log outf=GateVoltage_15.log
solve name=drain vdrain=0 vfinal=5.0 vstep=0.25

load infile=solve_tmp2
log outf=GateVoltage_25.log
solve name=drain vdrain=0 vfinal=5.0 vstep=0.25

load infile=solve_tmp3
log outf=GateVoltage_35.log
solve name=drain vdrain=0 vfinal=5.0 vstep=0.25

# extract max current and saturation slope

extract name="nidsmax" max(i."drain")
extract name="sat_slope" slope(minslope(curve(v."drain",i."drain"))))

#tonyplot can graph multiple structures on the same axes, and that is what this step does

tonyplot -overlay -st GateVoltage_15.log GateVoltage_25.log GateVoltage_35.log

quit

```

Appendix C – PMOS Athena and Atlas Code

```
go athena
```

```
#This initial step is used to define the mesh for the BCD structure. The mesh is
#important in determining on how many points of the device Athena will perform
#calculations. A mesh that is not dense enough will yield incorrect results, however a
#mesh that is too dense will require too many calculations and will make it impossible to
#run multiple simulations and quickly analyze results.
```

```
line x loc=0.0 spac=0.1
line x loc=1.66666 spac=0.05
line x loc=3.333333 spac=0.05
line x loc=5.0 spac=0.085
line y loc=0 spac=0.035
line y loc=1 spac=0.85
line y loc=5.0 spac=2.5
```

```
#The following line denotes the type of wafer on which the device is going to be
#constructed. For the CMOS devices, we will be using a silicon wafer, in a <100>
#orientation and doped with a boron level of 1e14
```

```
init orientation=100 c.boron=1e14 space.mul=2 TWO.D
```

```
#Here is where the arsenic epitaxial layer will be grown. Arsenic is chosen to create
#an n-type layer upon which the device will be constructed. The divisions parameter
#specifies the amount of new mesh layers to be applied to the newly grown epitaxial
#layer. The thickness is specified to be 4.5 micrometers (the default unit of length
#in Athena.
```

```
epitaxy time = 45 temp = 900 t.final = 1000 c.arsenic=1e16 \
thickness = 4.5 divisions = 20 \
dy = .05 ydy = 0.00
```

```
#As this is a PNP device, no Pwell infusion is necessary, as the epitaxial layer is NType
#arsenic
```

```
##### LOCOS here #####
```

```
#As discussed in the report, LOCal Oxidation of Silicon is an effective technique
#for isolating the seperate devices that are created on the wafer. This process
#grows a thick layer of Silicon Dioxide between neighboring devices, so that the
#performance of one device is not influenced by the operation of another.
```

```
#The following step creates the necessary mask to shield the device during the LOCOS
#process, and then etches away the area that is to be exposed to the growth of the Oxide.
```

#A thick layer of nitride is applied to not only serve as a barrier, but to
#also help diminish the "bird beak" effect that is common to the growth of an oxide
#layer.

```
deposit oxide thick = .01 div = 1
deposit nitride thick = .3 div = 6
deposit barrier thick = .1 div = 1
etch barrier left pl.x = .5
etch nitride thick = .35
etch oxide thick = .02
etch silicon dry thick = .25
```

#The 'barrier' layer is now removed, and the device is annealed in a water vapor
#environment so that rapid oxide growth can be achieved.

```
strip
method grid.ox = .075
diffuse temp = 1200 time = 60 weto2 hcl.pc=3
```

#The remaining deposited layers are now etched away, and the device has been
#successfully isolated.

```
etch nitride all
etch oxide thick = .05
```

#####

#The gate oxide is now grown on the device. Time and temperature are chosen
#to create a gate oxide of to the BCD-III spec of 28nm

```
diffus time=10 temp=1035 dryo2 press=1.00 hcl=3
```

Extract a design parameter

```
extract name="gateox" thickness oxide mat.occno=1 x.val=0.05
```

#In order to concentrate the current flow through the channel of the device,
#thereby helping reduce the leakage current, an additional arsenic implantation is
#performed.

```
implant arsenic dose=2.5e12 energy=250 pearson
```

#now that the channel is doped, the polysilicon can be deposited

```
depo poly thick=1 divi=10
```

#The polysilicon is lightly doped with phosphor


```

        implant phosphor dose=3.0e13 energy=20 pearson

#this step etches away the sides of the polysilicon, and then performs a brief
#annealing step which will grow an oxide around the polysilicon in order to protect
#it from acquiring any further doping characteristics

        etch poly left p1.x=4
        method fermi compress
        diffuse time=3 temp=900 weto2 press=1.0
        depo oxide thick=0.235 divisions=8
        etch oxide dry thick=0.235

#The p-type wells (source and drain) are then implanted into the device, and then
#diffused to the appropriate depth, as controlled by the time and temperature of
#diffusion

        implant boron dose=5e15 energy=25 pearson
        method fermi compress
        diffuse time=390 temp=925 nitro press=1.0

#A final oxide is grown to protect the device

        depo oxide thick=3.5
        etch oxide dry thick=3.4

# This step etches away the oxide in specific places so that aluminum contacts
# can be added to the source and drain wells.

        etch oxide start x=2 y = -6.25
        etch cont x = 2 y = -4.25
        etch cont x = 1.25 y = -4.25
        etch done x = 1.25 y = -6.25
        deposit alumin thick=0.4 divi=2
        etch alumin right p1.x = 2.25
        etch alumin left p1.x = .5

#The final steps are to mirror the device (because the CMOS transistor is a symmetric
#device, only half of it was created during this process, the structure can now merely be
#mirrored to attain the full device.

        structure mirror right

#Lastly, the aluminum contacts are defined as electrodes, which will allow Atlas to
#perform computations. X and Y coordinates intersecting the appropriate contact are
#chosen, and a name is given to the contact at the point of intersection.

        electrode name=gate x=5 y=-5.5
        electrode name=source x=1

```

```

electrode name=drain x=9
electrode name=substrate backside

#This step saves the created structure, and then calls the tonyplot software package
#in order to provide a picture of the created device.

structure outfile=PMOS_MQP.str
tonyplot PMOS_MQP.str

# extract a curve of conductance versus bias.

extract start material="Polysilicon" mat.occno=1 \
        bias=0.0 bias.step=-0.1 bias.stop=-5 x.val=4.5
extract done name="sheet cond v bias" \
        curve(bias,1dn.conduct material="Silicon" mat.occno=1 \
        region.occno=1)
outfile="PMOS_CvsBias.dat"
tonyplot PMOS_CvsBias.dat
structure outfile=PMOS_MQP.str

# plot the structure
tonyplot PMOS_MQP.str -set moslex01_0.set

#####
go atlas

# set material models. These models introduce real-world imperfections into the device
#and allow Atlas to generate answers that more accurately reflect the results of a
#physical device. srh = shockley-reed-hall, and governs the minority carrier
#recombination rate. cvt = Lombardi Model for N, G, E// and E (perpendicular) effects

models cvt srh print

#the polysilicon is defined as a contact, although there is no direct connection with the
#aluminum contacts. Then, the device is solved for its initial condition state (no bias
#state)

contact name=gate n.poly
method newton
solve init

#Because Silvaco cannot accurately solve for large bias intervals, the device must be
#ramped up to an appropriate voltage on which calculations are to be performed

solve vdrain=0.1 vstep=-0.2 vfinal=-2.0 name=drain

```

```
#The output command generates a structure file similar to that obtained from Athena,
#however many more conditions have been solved for, and are available to be viewed in
#tonyplot.
```

```
output
structure outfile=PMOS_OUTPUT.str
tonyplot PMOS_OUTPUT.str
```

```
# Ramp the gate. This step will monitor the device as the applied gate voltage is
# ramped from 0 volts to -5 volts and then generate a structure file using the results
# of the calculations. This will allow us to observe some of the V-I characteristics
```

```
log outf=AtlasMQP.log master
solve vgate=0 vstep=-0.25 vfinal=-5.0 name=gate
save outf=AtlasMQP.str
tonyplot AtlasMQP.log -set moslex01_1_log.set
```

```
# extract device parameters
```

```
extract name="nvt" (xintercept(maxslope(curve(abs(v."gate"),abs(i."drain")))) \
    - abs(ave(v."drain"))/2.0)
extract name="nbeta" slope(maxslope(curve(abs(v."gate"),abs(i."drain")))) \
    * (1.0/abs(ave(v."drain")))
extract name="ntheta" ((max(abs(v."drain"))) * $"nbeta")/max(abs(i."drain"))) \
    - (1.0 / (max(abs(v."gate"))) - ($"nvt")))
```

```
#these steps will act to adjust the current voltage levels of the device at which
#Atlas is making calculations.
```

```
solve vdrain=0.0
solve vgate=0.0 vstep = -.5 vfinal = -5.0 name = gate
```

```
#This step will ramp the gate voltage of the device, and monitor the capacitance of the
#device. This C-V curve will show us if our device is exhibiting acceptable capacitance
#characteristics.
```

```
log outfile=mos2ex15_CV19.log
solve vgate=-5.0 vstep=0.5 vfinal=5.0 name=gate ac freq=1e1 previous
tonyplot mos2ex15_CV19.log -set mos2ex15_CV.set
```

```
#The following process will acquire three separate curves from the behavior of
#the device, and then plot them all on the same axes. The curves that we are
#generating are the drain current vs. drain voltage characteristics at three distinct
#gate voltage biases.
```

```
# set gate biases with Vds=0.0
```

```

solve vgate=-1.5 outf=solve_tmp1
solve vgate=-2.5 outf=solve_tmp2
solve vgate=-3.5 outf=solve_tmp3

#load in temporary files and ramp Vds

load infile=solve_tmp1
log outf=moslex02_1.log
solve name=drain vdrain=0 vfinal=-5.0 vstep=-0.25

load infile=solve_tmp2
log outf=moslex02_2.log
solve name=drain vdrain=0 vfinal=-5.0 vstep=-0.25

load infile=solve_tmp3
log outf=moslex02_3.log
solve name=drain vdrain=0 vfinal=-5.0 vstep=-0.25

# extract max current and saturation slope

extract name="nidsmax" max(i."drain")
extract name="sat_slope" slope(minslope(curve(v."drain",i."drain")))

#tonyplot can graph multiple structures on the same axes, and that is what this step does

tonyplot -overlay -st moslex02_1.log moslex02_2.log moslex02_3.log -set moslex02_1.set

quit

```

Appendix D – BJT Athena and Atlas Code

```
go athena
```

```
#This initial step is used to define the mesh for the BCD structure. The mesh is
#important in determining on how many points of the device Athena will perform
#calculations. A mesh that is not dense enough will yield incorrect results, however a
#mesh that is too dense will require too many calculations and will make it impossible to
#run multiple simulations and quickly analyze results.
```

```
line x loc=0.0 spac=0.05
line x loc=5.0 spac=0.05
line y loc=0 spac=0.1
line y loc=2 spac=0.50
line y loc=5.0 spac=2
```

```
#The following line denotes the type of wafer on which the device is going to be
#constructed. For the CMOS devices, we will be using a silicon wafer, in a <100>
#orientation and doped with a boron level of 1e14
```

```
init orientation=100 c.boron=1e14 space.mul=2 TWO.D
```

```
#Here is where the arsenic epitaxial layer will be grown. Arsenic is chosen to create
#an n-type layer upon which the device will be constructed. The divisions parameter
#specifies the amount of new mesh layers to be applied to the newly grown epitaxial
#layer. The thickness is specified to be 4.5 micrometers (the default unit of length
#in Athena.
```

```
epitaxy time = 45 temp = 900 t.final = 1000 c.arsenic=1e16 \
thickness = 4.5 divisions = 25 dy = .05 ydy = 0.00
```

```
##### LOCOS is here #####
```

```
#As discussed in the report, LOCal Oxidation of Silicon is an effective technique
#for isolating the separate devices that are created on the wafer. This process
#grows a thick layer of Silicon Dioxide between neighboring devices, so that the
#performance of one device is not influenced by the operation of another.
```

```
#The following step creates the necessary mask to shield the device during the LOCOS
#process, and then etches away the area that is to be exposed to the growth of the Oxide.
#A thick layer of nitride is applied to not only serve as a barrier, but to
#also help diminish the "bird beak" effect that is common to the growth of an oxide
#layer. This code remains commented as the dimensions have not been finalized, due to
#our focus on the device operation. The process as described below is correct in all
#aspects except the etching coordinates.
```

```

#deposit oxide thick = .01 div = 1
#deposit nitride thick = .3 div = 6
#deposit barrier thick = .1 div = 1

#etch barrier left pl.x = .1
#etch barrier right pl.x = 4.9

#etch nitride thick = .35
#etch oxide thick = .02
#etch silicon dry thick = .25

#strip
#method grid.ox = .075
#diffuse temp = 1100 time = 60 weto2 hcl.pc=3

#etch nitride all
#etch oxide thick = .05
#####

#A thick oxide is deposited on the device in order to shield the regions
#which in which dopant deposition is unwanted.

depo oxide thickness=0.5 div=10

#The first step is to etch away the oxide, revealing the area on the surface
#of the device which we want to implant with Boron. This region will be the
#base.

etch oxide start x = 2 y=-5
etch cont x = 2 y = -4.52
etch cont x = 2.85 y = -4.52
etch done x = 2.85 y = -5

#Boron is now implanted into the base region of the BJT

implant boron dose=5e15 energy=100 pearson
diffus time=30 temp=1050 nitro

#The oxide is now removed, and a new oxide is applied. The new oxide will be etched
#in such a way that the base region is shielded while the emitter and collector
#regions are exposed for ion implantation

etch oxide all
depo oxide thick=.5

etch oxide start x=1.875 y=-5
etch cont x=1.875 y=-4.52
etch cont x=2.4 y=-4.52

```

```

    etch done x=2.4 y=-5

#The higher doped emitter is implanted first

    implant arsenic dose=5e15 energy=20 tilt = 0

#sections of the oxide are now etched away to prepare the device
#for the collector implantation step

    etch oxide start x = 4.5 y = -5
    etch cont x = 4.5 y = -4.52
    etch cont x = 5 y = -4.52
    etch done x = 5 y = -5

    etch oxide start x = 0.0 y = -5
    etch cont x = 0.0 y = -4.52
    etch cont x = 0.7 y = -4.52
    etch done x = 0.7 y = -5

#Collector implantation and diffusion

    implant arsenic dose=5e14 energy=20 tilt = 0
    diffus time=180 temp=1000 nitro

#All of the remaining oxide is partially etched to ensure that a clean
#contact can be made with the aluminum contact metal, and the base
#collector and emitter regions.

    etch oxide thick = .2

#Base contact region is etched here

    etch oxide start x = 3.25 y = -5
    etch cont x = 3.25 y = -4.5
    etch cont x = 3.75 y = -4.5
    etch done x = 3.75 y = -5

#Aluminum is now deposited over the whole of the device, and it
#is etched into seperate contacts for the emitter, base, and collector

    depo alum thick = .3 div = 3

    etch alum start x = 1 y = -5.5
    etch cont x = 1 y = -4.5
    etch cont x = 1.5 y = -4.5
    etch done x = 1.5 y = -5.5

    etch alum start x = 2.75 y = -5.5

```

```

    etch cont x = 2.75 y = -4.5
    etch cont x = 3.1 y = -4.5
    etch done x = 3.1 y = -5.5

    etch alum start x = 3.85 y = -5.5
    etch cont x = 3.85 y = -4.5
    etch cont x = 4.15 y = -4.5
    etch done x = 4.15 y = -5.5

    electrode name = collector x = .5
    electrode name = collector x = 4.5
    electrode name = emitter x = 2
    electrode name = base x = 3.5

#The finalized device is now graphed using TonyPlot

    structure outfile = finished_BJT.str
    tonyplot finished_BJT.str

##### ATLAS #####

go atlas

#set material models.  These models introduce real-world imperfections into the device
#and allow Atlas to generate answers that more accurately reflect the results of a
#physical device.

models srh cvt print

#Gummel plot.  The following steps will extract the necessary paramters so that
#a device Gummel Plot can be constructed.  The Gummel Plot will display the common
#emitter transfer characteristics of our constructed device

method newton autonr trap
solve vcollector=0.025
solve vcollector=0.1
solve vcollector=0.25 vstep=0.25 vfinal=2 name=collector
solve vbase=0.025
solve vbase=0.1
solve vbase=0.2

log outf=bjtex04_0.log
solve vbase=0.3 vstep=0.05 vfinal=1.5 name=base

#the Gummel Plot is graphed using TonyPlot
tonyplot bjtex04_0.log -set bjtex04_0_log.set

```



```

#IC/VCE with constant IB

#ramp Vb

log off
solve init
solve vbase=0.025
solve vbase=0.05

solve vbase=0.1 vstep=0.1 vfinal=0.7 name=base

# switch to current boundary conditions

contact name=base current

# ramp IB and save solutions
solve ibase=1.e-6
save outf=bjtex04_1.str master
solve ibase=2.e-6
save outf=bjtex04_2.str master
solve ibase=3.e-6
save outf=bjtex04_3.str master
solve ibase=4.e-6
save outf=bjtex04_4.str master
solve ibase=5.e-6
save outf=bjtex04_5.str master

# load in each initial guess file and ramp VCE
load inf=bjtex04_1.str master
log outf=bjtex04_1.log
solve vcollector=0.0 vstep=0.25 vfinal=5.0 name=collector

load inf=bjtex04_2.str master
log outf=bjtex04_2.log
solve vcollector=0.0 vstep=0.25 vfinal=5.0 name=collector

load inf=bjtex04_3.str master
log outf=bjtex04_3.log
solve vcollector=0.0 vstep=0.25 vfinal=5.0 name=collector

load inf=bjtex04_4.str master
log outf=bjtex04_4.log
solve vcollector=0.0 vstep=0.25 vfinal=5.0 name=collector

load inf=bjtex04_5.str master
log outf=bjtex04_5.log
solve vcollector=0.0 vstep=0.25 vfinal=5.0 name=collector

```

```
# plot results
tonyplot -overlay  bjtex04_1.log bjtex04_2.log bjtex04_3.log bjtex04_4.log bjtex04_5.log
-set bjtex04_1_log.set

quit
```

Appendix E – LDMOS Athena and Atlas Code

go Athena

This section defines the mesh lines for the wafer.

They are created by denoting an initial location x,y; and a spacing

These mesh lines are crucial; they define the number of calculation points

line x loc=0.0 spac=0.04

line x loc=10.00 spac=0.04

line y loc=0.0 spac=.5

line y loc=5.0 spac=2

Here we define the doping of the wafer

“TWO.D” specifies the 2-D plot; it is 1-D unless specified (dimension)

init orientation=100 c.boron=1e14 space.mul=2 TWO.D

#In combination, these two lines of code will display the specified outfile in tonyplot

structure outfile = LDMOS_MQP_Marc.str

tonyplot LDMOS_MQP_Marc.str

Here is where the arsenic epitaxial layer will be grown

We are unsure as to the purpose of the dy, ydy.

Specify a temp, time gradient, and a doping agent + concentration

Also, “division”, which is the additional mesh lines that will be added

epitaxy time = 45 temp = 900 t.final = 1000 c.arsenic=1e16 thickness = 4.5 dy = .05 ydy = 0.00 division = 25

this command will relax the number of mesh points for a specified area (less of them)

relax y.min = -2

structure mirror right

structure outfile = LDMOS_MQP_Marc.str

tonyplot LDMOS_MQP_Marc.str

LOCOS ISOLATION HERE#####

#####FOX ENHANCEMENT HERE#####

For the LDMOS, an additional oxide layer is grown known as the FOX enhancement. It helps control the Breakdown voltage and

the Ron of the device. It is done at the same time as the LOCOS because it requires much growth time. So it is done very early
on in the fabrication stage

```
deposit oxide thick=0.01 divi=1  
deposit nitride thick=0.3 divi=6  
deposit barrier thick=.1 divi=1
```

```
etch barrier left p1.x=1.5  
etch barrier right p1.x=18.5
```

```
etch barrier start x=8.5 y=-5  
etch cont x=8.5 y=-4.5  
etch cont x=15 y=-4.5  
etch done x=15 y=-5
```

```
etch nitride thick=0.35  
etch oxide thick=0.02  
etch silicon dry thick=0.1
```

```
strip
```

```
structure outfile = LDMOS_MQP_Marc.str  
tonyplot LDMOS_MQP_Marc.str
```

```
method grid.ox=0.075  
diffuse temp=1100 time=60 weto2 hcl.pc=3
```

```
etch nitride all  
etch oxide thick = .05
```

```
structure outfile = LDMOS_MQP_Marc.str  
tonyplot LDMOS_MQP_Marc.str
```

#gate oxide grown here round 1:-

```
diffus time=10 temp=1035 dryo2 press=1.00 hcl=3
```

next the poly-silicon is deposited and doped to improve conductivity

```
depo poly thick = 1 div = 10
```

```
implant phosphor dose = 3.0e13 energy = 20 pearson
```

```
structure outfile = LDMOS_MQP_Marc.str  
tonyplot LDMOS_MQP_Marc.str
```

```

etch poly left p1.x = 4.5

# the p-well drive is implemented

implant boron dose = 5e15 energy = 100
diffus time=150 temp=1100 nitro

structure outfile = LDMOS_MQP_Marc.str
tonyplot LDMOS_MQP_Marc.str

etch poly right p1.x = 13.5

etch oxide thick = .05

structure outfile = LDMOS_MQP_Marc.str
tonyplot LDMOS_MQP_Marc.str

depo oxide thick = .5

structure outfile = LDMOS_MQP_Marc.str
tonyplot LDMOS_MQP_Marc.str

etch oxide start x=4 y=-5.5
etch cont x=4 y = -4.4
etch cont x=2.25 y = -4.4
etch done x=2.25 y = -5.5

etch oxide start x=15.5 y=-5.5
etch cont x=15.5 y=-4.4
etch cont x=18 y=-4.4
etch done x=18 y=-5.5

structure outfile = LDMOS_MQP_Marc.str
tonyplot LDMOS_MQP_Marc.str

#gate oxide grown here round 2:-

diffus time=10 temp=1035 dryo2 press=1.00 hcl=3

structure outfile = LDMOS_MQP_Marc.str
tonyplot LDMOS_MQP_Marc.str

```

The N type dopants are then implanted

```
implant arsenic dose = 5e15 energy = 50
diffus time=180 temp=1000 nitro

structure outfile = LDMOS_MQP_Marc.str
tonyplot LDMOS_MQP_Marc.str

etch oxide thick = .03
```

The device is then prepared for the deposition of the contacts

```
depo alum thick = .5

structure outfile = LDMOS_MQP_Marc.str
tonyplot LDMOS_MQP_Marc.str

etch alum left p1.x=1

etch alum start x=4.5 y=-7
etch cont x=4.5 y=-5
etch cont x=15 y=-5
etch done x=15 y=-7

etch alum right p1.x=19

structure outfile = LDMOS_MQP.str
tonyplot LDMOS_MQP.str
quit
```